universität wien

DISSERTATION

Measurements of mineralization density profiles in bone formation sites: A novel tool for diagnosis of disturbances in primary mineralization of bone

angestrebter akademischer Grad

Doktorin der Naturwissenschaften (Dr.rer.nat.)

Verfasserin	Mag. Sonja Andrea Pfeffer
Matrikel-Nummer:	9721724
Dissertationsgebiet (lt. Studienblatt):	Biologie/Zoologie
Betreuer:	Univ.-Doz. Dipl.Ing. Dr. Paul Roschger

Wien, im Mai 2009

Erklärung

Ich erkläre an Eides statt, dass ich die hier vorliegende Arbeit selbst verfasst und nur die angegebene Literatur verwendet habe.

Wien, Mai 2009

Acknowledgement

First I would like to thank Univ. Prof. Dr. Klaus Klaushofer, the head of the Ludwig Boltzmann Institute of Osteology, for providing me an invaluable chance to work in his multidisciplinary research team.

Then I would like to thank my doctoral supervisor, Univ. Doz. Dipl.-Ing. Dr. Paul Roschger, for the inestimable scientific support during the work of acquisition, analysis and interpretation of the data. I highly appreciate the permanent encouragement during my thesis. The constant and profound feedback from him made possible for me to do this work with such a quality.

I also got a lot of technical assistance at the LBIO, wherefore I want to thank the following people: MTA Gerda Dinst, MTA Phaedra Meßmer, MTA Sabrina Thon, MTA Daniela Gabriel. Beside this assistance, I thank these persons also for the collegial and friendly ambiance and communication. I want to express also my thanks to my other collegues for their supports and their profitable discussions: Dr. Kamilla Nawrot-Wawrzyniak, Dr. Stéphane Blouin, Andreas Roschger, Dr. Barbara Misof, Dr. Nadja Fratzl-Zelman.

I thank Dr. Ruth Zöhrer, who introduced me into this institute. She has supported me as friend during all my student-time in Salzburg and Vienna.

Many thanks also to Eleonora Loy for her help, providing of useful informations and her encouragement.

Last but not least I thank my entire family for their love, their patience and their confidence during all the years of my academic studies.

MEASUREMENTS OF MINERALIZATION DENSITY PROFILES IN BONE FORMATION SITES: A NOVEL TOOL FOR DIAGNOSIS OF DISTURBANCES IN PRIMARY MINERALIZATION OF BONE.

ABSTRACT

The degree of bone matrix mineralization is playing a pivotal role in tuning stiffness, strength and toughness of bone and is therefore an important determinant of bone quality. Mature trabecular and osteonal bone is composed by bone structural units (BSU) mineralized up to different degrees of mineral content, which generates a characteristic bone mineralization density distribution (BMDD). Young BSUs have the lowest and old BSUs the highest degree of mineralization. The exact knowledge of the underlying mineralization process is still lacking, but it could be shown that once mineralization has been started in the newly formed bone matrix (osteoid) the mineral content is rapidly increasing within few days up to 70 % of its final value and is referred as primary mineralization. The last 30% of increase in mineral content occurs only slowly in a time scale of month to years and is referred as secondary mineralization. The present work focuses on the measurement of the Ca-content where the transition from fast to slow mineralization occurred, which had been designated by us as Ca_{TURN}. Such measurements would allow us to detect bone diseases affecting the primary mineralization process and to contribute in the development of therapeutic strategies directly targeting the mineralization process.

For this purpose sectioned bone areas of human transiliac biopsies embedded in polymethylmethacrylate were imaged with a pixel resolution of 0.5 µm by quantitative backscattered electron imaging (qBEI). BSUs exhibiting a mineralization front were selected for analyses of mineralization density profiles (*BM-profiles*) perpendicular across the mineralization front. The obtained data plots could be described by two linear fits of different slopes, an initial steep slope followed by a flat one. The intersection point of the two lines determined the value of Ca_{TURN}.

Biopsies from children with a genetic disorders like osteogenesis imperfecta (OI-type I, n=5 and OI-type VII, n=4) showed an increased Ca_{TURN}, while children with an autosomal dominant hypocalcemia (ADH) an inherited form of hypoparathyroidism caused by an activating mutation of calcium sensing receptor (CaR) (n=3) exhibited a decreased Ca_{TURN} , compared to healthy children (n=13). Biopsies from patients with postmenopausal osteoporosis (n=9) treated with Ca and Vit D had a Ca_{TURN} not different from that of adult controls (n=8), while patients with an unclear differential diagnosis of bone diseases (n=10) exhibited all a reduced $Ca_{TURN.}$ When the Ca_{TURN} parameter where correlated with parameters of bone mineralization density distribution (BMDD) describing the average (Ca_{MEAN}) or the typical (Ca_{PEAK}) Ca-content of the entire cancellous bone compartment a strong positive linear correlation was revealed for the children with genetic disorders, while no such correlations were found for the adult patients.

The data suggest that the investigated genetic disorders are affecting the primary mineralization process, and that the final amount of Ca-content the bone matrix is reaching, is some how predetermined by the primary mineralization process. This new findings also proves the concept that a pathological altered mean degree of mineralization of bone can be a result of altered bone turnover and / or intrinsic bone mineralization process. Indeed, the changes seen in BMDD of OI and CaR mutated patients seem to be predominantly an effect of changes in the primary mineralization process, while the effects seen in the adult patient group with metabolic bone diseases seems to be mainly due to changes in bone turnover.

DIE ANALYSE VON MINERALISATIONSPROFILEN AN KNOCHENNEUBILDUNGSZONEN: EIN NEUES DIAGNOSEVERFAHREN FÜR STÖRUNGEN DER PRIMÄREN KNOCHENMINERALISATION.

ZUSAMMENFASSUNG

Der Mineralisationsgrad der Knochenmatrix stellt eine Schlüsselrolle in der Feinabstimmung von Steifigkeit, Festigkeit und Härte des Knochens dar und ist ein wichtiger Faktor für die Knochenqualität. Reife trabekuläre und osteonale Knochen setzen sich aus einzelnen unterschiedlich mineralisierten Knochenstruktureinheiten (BSU) zusammen, die eine charakteristische Knochenmineralisationsdichteverteilung (BMDD) erzeugen. Die jungen, neu gebildeten BSU's sind noch nieder mineralisiert, während die alten BSU's den höchsten Mineralisationsgrad aufweisen. Das genaue Wissen um den zugrundeliegenden Mineralisationsprozess ist noch unvollständig.

Man konnte zeigen, dass der Mineralgehalt in einer neugeformten Knochenmatrix (Osteoid) innerhalb von nur wenigen Tagen auf 70% des Endwertes ansteigt, sobald der Mineralisationsprozess gestartet wurde. Diesen Vorgang bezeichnet man als primäre Mineralisation. Bis die restlichen 30% Mineralgehalt erreicht werden, dauert es dann Monate bis Jahre und man bezeichnet diesen Vorgang als sekundäre Mineralisation. In dieser Arbeit lag der Fokus auf der Ermittlung des Kalziumgehalts, der den Übergang von der schnellen zur langsamen Mineralisation beschreibt. Dieser Punkt wurde von uns als Ca_{TURN} bezeichnet. Durch diese Analysen könnten Knochenerkrankungen detektiert werden, deren Auswirkungen den primären Mineralisationsprozess betreffen, und es könnte ein Beitrag zur Entwicklung therapeutischer Strategien, die direkt in den Mineralisationsprozess einwirken, geleistet werden.

Zu diesem Zweck wurden humane Beckenkammbiopsien (n=72) in Polymethylmethacrylate eingebettet. Angeschnittene Knochenflächen wurden mittels quantitativer Rückstreuelektronenmethode (qBEI) mit einer Bildauflösung von 0,5µm Pixelgröße im Rasterelektronenmikroskop untersucht. Für die Analyse wurden BSU's mit einer sichtbaren Mineralisationsfront ausgesucht und im rechten Winkel zur Mineralisationsfront quer durch das frisch angebaute Knochenpaket ein Mineralisationsdichteprofil *(BM-Profil)* aufgenommen. Die erhaltenen Diagramme konnten durch zwei lineare Fits mit unterschiedlichen Anstiegen dargestellt werden. Der Schnittpunkt der beiden Geraden bestimmte den Wert des Ca_{TURN}.

Biopsie-Ergebnisse von Kindern mit der genetischen Erkrankung Osteogenesis Imperfecta (OI-Typ I, n=5 and OI-Typ VII, n=4) wiesen einen erhöhten Ca_{TURN}-Wert gegenüber der Kinder-Kontrollgruppe auf. Im Gegensatz dazu zeigten Kinder mit einer autosomal dominanten Hypokalzämie (ADH), einer vererbten Form des Hypoparathyreoidismus, die durch eine Mutation am Calcium Sensing Receptor (CaR) (n=3) verursacht wird, einen verminderten Ca_{TURN}-Wert. Biopsie-Ergebnisse von postmenopausalen osteoporotischen Frauen (n=9), behandelt mit Kalzium und Vitamin D, hatten einen Ca_{TURN}, der sich nicht von der Erwachsenen- Kontrollgruppe (n=8) unterschied. Jedoch bei allen PatientInnen mit Knochenerkrankungen unklarer Differentialdiagnose (n=10) zeigte sich ein reduzierter Ca_{TURN}-Wert. Korreliert man die Parameter der Knochenmineralisationsdichteverteilung (BMDD) mit dem Ca_{TURN}-Parameter, so ergab sich beim Ca_{MEAN} (BMDD-Parameter) und beim Ca_{PEAK} (charakteristischer Kalziumgehalt des gesamten spongiösen Knochenkompartiments) eine eindeutig lineare Korrelation bei den Kindern mit genetischen Veränderungen während innerhalb der Erwachsenen-Patientengruppe keine Korrelation festgestellt wurde.

Die Ergebnisse zeigen, dass der primäre Mineralisationsprozess bei den untersuchten genetisch erkrankten PatientInnen negativ beeinflusst wird, und dass der endgültige Kalziumgehalt, den die Knochenmatrix erreichen kann, abhängig vom primären Mineralisationsprozess ist. Diese neuen Untersuchungsergebnisse geben Evidenz, dass ein

pathologischer Grad der Mineralisierung des Knochens das Resultat eines veränderten Knochen-Turnovers und / oder eines veränderten Knochenmineralisationsprozesses sein kann.
Tatsächlich scheinen die Veränderungen im BMDD bei PatientInnen mit genetischen Erkrankungen wie Osteogenesis Imperfekta oder Calcium Sensing Receptor Mutationen vorwiegend die Folge der Veränderung im primären Mineralisationsprozesses zu sein, während die Effekte, die bei den Erwachsenen-PatientInnen gefunden wurden, hauptsächlich Folgen der Änderungen im Knochen-Turnover zu sein scheinen.

1. INTRODUCTION

I was working for my Thesis on the Ludwig Boltzmann-Institute of Osteology (LBIO) under supervision of Univ. Doz. Dipl. Ing. Dr. Paul Roschger (LBIO). The LBIO is a multidisciplinary research institute for bone, embedded in a clinical network at the Hanusch Hospital of WGKK and the AUVA Trauma Centre Meidling in 1140 Vienna and 1120 Vienna, respectively (*www.osteologie.at*). The primary goal of the Institute is the improvement of patient care. For this purpose, the study of bone, a highly complex hierarchical organized structure, is undertaken at all hierarchical levels. Especially, the quality of bone is addressed, which is contributing to the mechanical performance of bone.

1.1. Objective and Scope of the Thesis

Humans as all vertebrates have a skeletal system comprised of bone, a material with outstanding mechanical properties. However, disorders affecting the structure and material of bone, leads to enhanced fractures, which are associated with elevation in morbidity, mortality, loss of life quality and high socioeconomic costs. The increase in life expectancy for the population is the main factor today causing a remarkable increase in fracture incidence. Thus, the estimation of the bone fracture risk of a patient is the essential goal for correct treatment decisions for clinicians to prevent fractures and a challenge for material scientists. Only on the basis of an appropriate fracture risk assessment a high fracture risk can be diagnosed and the patient can get the correctly targeted treatment. Further, the success of a therapy can be evaluated. To date the prediction of fracture risk is mainly based on non invasive measurements like bone mineral density (BMD) or mineral content (BMC - a measure of the total mineral mass) as measured by dual energy x-ray absorption analysis (DXA) and biochemical bone markers in the serum and urine. However, only about 50% of the fracture risk in osteoporosis the most common skeletal disorder can be explained by these diagnostic tools (Marshall et al. 1996). The reason for this limitation is, that the total bone mass (bone

quantity) alone does not determine the fracture risk but additionally, the quality of the bone material contributes essentially to bone strength (Bouxsein 2003; Fratzl et al. 2004a; Seeman 2008). Generally, there are three levels at which the deterioration of the mechanical properties of a bone may occur:

1) the amount of bone material
2) the quality of bone architecture
3) the quality of bone material

Beside the amount of bone material **(1)** it was found that e.g. the trabecular architecture **(2)** such as connectivity, orientation, etc. in cancellous bone and geometrical properties of cortical bone such as outer diameter, thickness and porosity etc. have a significant influence on the mechanical integrity. Finally, alterations in the quality of the material **(3)** the trabecular and cortical motifs are composed of can play a pivotal role in loosing the mechanical competence of the whole bone. Important determinants of bone material quality **(3)** are the properties of the collagen/mineral nano-composite material like, particle density, size, shape, as well as the arrangement of mineral particles and the fibrillar collagenous matrix. In contrast to clinical BMD measurements, the assessment of bone trabecular architecture and aspects of bone material quality cannot be done in vivo, but needs a bone biopsy and a combination of modern physical techniques.

At the LBIO, the material level of bone is approached in a multidisciplinary way by a worldwide unique combination of modern physical techniques including a long-term collaboration with the Max Planck Institute of Colloids and Interfaces, Dept. of Biomaterials Potsdam/Germany (Director: Prof. Dr. Peter Fratzl). Quantitative backscattered electron imaging (qBEI) (Roschger et al. 1995; Roschger et al. 1998; Roschger et al. 2008b) is employed to assess the mineral content spatially resolved within the bone matrix, which is crucial for the elastic properties of the bone material. In combination with confocal laser scanning microscopy (CLSM) the dynamics of bone mineralization are determined. Polarized light microscopy (pLM) allows to visualize the lamellar arrangement of

collagen fibrils in trabecular and osteonal bone compartments. The arrangement of the fibrils plays a pivotal role in resistance to crack propagation and thus in bone strength. Fourier transform infrared microspectroscopy (FTIR) (Paschalis et al. 2001) and RAMAN (Kazanci et al. 2007) (are applied to characterize the chemical bonds in the collagen/mineral composite. Especially the collagen cross-link status modifies the mechanical properties of the composite. Scanning small angle x-ray scattering (sSAXS) (Rinnerthaler et al. 1999) is used to determine important bone composite parameters like mineral particle thickness, orientation, arrangement and inter-particle distance. The application of the nanoindentation technique on the atomic force microscope (AFM) (Gupta et al. 2005) enables us to make mechanical testing experiments of the bone material with about a 5µm spatial resolution. Parameters, like E-modulus and hardness are evaluated from each indentation experiment and are correlated with other composite parameters.

1.2. Aim of the Thesis

The bone material / matrix is a fiber nanocomposite of carbonate hydroxyapatite mineral and collagenous fibers. The degree of bone matrix mineralization is playing a pivotal role in tuning stiffness, strength and toughness of bone and is therefore an important determinant of bone quality. On one hand deficiency in mineral content leads to a less stiff bone and deformation occurs like in rachitic (Vit D deficient) patients (Lips et al. 2009). On the other hand hypermineralized bone matrix like osteogenesis Imperfecta (OI) leads to a brittle bone (glas bone) and the patients suffer on multiple fractures (Marini 2006).

Each individual has its characteristic bone mineralization density distribution (BMDD) like a fingerprint (Ruffoni et al. 2007; Roschger et al. 2008b). It is generated by the fact that bone is a living system, which is continuously destructed and renewed by bone cells the so called multicellular units (cycles of remodeling) forming basic structural units (BSUs), bone packets in trabecular

and osteons in cortical bone. Two independent processes are responsible, which lead to a specific BMDD (Fig. 1):

1) The frequency of bone remodeling, which leads to a certain bone turnover rate.
2) The time course of mineralization (the mineralization law) of newly apposed bone matrix (osteoid)

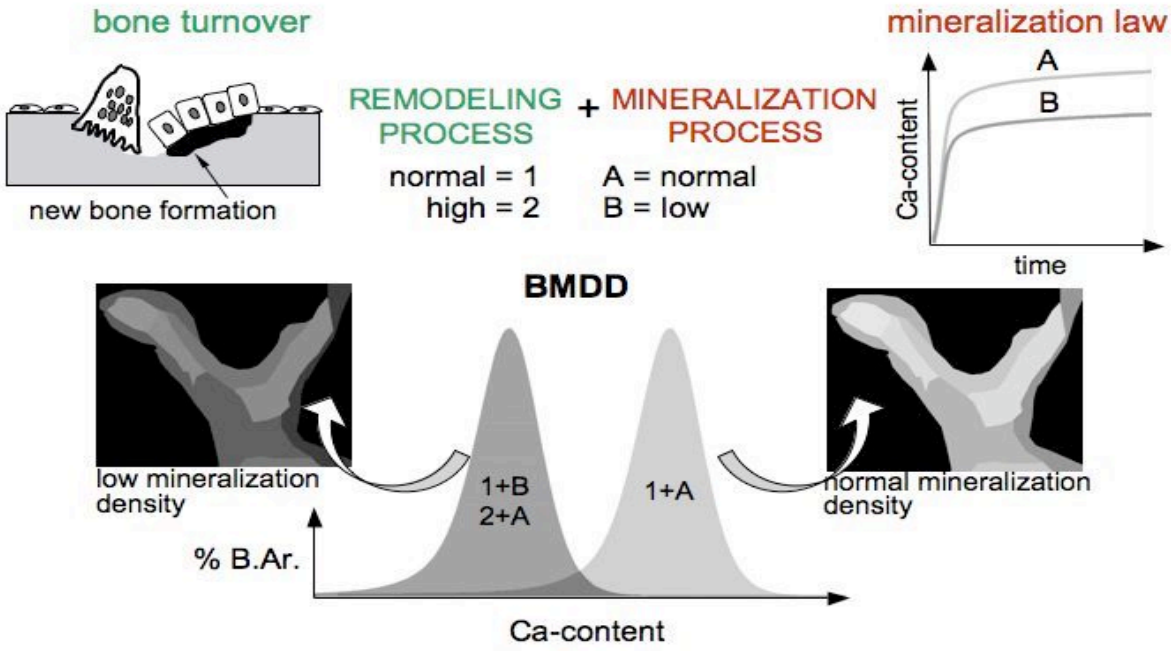

Figure 1: Schematic drawing of the generation of specific BMDDs. Two processes are responsible for its shape: bone remodeling and mineralization kinetics of bone matrix. Remodeling leads to the formation of non-mineralized bone packets (osteoid), which are mineralized following a certain mineralization law (describing the increase in Ca-concentration with time, see top right). The mineralization law shows an initial fast (primary mineralization) phase followed by a slow (secondary mineralization) phase of increase in mineral content. In consequence, a mosaic like structure of bone packets with different mineral content corresponding to the different tissue age (middle left and right) is generated. The effect of three different scenarios on the BMDD is sketched (bottom): (1+A) normal turnover and normal mineralization; (2+A) high turnover and normal mineralization; (1+B) normal turnover and altered mineralization (after: Nawrot-Wawrzyniak et al. 2009).

The exact knowledge of the underlying mineralization process is still lacking, but it could be shown that once mineralization has started in the newly formed bone matrix, the mineral content is rapidly increasing within few days up to 70 % of its final value and is referred as primary mineralization. The last 30% of increase in mineral content occurs only slowly in a time scale of month to years and is referred as secondary mineralization (Boivin and Meunier 2002; Misof et al. 2003). This biphasic kinetic of mineralization of bone has also been confirmed by mathematical (computed) modeling of the BMDD (Ruffoni et al. 2007; Ruffoni et al. 2008). In consequence of bone turnover and mineralization kinetics, mature trabecular and osteonal bone is composed of differently mineralized bone packets (bone structural units (BSUs)) generating a characteristic bone mineralization density distribution (BMDD). Young BSUs have the lowest and old BSUs the highest degree of mineralization.

Generally, bone diseases can affect process one (1) (bone turnover) and/or process two (2) (mineralization). Both can lead to similar deviations from normal BMDD. For instance high bone turnover would shift the BMDD towards lower mineralization (Fig. 1), however the same can happen, if the mineralization law is changed leading to lower mineralization at normal bone turnover. Thus it is from high clinical interest to know which disorder the patient is presenting to chose the correct therapeutic strategy. High bone turnover would usually be treated by antiresorptive drugs while in cases of deficiency in mineralization other therapeutic strategies have to be applied or developed first.

The present thesis focuses on transiliac biopsies of patients with a broad spectrum of metabolic and genetic bone diseases. We used the qBEI method for the first time to determine the Ca-content at the transition from fast to slow mineralization, which had been designated by us as Ca_{TURN} (Roschger et al. 2008b). A further tool of differential diagnosis in bone diseases, new insights into normal and pathological mineralization processes and help in the development of new drugs targeting directly the mineralization process can be expected.

2. CHARACTERISTICS OF BONE

The germ layer mesoderm in the early embryonic stage is the origin of the development of all the skeletal tissues components. The mesoderm differentiates into cells producing connective tissue, including bone, cartilage, dentin as well as cementum. Only dental enamel is generated by cells coming from another germ layer, the ectoderm (Ortner and Turner-Walker 2003). Bone constitutes the largest proportion of connective tissue mass in the human body. Unlike most other connective tissue matrices, it is mineralized and constantly regenerated throughout life. Bone as an organ is composed of the cortical and trabecular bone, the bone marrow, the cartilaginous joints, and the growth plate in developing individuals. Approximately 65wt% of the tissue consists of mineral, water comprises about 5 to 8wt% and the rest is made up of extracellular matrix or organic material. Nearly 95wt% of the mineral phase consists of carbonated hydroxyapatite. About 90wt% of the organic phase consists of type I collagen and 10wt% as a variety of non-collagenous proteins and proteoglycans. The absolute amounts of these constituents vary with age, sex, tissue site, health and dietary status (Urist 1980).

Bone as living material has outstanding mechanical properties forming the skeletal system together with cartilage and fulfills three important functions:

1) mechanical support, movement
2) protection of internal organs and bone marrow
3) metabolism, as a reservoir of calcium- and phosphate ions
   (Cashman 2002)

The biomaterial bone is characterized by its complex hierarchical structure, which is essential for its extraordinary biomechanical properties. Each level of structural organization has to be optimized to achieve the overall optimal mechanical performance of bone at organ level. (Paris et al. 2000; Roschger et al. 2008b).

2.1 Hierarchical Structure

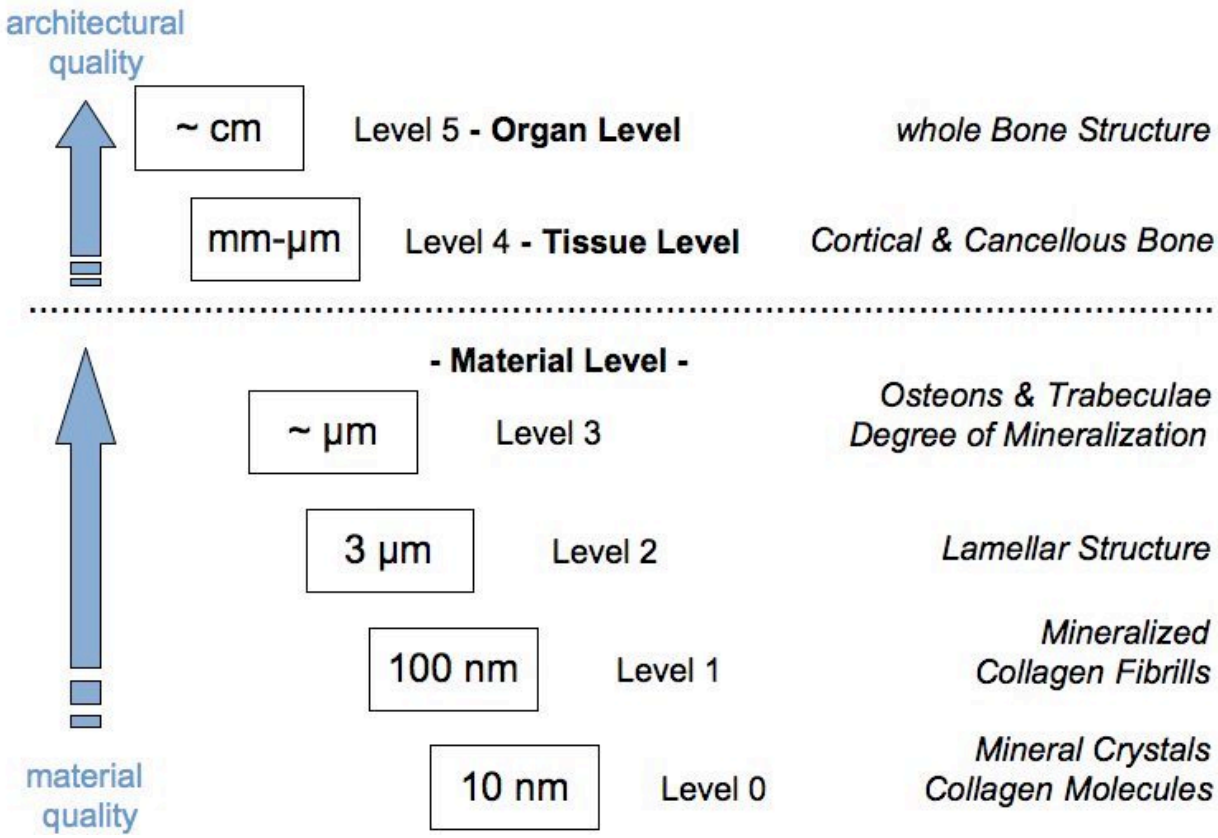

Figure 2: The hierarchical organization of bone structure. The strength of bone is the product of structural optimization at each level of bone structure.

2.1.1. Collagen and Mineral (level 0)

Bone is a nano-composite material composed at the lowest nanostructural level of mineral (carbonated hydroxyapatite $Ca_{10}(PO_4)_6(OH)_2$ and collagenous (mainly collagen type I) and non-collagenous organic proteins.

Collagen: The collagen is synthesized as procollagen first within the osteoblasts. Two α1-chains and one α2-chain are synthesized and the chains are intertwined to form a triple helix, whose amino acid sequence consists of Gly-X-Y repeats, each with a length of about 1400 residues. In about one-third of the cases, X is a proline and Y is a hydroxyproline. The presence of

hydroxyproline is essential, as it stabilizes the triple helix and is a unique characteristic of collagen molecules (Bilezikian et al. 1996). The triple helix of the procollagen has propeptide extensions at both N- and C-terminals. After excretion outside the osteoblasts, enzymatic cleavage converts the procollagen to collagen and the helical molecules assemble spontaneously into collagen fibrils. Collagen can stretch like an elastic band and allows bone to deform to a certain extent without fracturing. The flexibility of collagen can be altered due to chemical changes, thus reduces the toughness of bone and increases its fragility (Paschalis 2006) (Vashishth et al. 2001). Collagen diseases can be commonly attributed to genetic defects, which are affecting the biosynthesis, assembly, posttranslational modification, secretion, or other processes in the normal production of collagen. Collagen abnormalities and altered cross-link profiles are associated with osteoporosis (McLean et al. 2004; Blouin et al. 2009) , osteopetrosis (Wojtowicz et al. 1997) and osteogenesis imperfecta (Prockop et al. 1989; Kuivaniemi et al. 1991).

Mineral: The inorganic constituent of bone comprises poorly crystalline hydroxyapatite with the stoichiometric formula $Ca_{10}(PO_4)_6(OH)_2$ among others crystal lattice substitutions like carbonate, fluoride, citrate and potassium. The crystals are platelets or spicules, have a thickness of 2 to 4 nm and a width and length of tens of nanometers (Fratzl et al. 2004a). The crystal lattice spacing along *a* and *b* axis is 0.9432 nm and of the *c*-axis of the hexagonal lattice (the long axis) spacing is 0.8881 nm (Veis 2003) (Burger et al. 2008). Depending on the crystals' maturation, various amounts of carbonate ions are incorporated in the crystals lattice leading to carbonated apatite (Legros et al. 1987; Fratzl et al. 2004a). The crystal size, shape and thickness is a determinant of intrinsic bone material properties /quality of the collagen mineral composite. Thus alterations in mineral particles size, as it was observed in osteoporotic patients with fluoride treatment, was the reason that despite the increased formation of new bone this treatment failed to have any beneficial effect to fracture risk. Obviously the mechanical competence of the bone matrix formed under sodium fluoride (NaF) treatment was deteriorated (Fratzl et al. 1994; Roschger et al. 1997).

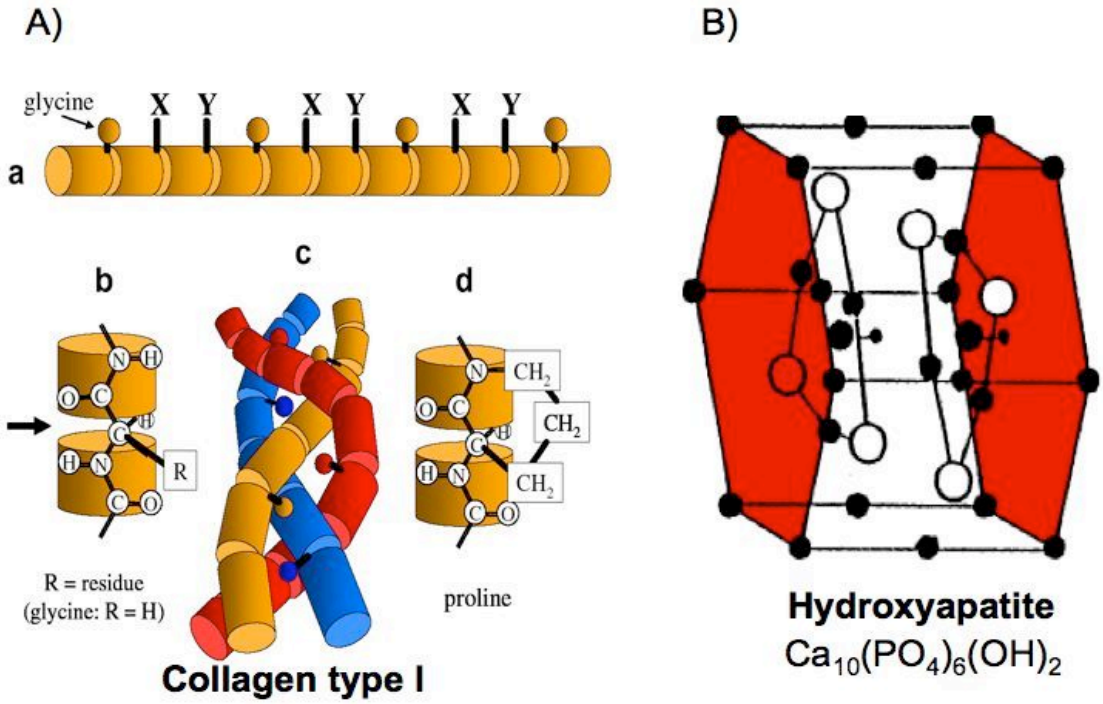

Figure 3: Level 0 - collagen molecule and mineral (carbonated apatite):
A) collagen type I: a) large protein with a highly repetitive amino acid sequence based on -Gly-X-Y- (Gly = glycine, X = proline, Y = hydroxyproline). Every third residue is Gly. (b) Gly is the smallest amino acid where the residue is just a hydrogen atom. (c) The collagen type I molecule is formed a triple helices, which are composed of two α1 and one α 2 chains.
(d) Proline and hydroxyproline have residues connecting back to the polypeptide chain. (after: Fratzl and Weinkamer 2007).
B) Mineral: hydroxyapatite = $Ca_{10}(PO_4)_6(OH)_2$, depending on crystal maturation various amounts of carbonate ions are incorporated in the crystal lattice in exchange with PO_4^- or OH^- leading to carbonated apatite.

Techniques used for analysis at collagen and mineral level:

- Small-Angle X-ray Scattering (SAXS)
- Wide Angle X-ray Scattering (WAXS)
- Fourier-Transforming InfraRed microspectroscopy (FTIR)
- Raman spectroscopy (Raman)
- Energy Dispersive X-ray spectroscopy (EDX)

2.1.2. Mineralized Fibril (level 1)

The mineralized collagen fibril is the basic building block of bone. The collagen fibrils are formed in the extracellular space by processes of self-assembly. The intertwined collagen molecules (two α1 chains and one α2 chain) form a triple-helical molecule of ~300 nm in length and ~1.5 nm in diameter. The collagen triple helices molecules form fibrils (Fratzl et al. 2004a), in which the single molecules lay parallel with a displacement of 67 nm between them in a staggered array, stabilized by intermolecular cross-links. Thereby hole zones of 35 nm and the overlap zones of 32 nm length are generated within the fibril leading to a banded structure. Many collagen fibrils together form a collagen fiber. The intra- and inter- fibrillar molecular cross-links play thereby a pivotal role for the mechanical strength of the mineralized fibrils.

The collagen fibril is reinforced by small nano-sized mineral particles, plate-like mineral crystals of carbonated hydroxyapatite. They are aligned with their c-axis parallel to the longitudinal axis of the collagen fibrils. Most likely they are also arranged in a staggered way (as this arrangement is most useful for mechanical performance), so that the mineral platelets overlap in the hole zones of the fibril. By this way a nano composite material is formed combining two mechanical properties of the individual components, collagen - soft and tough - and mineral - stiff and brittle - to a material which has both properties - stiff and tough (Ashby 1983; Fratzl 2006). Thus, mineral dictates much of the tissue stiffness and collagen has a profound effect on bone's post-yield properties, e.g. energy absorption (Burr 2002).

Important contributions to the fracture resistance and defect tolerance of bone composites arise from the nanometer scale. It was shown, that mineral nanoparticles and the mineralized fibrils deform both first elastically, but to different degrees, in a ratio of 12:5:2 between tissue, fibrils and mineral particles (Fig. 4). The different degrees of deformation of different components arranged in a parallel and staggered way within the tissue can be explained by a shear deformation between the components (Jager and Fratzl 2000) This means that

there is a shear deformation within the collagen fibrils making the difference between the strain in collagen and mineral possible. However, there must also be some shear deformation between adjacent collagen fibrils to accommodate the different strains in fibrils and the entire bone tissue. This shear deformation occurs presumably in a thin “glue” layer between fibrils in bone. They may consist of proteoglycans and non-collagenous phosphorylated proteins (Fratzl and Weinkamer 2007).

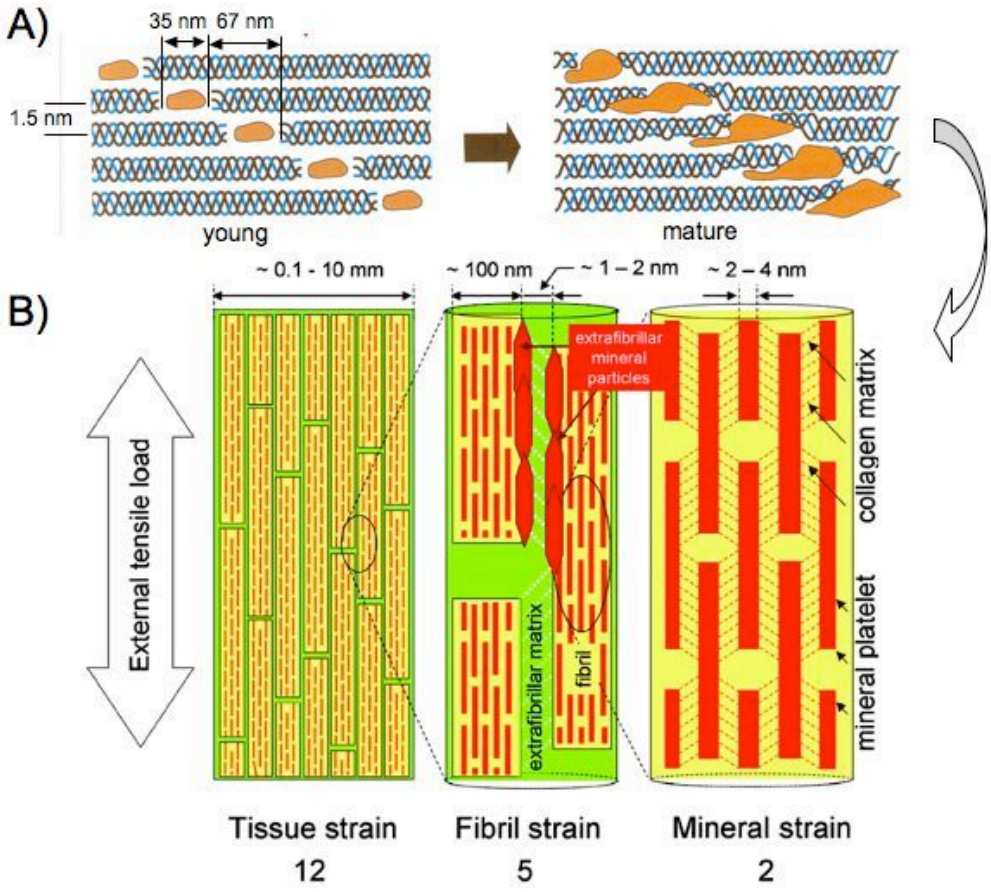

Figure 4: Level 1 – mineralized collagen fibrils:
A) Sketch of arrangement of staggered collagen molecules with embedded plate-like mineral crystals.
B) Mechanical model of deformation mechanism: The tensile load is transferred to all the mineral particles by shear forces generated in the collagen matrix functioning as glue. The same principle is working between the staggered arrangements of the mineralized fibrils and the inter-fibrilar matrix at the next higher hierachical level (Jager and Fratzl 2000; Fratzl et al. 2004a; Fratzl et al. 2004b; Gupta et al. 2006)

Techniques used for analysis at fibril level:

- Scanning Small-Angle X-ray Scattering (SAXS)
- Scanning x-ray diffraction (XRD)
- Transmission Electron Microscope (TEM)
- Atomic force microscopy (AFM)

2.1.3. Arrangements of Fibrils / lamellae (level 2)

The basic building blocks of bone, the mineralized fibrils, are mostly aligned in bundles or arrays. They form various patterns and build the final material of the tissue motifs, like trabecular and osteonal bone, primary periosteal bone, membranous bone, plexiform bone, callus, dentin, mineralized turkey leg tendon etc.. The pattern of fibril arrangement is highly responsible for the anisotropy in mechanical properties found in bone tissue. Indeed, a crack propagation perpendicular to the longitudinal axis of the collagen fibril bundle needs of two orders more energy than parallel to fibril axis (Peterlik et al. 2006) (Fratzl and Weinkamer 2007).

DIFFERENT PATTERNS OF FIBRIL BUNDLE ARRANGEMENTS ARE DISTINGUISHED:

WOVEN BONE: Fibrils are arranged in loosely packed and randomly oriented bundles with different diameters. It contains also a large proportion of non-collagenous material. It is built very quickly, e.g. the embryonic and/or fetal skeleton and in the callus after a bone fracture.

PARALLEL-FIBRILAR PATTERN: The fibrils and fibres are predominantly oriented parallel to each other and roughly parallel to the long bone axis. This is the case in cortical long bone of mouse, rats. Extreme amount of parallel arranged fiber bundles can be found in turkey leg tendons.

ROTATED PLYWOOD-LIKE STRUCTURE OF LAMELLAR BONE: This is the most common matrix structure of mature human bone of trabecular bone packets and cortical osteons. In trabecular bone the lamellae are aligned parallel to the trabecular surface. In osteonal bone the lamellae are arranged in concentric rings around

the haversian canal. The arrays of collagen fibrils orientation is changing in a regular manner to form a complex rotated plywood-like structure having a typical lamellar unit of approximately 5µm in thickness, in which the changing of the predominant fibril orientation is completed once. In polarized light microscopy the lamellar arrangement becomes visible by alternating contrast bright and dark. This type of bone matrix is formed more slowly than woven or parallel fibred bone.

RADIAL FIBRILAR PATTERN: This pattern is characteristic of the bulk of dentin, which forms the inner basis of the teeth. The collagen fibrils are arranged in plane randomly oriented perpendicular to the longitudinal axis of tubular canals.

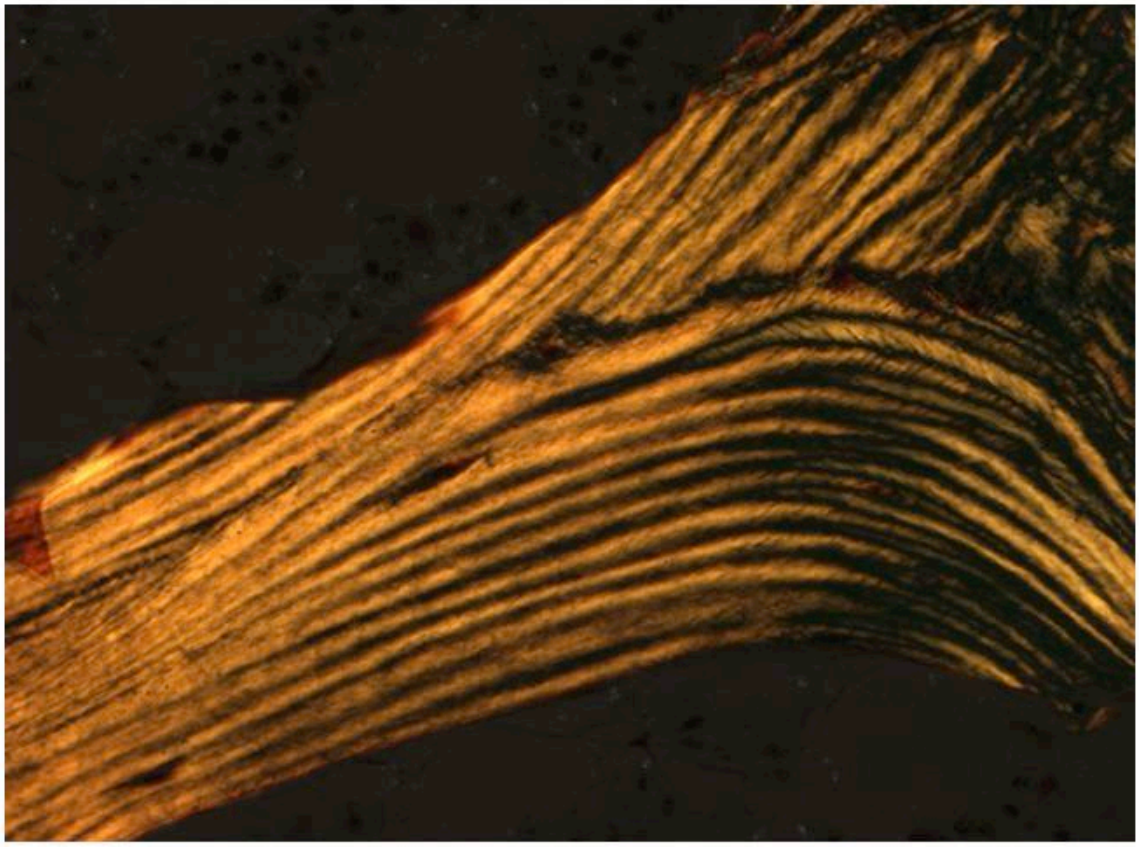

Figure 5: Level 2 – lamellar arrangement of collagen fibrils: Polarized light microscopy (pLM) visualizes the changing orientations of collagen fibrils between the lamellae of trabecular bone.

Techniques used for analysis at lamellar level:

- polarized-Light Microscope (p-LM)
- Raman Microscopy
- Scanning Small angle X-ray scattering (scanning-SAXS)

2.1.4. Bone Structural Units (BSU) (level 3)

The trabecular and cortical bone motifs are composed by BSUs. BSU denotes a unit bone matrix, which is formed during a complete remodeling cycle by one bone multicelluar unit (BMU). In trabecular bone it is called bone packet and in cortical bone osteon. Characteristically, they have a lamellar bone structure with a uniform lamellar orientation and a certain rather uniform mineral content. Adjacent BSU are separated by cement lines / surfaces, a non collagenous protein (NCP) rich mineralized matrix built by the BMU.

Since the mineral content in the BSU is increasing with time, the mineral content of a single BSU in an individual depends on the time passed after its formation. Therefore, the mineral content between the BSUs can vary between 0 to 65wt %. Thus, a bone tissue exhibits a characteristic pattern due to the different ages of BSUs, which can be quantified as mineralization density distribution (BMDD) (Roschger et al. 2008b). Hence, the BMDD is also reflecting rather the actual tissue age than the age of the individual. Further, the mineral content is tuning the stiffness, toughness and strength of the bone, so that the BMDD is an important factor in determining the bone material quality. It was found that the BMDD of healthy adults exhibited relatively small variations independent of skeletal site, gender, age and ethnic origin (Roschger et al. 2003) representing most likely an evolutionary optimum. Hence, already small deviations caused by diseases might be of biological relevance for an increase of fracture risk in the patient. For instance diseases like osteoporosis are associated mostly with an increased bone turnover, which means that the frequency of bone remodeling sites is increased. This leads to an elevation of younger BSUs with lower mineral content. Such a BMDD is shifted towards lower mineralization density compared to normal.

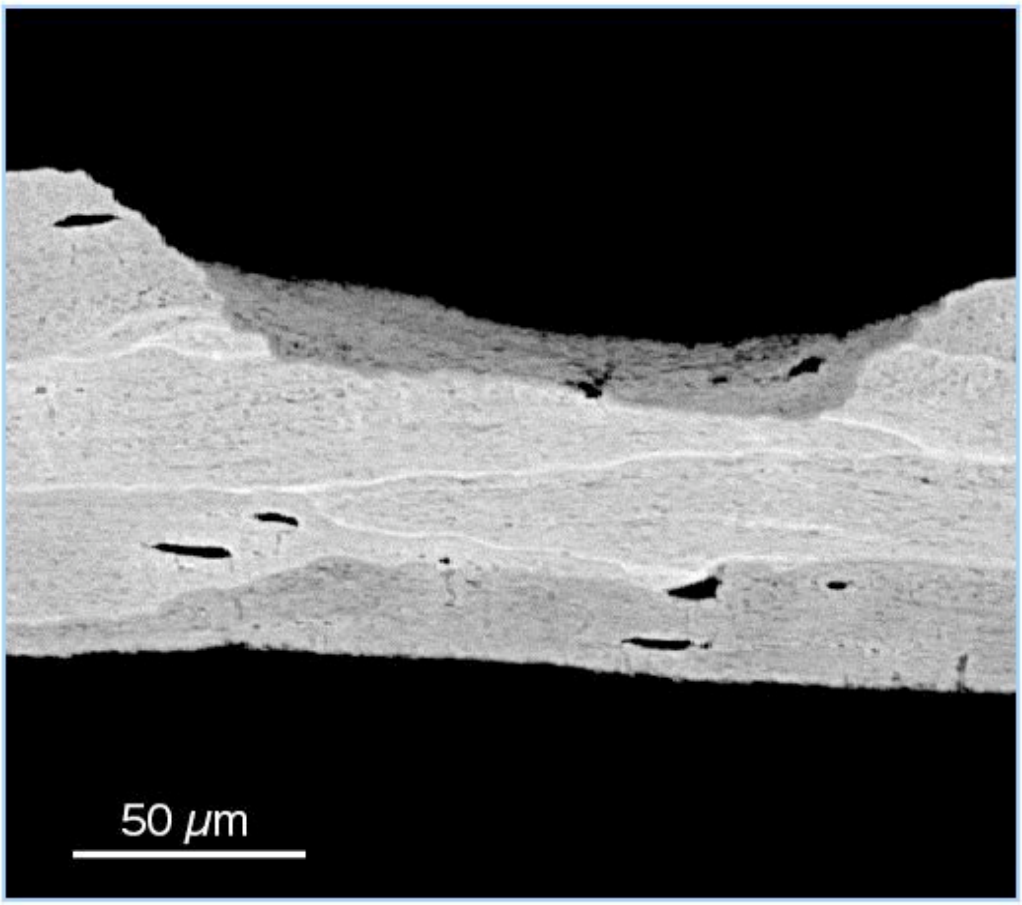

Figure 6: Level 3 - trabecular bone packets: Quantitative backscattered electron images (qBEI) showing bone packets (BSUs) of different mineral content reflecting their different tissue age. Dark gray new bone packets low with mineral content, light gray old bone packtes with high mineral content. White lines between the packets are highly mineralized cement lines. (Source: LBIO)

Techniques used for analysis at BSU level:

- quantitative Backscattered Electron Imaging (qBEI)
- Microradiography (MR)
- Synchrotron Radiation Micro Computer Tomography (SR-µCT)
- Electron induced X-ray Fluorescence Energy Dispersive X-ray analysis (ERF-EDX)
- Synchrotron induced X-ray Fluorescence micro Computer Tomography (SR-XRF µCT)

2.1.5. Bone Tissue / Trabeculae and Osteons (level 4)

The mature human bone tissue appears with two types of inner bone architecture, the cancellous and the cortical / compact bone, made by the BSUs as a result of a modeling and remodeling process throughout the entire lifetime of an individual. Cancellous bone is formed by plate and rod like trabecular features and forms a spongy like structure with a high porosity (>70%). The thickness of the struts in trabecular bone is fairly constant between one and three hundred micrometers (Fratzl and Weinkamer 2007) (Parisien et al. 1988; Han et al. 1996)

The trabeculae are interconnected in a honeycomb pattern, thereby providing maximum mechanical strength and ensuring resistance to compression stresses (Eriksen et al. 1994). Trabecular bone makes up the vertebral body and in the epiphyseal and metaphyseal region of long bones.

Cortical or compact bone is composed by osteons or haversian systems consisting of bone lamellae arranged in concentric layers along the long axis that surround a central canal containing nerves and blood vessels. The porosity of cortical bone is less then 10%. The cortical bone shell can reach a thickness between several tenths of a millimeter e.g. in vertrebrae, to several millimeters or even centimeters e.g. in the diaphysis of long bones. Cortical bone accounts for nearly 80% of the skeletal mass (Stein et al. 1999) and fulfills mainly protective and mechanical functions. It allows the body to withstand the forces of tension, torsion and compression due to its tight network-like structure of osteons.

Techniques used for analysis at tissue level:

- Light Microscopy (bright field, polarized light, fluorescence light), histological staining, tetracycline double labeling;
- quantitative Backscattered Electron Imaging (qBEI)
- Microradiography
- X-ray Micro Computer Tomography (µCT)

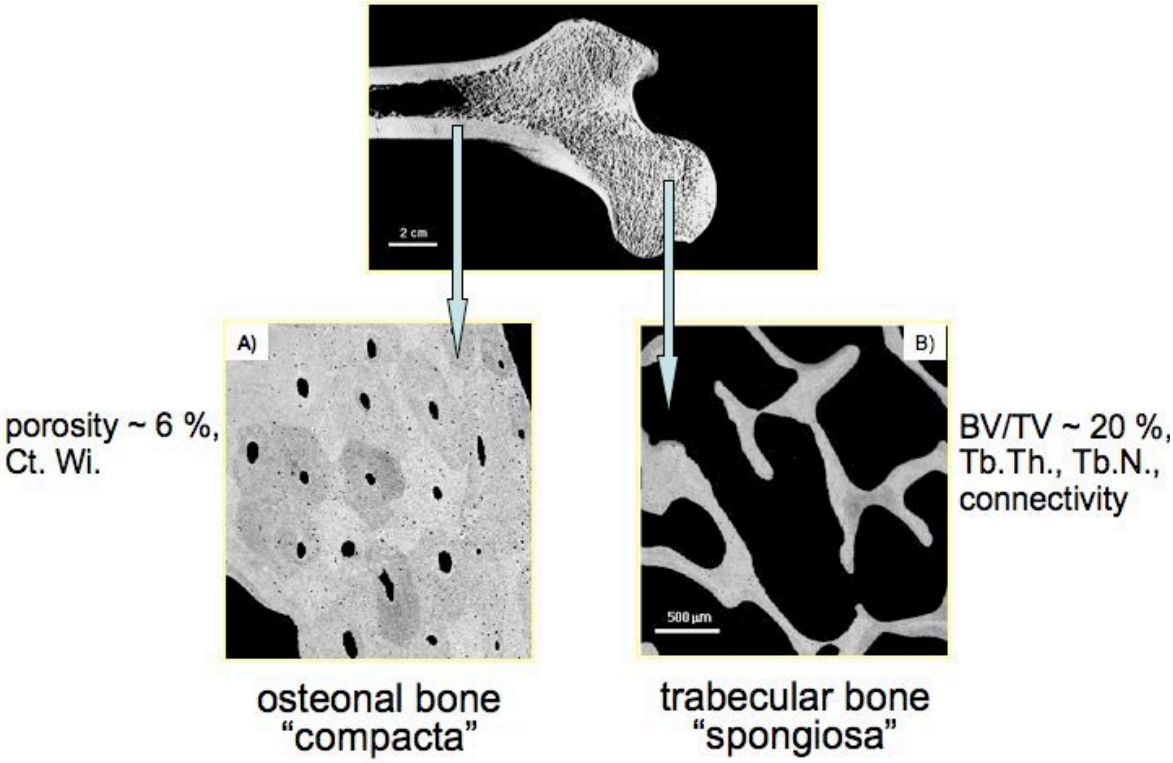

Figure 7: Level 4 – cortical and cancellous bone:
Longitudinal section of proximal human femur as overview and as details in higher magnification by backscattered electron imaging A) Cortical / compact bone: composed by osteons (central haversian canal surrounded by cylindrical arranged lamellar bone) and interstitial bone (old residual bone matrix). Structural parameters: porosity (<30%), Ct.Wi.= cortical width (~1mm) B) Trabeculae of cancellous bone (spongiosa). Structural parameters: BV/TV= bone volume per tissue volume (<70%), Tb.Th.= trabecular thickness (~120 µm), Tb.N.= trabecular number (~1.6/mm), Connectivity= degree of connection between trabeculae. (Source: LBIO)

2.1.6. Whole Bone (level 5)

In the human skeleton between three different shapes/types of bone can be distinguished:

1) *Plate-shaped bones* like skull bones, scapula, mandible and ilium;
2) *Long bones* like tibia, femur, humerus, etc.;
3) *Short bones*, like wrist, ankles and vertebrae.

The shape, outer geometry, size and inner architecture of these bone types are the result of embryonal bone development based on a combination of intramembranous and endochondral ossification. The bones are designed in strong relation to their mechanical function under the rule to achieve a maximum on strength with a minimum usage of bone material. Thus, flat bones consist of two compact bone layers, sandwiching a zone of cancellous bone in-between making a stiff and strong plate to protect e.g. the sensitive brain by the scull. The long bones of the human skeleton, such our limbs are built as tubes to withstand best the bending stress caused by different movements. The short bones like vertebrae are connected to form the spinal column. The thin cortex is filled with cancellous bone to make these bone not to heavy, but still can withstand high compression loads. Additionally, intervertebral cartilage disks act as shock absorber between the vertebrae.

Techniques used for analysis at organ level:

- Radiography
- Dual Energie X-ray Absorption (DXA)
- X-ray Computer Tomography (CT)
- peripheral quantitative Computer Tomography (pqCT)
- Nuclear Magnetic Resonance Imaging (NMR)

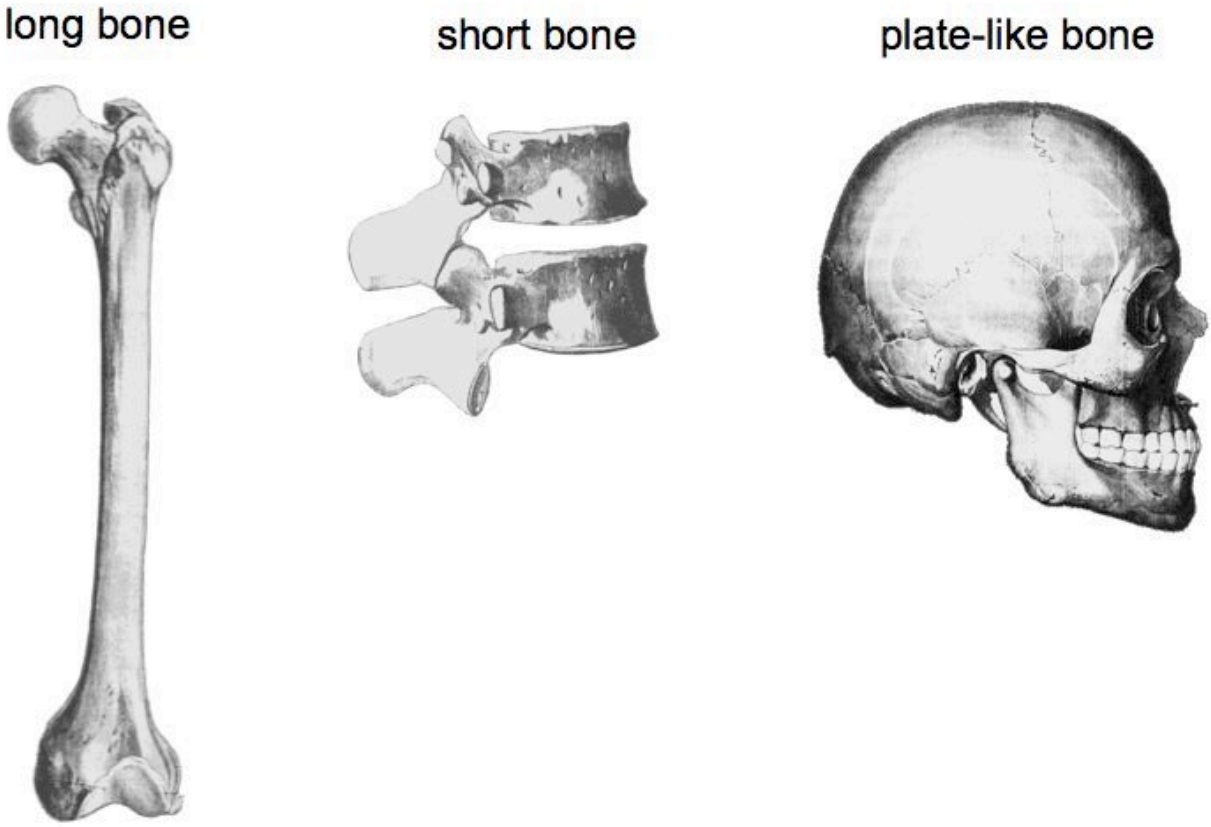

Figure 8: Level 5 - Wohle bone (geometry, shape, size):
The three different bone shapes: long bones e.g. femur; short bones e.g. vertebra;. plate-like bones e.g. skull.

2.2. Bone Cells

For the development and maintenance of bone essentially four different types of cells are engaged. The osteoblasts, the osteoclasts, the bone lining cells, which all are located on bone surfaces (inner and outer) and the osteocytes, which permeate the mineralized interior of the bone matrix (Marks and Hermey 1996). The main function of the osteoblasts is the production of new extracellular matrix, its apposition on the surface of bone motifs (trabeculae and haversian canals) and its controlled mineralization. The lining cells, which are covering the entire quiescent bone surface, are thought to control the access to the pure bone matrix at the bone surface, which is important for Ca-homeostasis and attachment of osteoblasts and osteoclasts. The osteoclasts are responsible for resorbing old bone matrix. The osteocytes are dispersed throughout the mineralized matrix and are interconnected to a network. It is assumed that they play a pivotal role in mechanosensing and Ca, P, homeostasis. In the adult skeleton, the osteocytes make up >90-95% of all bone cells compared with 4-6% osteoblasts and ~1-2% osteoclasts Bone (Bonewald and Johnson 2008) .The bone cells, which are responsible for bone formation, -repair and -remodeling respond to hormonal, mechanical and other extrinsic signals. Osteoblasts, osteocytes and bone lining cells originate from mesenchymal stem cells of the bone marrow, which differentiate over osteoprogenitor cells to preosteoblasts and then to mature osteoblasts. Osteoclasts originate from hematopoietic stem cells, which differentiate over mononuclear precursor cells to preosteoclasts and subsequently to multinucleated active osteoclasts.

2.2.1 Osteoblasts

Osteoblasts are large cuboidal cells (20 - 30 µm), responsible for the formation of osteoid, the unmineralized collagenous matrix of bone tissue (Fig. 9). Osteoblasts contain the normal basic ingredients of a cell – a single nucleus, endoplasmatic reticulum, well-developed Golgi bodies and numerous ribosomes and mitochondria – reflecting the requirement for abundant protein synthesis in

osteoid formation. These proteins include pro-α collagen (a basic component of collagen), osteocalcin (OC) and bone morphogenic protein (BMP). When human osteoblasts have completed their matrix forming function after an average lifespan of 1 to 10 weeks, approximately 50-70% die by apoptosis and 15% become transformed into bone lining cells or into osteocytes (Aubin and Liu 1996; Dempster 2006; Fernandez-Tresguerres-Hernandez-Gil et al. 2006a)

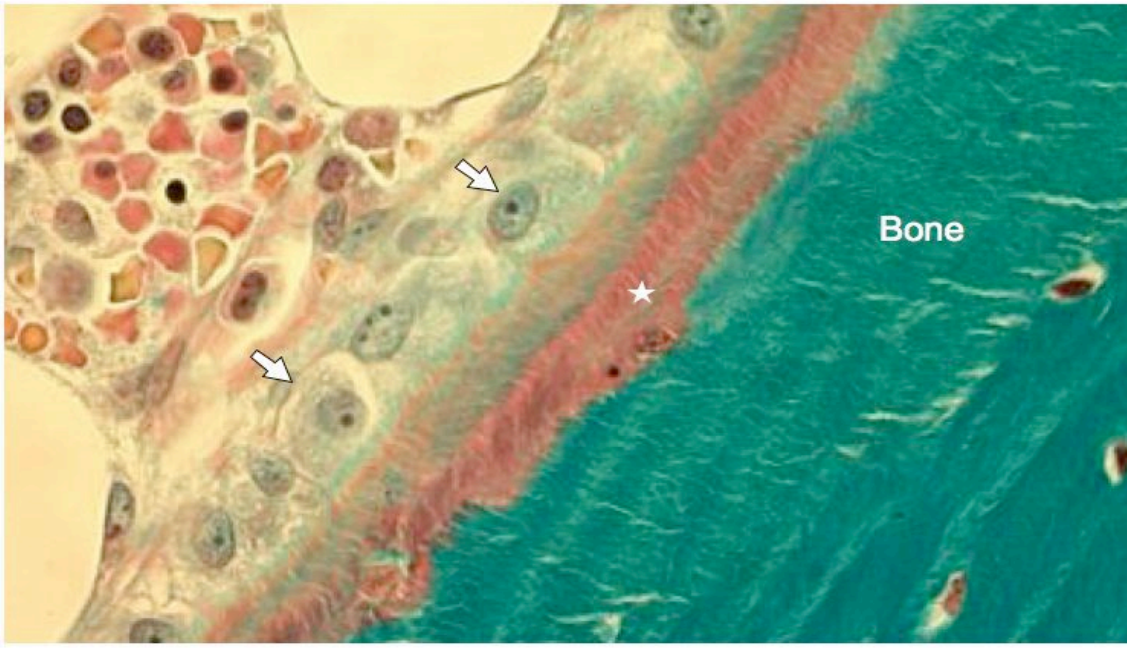

Figure 9: Light microscopic (LM) image of detail from trabecular bone: undecalcified bone section (3 µm thick) stained by Trichrome Goldner staining; white arrows indicate osteoblasts; white star designates the unmineralized osteoid seam (orange); mineralized bone (green).(Source: LBIO)

Cytokines which are involved in osteoblast differentiation are the Hedgehogs (Hh), bone morphogenic proteins (BMPs), transforming growth factor beta (TGF-β), parathyroid hormone (PTH) and WNTs. The activation of the transcription factor Runx2 (also known as Cbfa1) is a point of convergence of many involved signal transduction pathways. Runx2 is a master switch for osteoblast differentiation and regulate Osterix, a zinc finger-containing transcription factor, which is essential for bone formation.

Differentiation markers of osteoblasts are alkaline phosphatase (ALP), type I collagen (Col1), bone sialoprotein (BSP), osteopontin (OPN) and osteocalcin

(OC). ALP is used as an early marker, whereas OC is a late marker for osteoblast differentiation (Ortner and Turner-Walker 2003) (Krause et al. 2008).

The osteoblasts and the osteocytes communicate with each other by transmembran proteins or integrins, which act as a link between cells or between a cell and the extracellular matrix, allowing the passage of messengers such as calcium, cytokines and prostaglandins. In these cells the intercellular connection is Connexin 43.

The osteoblast functions are:

- synthesize the collagen and non-collageneous proteins of the organic bone matrix,
- direct the arrangement of the extracellular matrix fibrils,
- contribute to the mineralization of the osteoid material, due to alkaline phosphatase,
- mediate in the resorption carried out by the osteoclasts through the synthesis of specific cytokines and
- synthesize growth factors (Fernandez-Tresguerres-Hernandez-Gil et al. 2006a).

2.2.2 Osteoclasts

The osteoclast is a giant multinucleated bone resorbing cell, up to 100 μm in diameter with abundant mitochondria, numerous lysosomes and ribosomes. It derives from hematopoietic precursors of the monocyte/macrophage lineage. They are formed through fusion of mononuclear cells (Teitelbaum et al. 1997; Parfitt 1998; Teitelbaum and Ross 2003).

A large group of cytokines and colony-stimulating factors are involved in hematopoiesis and osteoclast development (Manolagas et al. 1996). This group includes the interleukins IL-1, IL-3, IL-6, IL-11, leukemia inhibitory factor (LIF), oncostatin M (OSM), ciliary neurotropic factor (CNTF), tumor necrosis factor (TNF), granulocyte macrophage-colony stimulating factor (GM-CSF), M-CSF

and c-kit ligand. As opposed to the previously mentioned cytokines they stimulate osteoclast development, IL-4, IL-10, IL-18 and interferon-γ inhibit osteoclast development (Manolagas 2000).

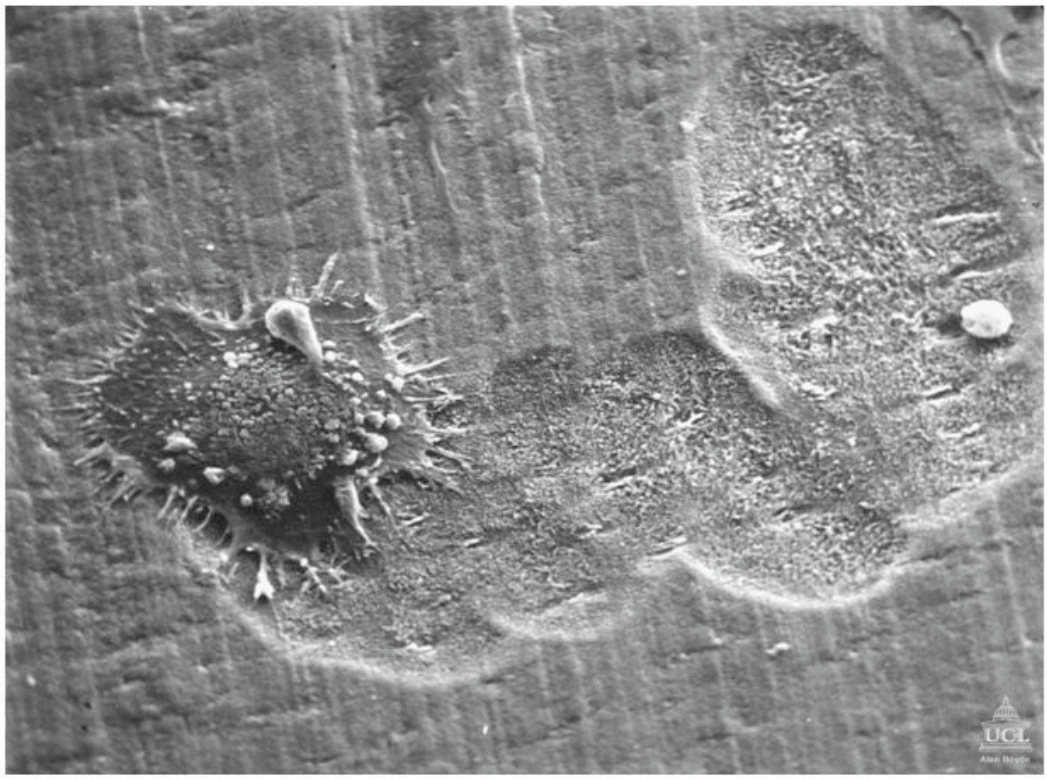

Figure 10: Secondary electron imaging in SEM of bone resorbing osteoclast with generation of resorption pits (resorption lacunae)
(Source: http://www.cdb.ucl.ac.uk/research/arnett/arnett_lab/index.html)

Mature osteoclasts are characterized by the presence of a ruffled border, which consists of a complex infolding of plasma membrane and a prominent cytoskeleton. Osteoclasts have abundant Golgi complexes, abundant mitochondria and transport vesicles loaded with lysosomal enzymes. The key to the resorption process is the capacity of the osteoclast to form a microenvironment between itself (ruffled border plus sealing zone) and the underlying bone matrix. This compartment is acidified by H^+-ATPase, an electrogenic proton pump and a chloride channel to a pH of ~4,5. The acidified milieu releases the mineralized constituent of bone, the hydroxyapatite, and exposes the organic bone matrix, mainly collagen type I, that is subsequently degraded by the lysosomal enzyme cathepsin K. The bone degradation

depends on physical intimacy between osteoclast and bone matrix (sealing zone) provided by integrins. Integrins are the principal cell/matrix attachment molecules, which mediate osteoclast/bone recognition (Ross 2008) (Hadjidakis and Androulakis 2006). After the resorption phase the osteoclasts detach itself from the bone resorbing surface and apoptosis occurs (Ortner and Turner-Walker 2003). The average lifespan of human osteoclasts is about 2 to 6 weeks (Frost 1963).

Coupling of osteoclast and osteoblast action: The number of osteoclasts and that of the osteoblasts have to be coupled to achieve the correct balance between bone formation and resorption. The osteoblasts are fundamental to the formation of osteoclasts because the macrophage colony-stimulating factor (M-CSF) produced by the osteoblasts is required in the early phases of osteoclastogenesis for the formation of giant multinucleate cells. The osteoclast differentiation from hematopoietic progenitor cells depends on activation of a receptor, called RANK (receptor activator of NFκB signaling), consistent with evidence that transcriptional regulation by NFκB is important for osteoclast development. Osteoblasts express on their surface RANKL, the ligand for RANK, a transmembran cytokine belonging to the TNF-family. The interaction between RANKL and its receptor RANK initiates osteoclastic activity and differentiation and increasing resorption. The effects of RANKL are inhibited by osteoprotegerin (OPG) a circulating protein belonging to the superfamily of TNF receptors. When OPG and RANKL bind together, the union between RANK and RANKL is inhibited and thus the osteoclastic differentiation is also inhibited. This shows that OPG, RANK and RANKL are important regulators of osteoclastogenesis (Fernandez-Tresguerres-Hernandez-Gil et al. 2006a) (Blair et al. 2007).

Most therapies for osteoporosis targeting inhibition of osteoclastic activity such as estrogens, selective estrogen receptor modulators (SERMs), bisphosphonates and calcitonin, are anticatabolic. They reduce bone loss by inhibiting bone resorption and bone remodeling.

A

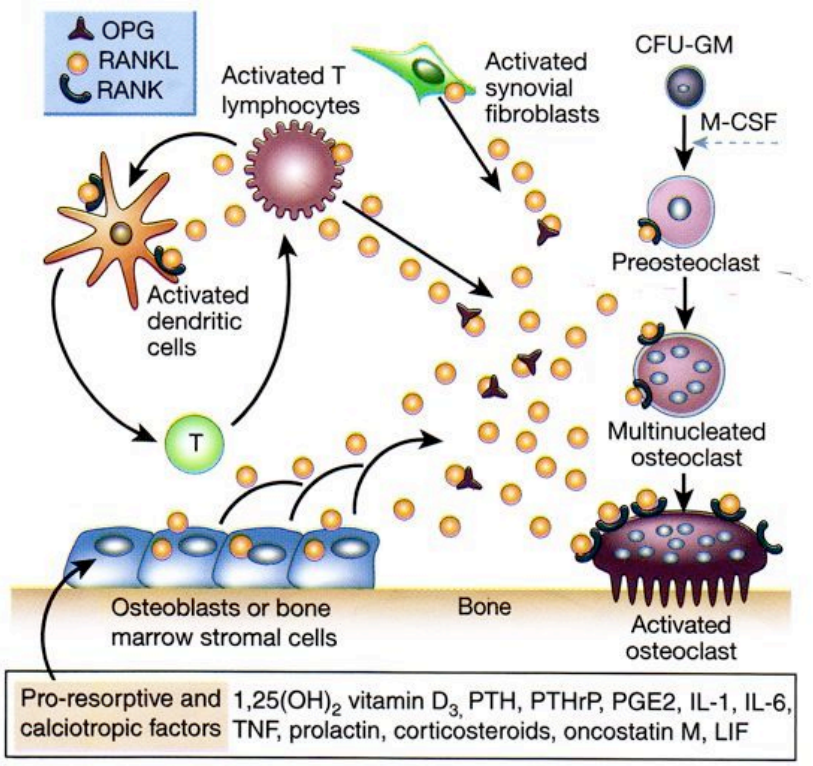

B

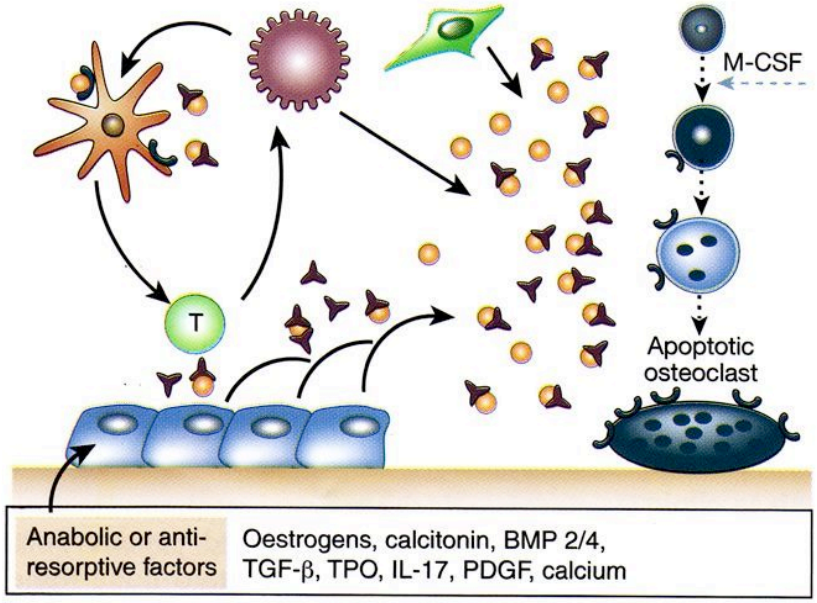

Figure 11: RANK Ligand (RANKL) is the primary mediator of the osteoclast formation, function and survival. A) OPG/RANKL ratio is low B) OPG/RANKL ratio is high. (After: Boyle et al. 2003).

2.2.3 Osteocytes

Some osteoblasts (15%) become trapped within the matrix and are transformed into osteocytes, when the bone matrix is mineralized. Therefore the osteocytes are located in the interior of the bone matrix. They are smaller than osteoblasts, but they have numerous dentritic cell processes. Protein-forming organelles are reduced, because they are not involved in matrix formation (Ortner and Turner-Walker 2003). The osteocytes comprise approximately 90% of all cells in mature bone (10 times the percentage of osteoblasts), they live in almond-shaped cavities / lacunae within the bone matrix, from which small channels, the so-called canaliculi are running radial into matrix carrying cytoplasmic extensions. A single osteocyte may typically have 50 – 70 such canaliculi. This network of canaliculi also permits the transport of nutrients, waste products and chemical signals between blood vessels and bone cells. They form a huge internal bone surface of 5.000 m^2, which is believed to have an important role in the calcium and phosphorus homeostasis. Recently, it has been established that they have an important function in the regulation of phosphate homeostasis. Therefore the osteocyte network may also function as an endocrine gland (Bonewald 2008). Osteocytes may live for several years before being replaced as part of the normal mechanism of bone remodeling (Ortner and Turner-Walker 2003) which may in some instances be stimulated by osteocyte apoptosis (Fernandez-Tresguerres-Hernandez-Gil et al. 2006a).

The control of bone remodeling, via detecting the mechanical variations of the loads, designated as mechanotransduction is believed to be crucial function of the osteocytes. The Sclerostin (SOST) gene encodes a protein, which is exclusively expressed in osteocytes in mineralized cortical and cancellous bone. SOST is a key regulator of bone formation (Lowik and van Bezooijen 2006; ten Dijke et al. 2008). The loss-of-function mutations of the SOST gene in humans were associated with sclerosteosis due to high bone mass. Bone biopsies from sclerosteosis and Van Buchem patients showed many more cuboidal osteoblasts than the normal control, which may be caused by increased Wnt signaling. SOST seems to be a negative regulator of osteoblast

development and bone formation. In vitro, SOST was found to inhibit BMP-induced osteoblast proliferation and differentiation, to suppress mineralization by osteoblastic cells and to stimulate osteoblast apoptosis. The SOST effects may exert by opposing the action of growth factors like BMP's and Wnts. The inhibition of SOST expression is an ideal candidate for a therapeutic agent. Patients with low bone mass, such as osteoporosis, SOST inhibition would lead to variable increases in bone mass without any unwanted skeletal effects (ten Dijke et al. 2008).

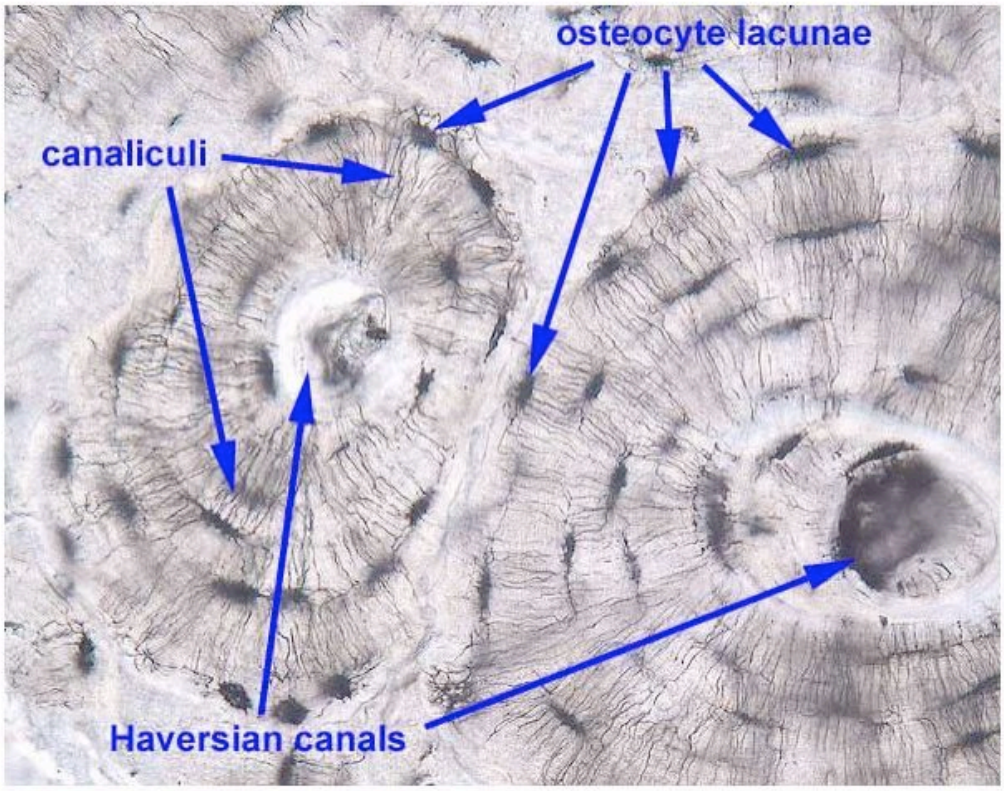

Figure 12: Light microscopic (LM) image of osteocytes network in the mineralized bone matrix (source: www.siumed.edu)..

2.2.4 Lining Cells

The quiescence bone surface is covered by a 1-2 µm thick layer of unmineralized collagen matrix, on top of which there is a layer of elongated and flat cells, called lining cells with spindle shaped nuclei and scarce organelles (Manolagas 2000). They can express *osteoblastic markers* such as bone sialoprotein, osteopontin, osteonectin and alkaline phosphatase, as well as parathyroid hormone receptor.

It is assumed that they play an important role to control the access of osteoclast to native bone matrix. Thus, the lining cells can secret collagenase, which removes the matrix before osteoclasts can attach to bone. Further, it has been shown that under certain circumstances, e.g. mechanical force or stimulation by PTH, bone lining cells can reconvert to osteoblasts. Another important function of the lining cells is to create specialized compartments on the surface of trabecular bone in which the remodeling process takes place. (Dempster 2006). (Manolagas 2000).

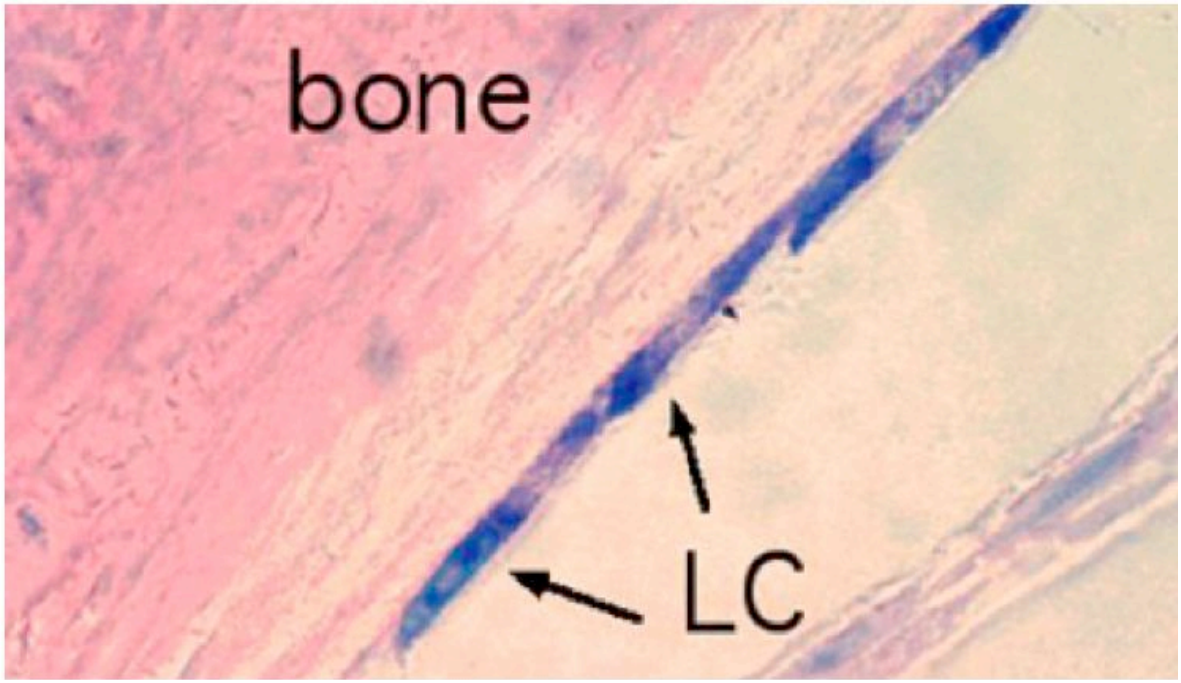

Figure 13: A light microscopic (LM) image of undecalcified trabecular bone section (3µm thick) stained by Giemsa staining: LC= lining cells (dark blue); dark pink= mineralized bone, light pink= osteoid (region adjacent to lining cells) (source: LBIO).

2.3. Bone Development, Growth and Maintenance

During embryonic development and growth of the skeleton 206 separate bones are formed. Between three principles in bone formation and its combination can be distinguished: a) intramembranous, b) endochondral ossification (Maes et al. 2007) and c) perichondral ossification.

2.3.1 Intramembranous Ossification

The bone is formed after a template of a dens membranous tissue of collagen bundels. A mesenchymal group of cells within a highly vascularized area of the embryonic tissue proliferates and differentiates directly into preosteoblasts and then into osteoblasts. These cells synthesize a characteristic bone matrix:

- it consists of collagen fibers which are not preferentially oriented, appear as irregular bundles and form a dense membranous tissue
- it includes a large number of osteocytes which are also larger in size
- its mineralization is delayed and does not proceed in an orderly fashion but in irregularly distributed patches, however reaches finally a higher level of mineral content than lamellar bone.
- these motifs of woven bone serves as scaffold on which primary lamellar bone is layed down. The primary bone is in the following replaced by secondary/remodeled lamellar bone (Baron 1999; Mackie et al. 2008).

Bones formed in this manner are the flat bones of the skull (calvaria bones and mandibles) and parts of the clavicles.

2.3.2. Endochondral Ossification

In contrast to intramembranous ossification, in endocortical ossification bone is formed by a cartilage template, like in short and long bones. Endochondral ossification starts that in centre of a cartilage template, e.g. vertebra. The

chondrocytes become hypertrophic and the cartilage matrix starts to mineralize. Simultaneously blood vessels are invading to the hypertrophic zone and osteoblasts and osteoclasts are accumulating. The osteoblasts lay down the first bone matrix on the mineralized cartilage motifs, while the osteoclasts are resorbing the mineralized matrix (bone and cartilage). Both processes together lead finally to a young trabecular bone, which further gets continuously (re)modeled.

2.3.3. Perichondral Ossification

This type of ossification is a kind of combination of intramembranous and endochrondal ossification and occurs in all long bones. The long bone is also formed after a cartilage template. The first ossification center is at the midshaft region of the diaphysis. From the surrounding perichondrium tissue osteoblasts start first to develop and to form a bone collar around the cartilage template by intramembranous ossification. Additionally, blood vessels and osteoclasts accumulate within the perichondrium, and subsequently invade to the underlying hypertrophic mineralizing cartilage region. Subsequently, the endochondral ossification process starts involving osteoblasts and osteoclasts.

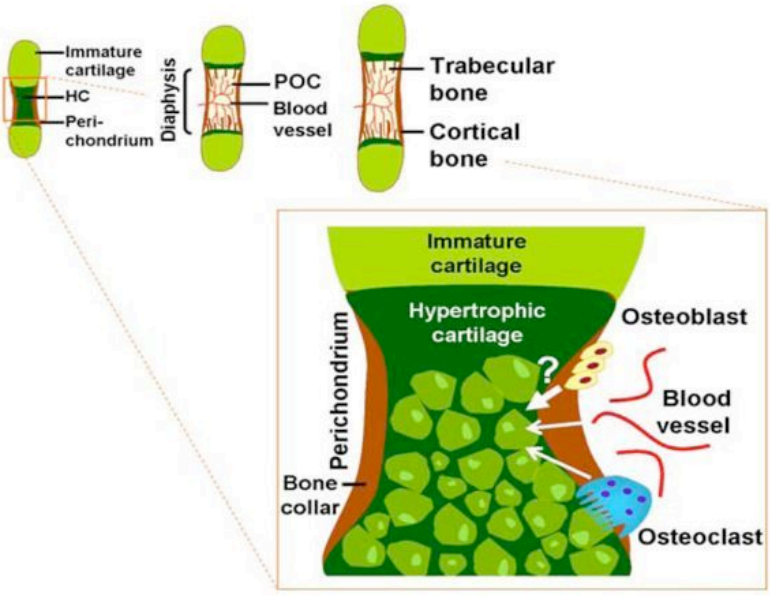

Figure 14: Early events during peri- and endochondral ossification of long bone: 1. Osteoblasts develop from the surrounding perichondrium at midshaft region and form a membranous bone collar. 2. Within the cartilageous scaffold chondrocytes differentiate into hypertrophic chondrocytes (HC) and the cartilage gets mineralized (start of primary ossification center). 3. Blood vessels and osteoclasts accumulate within the perichondrium and invade and erode the hypertrophic cartilage (endochondral ossification); formation of the primary ossification center (POC).(After: Maes 2007).

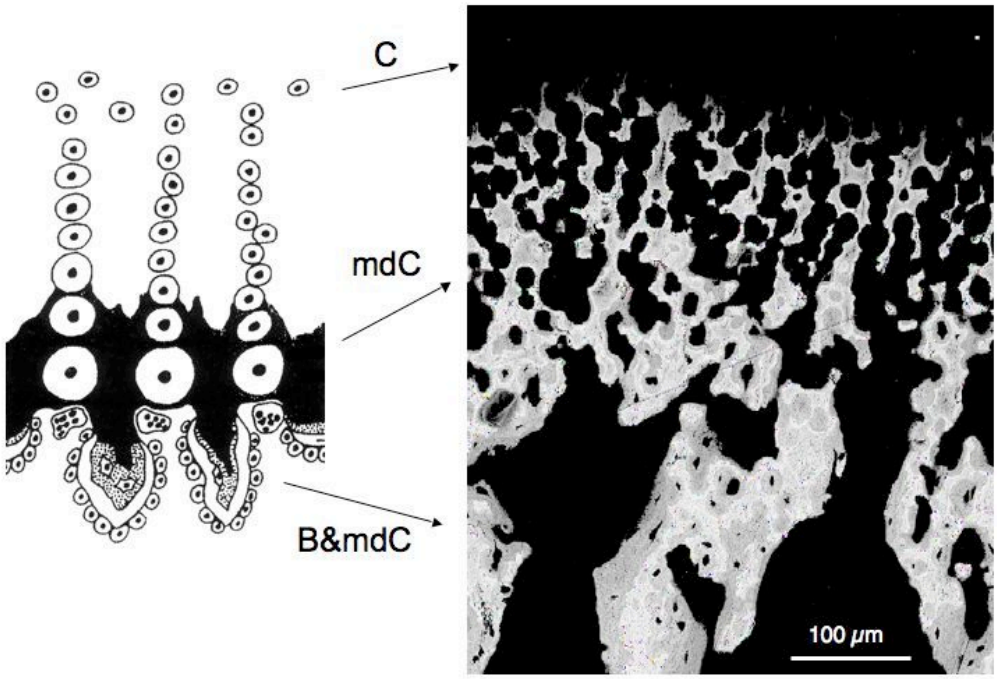

Figure 15:A Schematic of the zones of bone growth at the epiphyseal growth plate (left) and a backscattered electron image of the same region. ***C*** *= uncalcified growth cartilage,* ***mdC*** *= mineralized cartilage and* ***B&mdC*** *= Bone and mineralized cartilage (bone matrix dark gray, cartilage matrix light gray).(Source: LBIO).*

2.3.4. Growth of Bone

In general, the growth in size and/or length of bone is accomplished by cartilagous growth plates. At the periphery of this cartilage (the perichondrium), the mesenchymal cells continue to proliferate and differentiate. This process is called appositional growth. Deeper in this tissue the cells differentiate into prechondroblasts and then into chondroblasts. These cells secrete the cartilaginous matrix. Like the osteoblasts, the chondroblasts become embedded in their own matrix, where they lie in the chondrocyte lacunae as chondrocytes. In contrast to the osteocytes, the chondrocytes continue to proliferate for some time and form regular columns called isogenous groups. Subsequently, the chondrocytes enlarge progressively, become hypertrophic and apoptotic (Baron 1999). This zone of cartilaginous matrix starts to mineralize and gets ossified by endochondral ossification, which increases the dimension of bone.

2.3.5. Modeling / Remodeling

Bones are designed to optimally resist impacts by their functional activities. Thus, the tissue must be constantly reshaped and remodeled to adapt for changes in stress environment and to maintain its mechanical competence.

Modeling refers to new bone apposition of bone matrix on sites it has not been before, whereas remodeling refers to its replacement on surfaces previously containing bone (Boskey 2006). This means, that all growth of bone until adolescence and all adaptation to mechanical stress modeling processes are essentially involved too. In this situation the osteoblasts are working at forming sites apart not in close neighborhood with the osteoclasts as in remodeling. E.g. the process of growth in the diameter of the shaft is the result of a deposition of new bone beneath the periosteum that will continue throughout life. In this case, resorption does not immediately precede formation, but takes place in the endosteal region.

Bone remodeling occurs by removal of old bone (resorption) by osteoclasts, followed by new bone formation by osteoblasts. A key molecular regulator system of bone resorption are RANK, RANK ligand (RANKL) and osteoprotegerin (OPG) (Blair et al. 2007). The remodeling process allows bone to fulfill its structural and metabolic functions. Thus, bone is a dynamic tissue that accomplishes by constant resorption and formation

* the maintenance of bone tissue
* the repair of damaged tissue
* the homeostasis of the phosphocalcic metabolism.

Through this balanced phenomenon of remodeling, about 5% of cortical bone and 20% of trabecular bone, approximately 5 to 10% of total bone, are renewed per year. Cortical bone makes up 80% of the total volume, but the metabolic rate is 10 times lower, because the surface area to volume ratio is much smaller. Bone remodeling or bone turnover occurs throughout a person's life. The remodeling of each packet takes place in temporally constant cycles of 3-4 months, but differs for cortical and trabecular bone. Only up to the third decade the balance is positive, in the third decade of life, when bone mass has reached its maximum, the level is maintained with small variations until the age of 50. From this time on resorption predominates and the bone mass begins to decrease.

At the microscopic level, bone remodeling takes place in small areas of the intra -cortical and the trabecular surface, known as *basic multicellular units* (BMU). In cortical bone, the BMU moves through the bone matrix, excavating and replacing a tunnel. In trabecular bone, the BMU moves across the trabecular surface, excavating and replacing a trench (Manolagas 2000). Resorption always precedes formation and in the young skeleton the amount of resorbed bone is similar to the newly formed bone. The average lifespan of each remodeled unit in humans is 6-9 months, much longer than the lifespan of its executive cells [lifespan of osteoblasts (active) ~ 3 months, lifespan of osteoclasts ~ 2 weeks] of which the greater part is taken up by bone formation.

In a recurring sequence of 10 years the skeleton is completely renewed (Parfitt 1994; Fernandez-Tresguerres-Hernandez-Gil et al. 2006b).

The Remodeling Cycle:

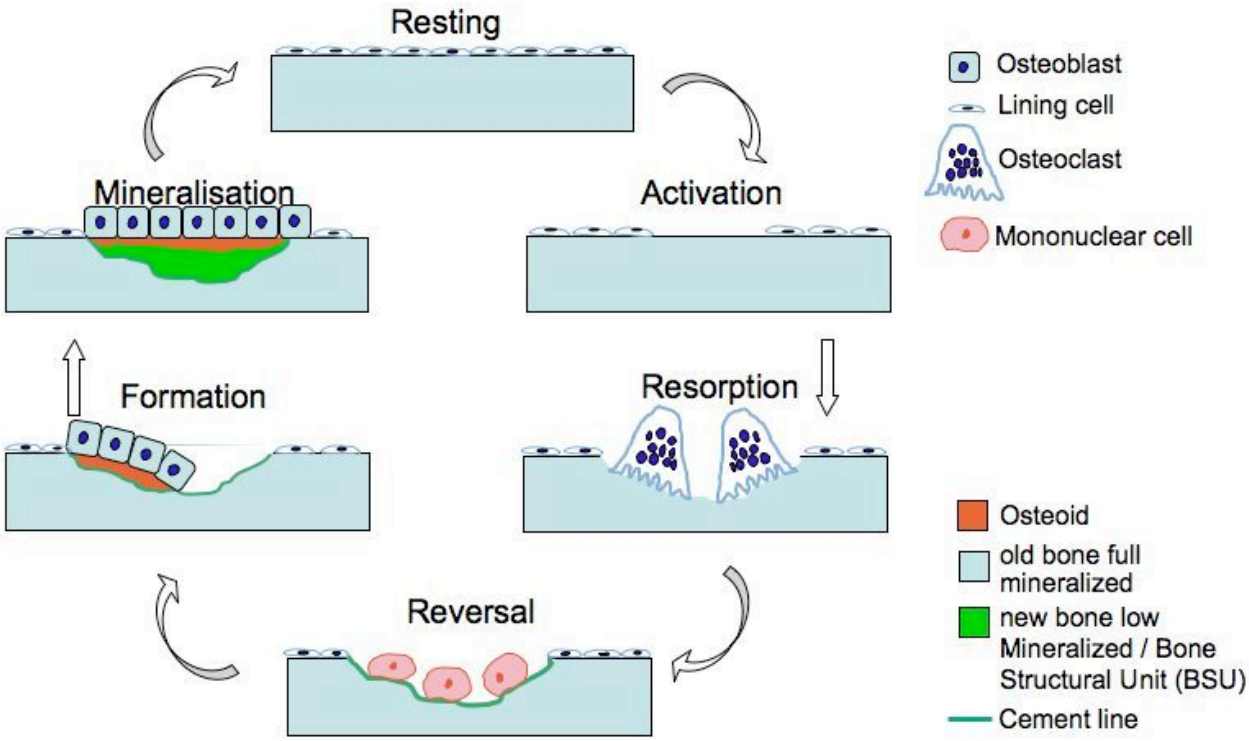

Figure 16: Bone remodeling cycle characterized by six phases

Bone remodeling can be divided into six different phases (Fig. 16).

1. Resting phase:

During this phase, no resorption or formation of bone takes place the lining cells are covering the bone surface.

2. Activation phase:

The process of activation involves retraction of lining cells and digestion of the endosteal membrane by collagenase action. The mineralized surface attracts the circulating osteoclasts coming from the nearby vessels. The osteoclast

formation, activation and activity are regulated by local cytokines (RANKL, Interleukins (IL1 und IL6), colony stimulating factors (CSF's) and systemic hormones (PTH, vitamin D, calcitonin) (Blair et al. 2007).

3. Resorption phase:

The osteoclasts begin to dissolve the mineral matrix and decompose the osteoid matrix. This process is completed by the macrophage and permits the release of the growth factors, transforming growth factor beta (TGF-β), platelet derived growth factor (PDGF) and insulin-like growth factor I and II (IGF-I, IGF-II).

4. Reversal phase:

After osteoclasts withdraw and or apoptosis the reversal phase, the first step in the repair process, starts. Not cleaned out collagen in the resorption lacuna is removed by specific mononuclear cells, which deposit a thin layer of proteoglycans to form the cement line. After this surface preparation, the formation of new bone is starting.

5. Formation phase:

The osteoblasts lay down unmineralized matrix (type 1 collagen) in a well organized way (lamellar fibril arrangement) into the resorption lacuna. This layer of new bone is called osteoid.

6. Mineralization phase:

After a certain maturation time the mineralization starts. The process is biphasic with an initial *fast* (primary mineralization) followed by a *slow* (secondary mineralization) phase. As more and more extracellular matrix is produced, some of the osteoblasts are implemented in the mineralized bone and become osteocytes. When the resorption space is filled osteoblasts become lining cells or die through apoptosis.

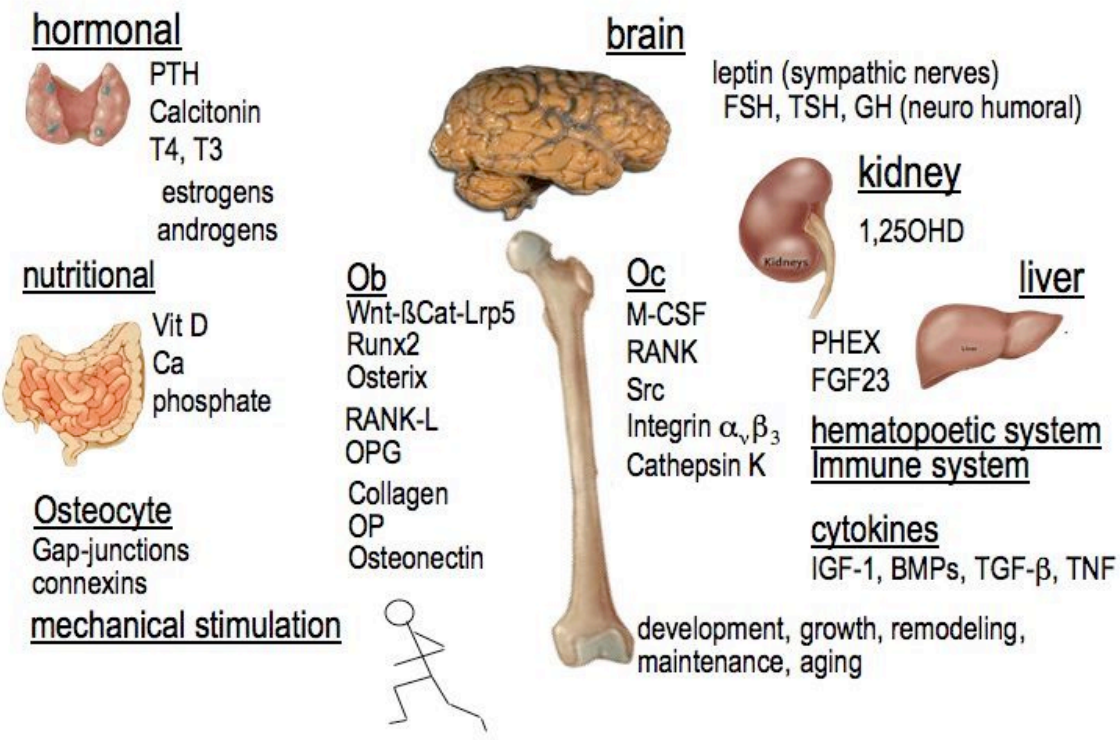

Figure17: Skeletal remodeling in health and disease. The skeletal maintenance is accomplished by multiple factors including hormonal, nutritional, cellular (osteocyte, osteoblast = Ob, osteoclast = Oc), hematopoetic system, brain, kidney, liver and mechanical stimulation (source: LBIO).

2.4. Bone Quality

The strength of bone is not determined only by its mass, but by its the structural and material properties. Thus, bone quality can be understood as an umbrella term that describes the set of characteristics for all hierarchical levels of bone that influences bone strength at a constant bone mass.

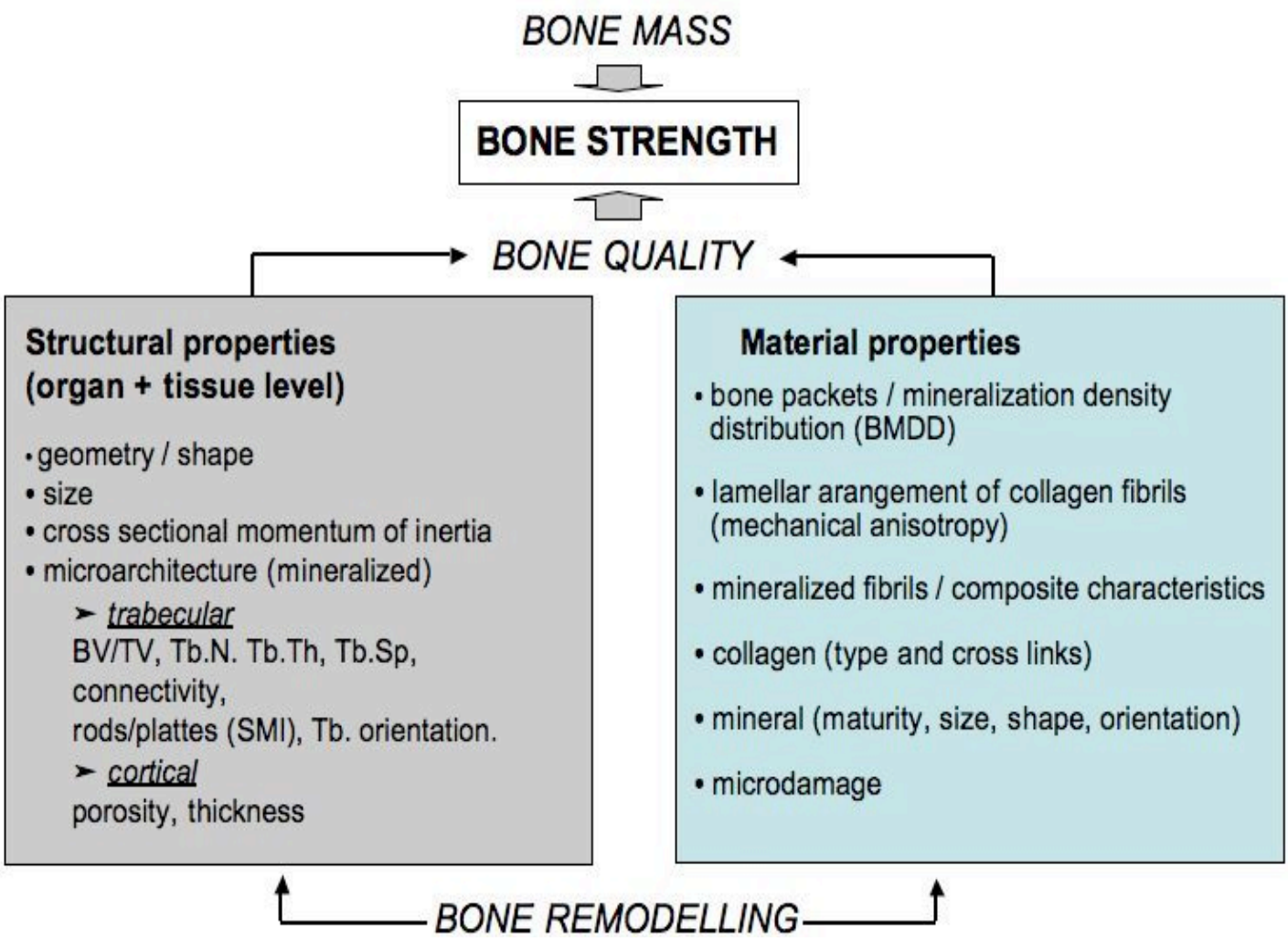

Figure 18: Bone quality framework – contribution to bone strength

3. MEASUREMENTS OF BONE MINERALIZATION PROFILES (BM-PROFILE)

3.1. Subjects and Diseases

Controls for Young individuals:

As controls served biopsies from individuals (n=13) (age, 2.1 to 20.8 yrs) without any sign of metabolic bone diseases. These biopsies were already used in previous studies (Roschger et al. 2008a; Fratzl-Zelman et al. 2009).

Controls for Adult individuals:

Transiliac biopsies from healthy premenopausal women (n=8) (premenopausal woman) used already in previous studies were employed for adult controls (Roschger et al. 2003)

Osteogenesis imperfecta (OI)*:*

OI type I is a genetic disorder associated with increased bone fragility. In the majority of patients, mutations affecting collagen type I can be attributed to the typical OI phenotype (Roschger et al. 2008a). One of the exceptions of OI where the altered collagen synthesis is not caused by a genetic mutation of collagen type I is OI type VII. This form of OI is caused by the posttranslational modification of the collagen in the extra cellular space due to CRTAP (cartilage-associated protein) mutations. CRTAP is a cofactor important for this process (Morello et al. 2006)

Biopsies from patients (n=5) (age 3.3 to 13 yrs) with **OI type I** (Roschger et al. 2008a) and **OI type VII** (n=4) (age 2.3 to 12,2 yrs) (Ward et al. 2002) were studied.

***Hypoparathyroidism**:*

Hypoparathyroidism (hypoPT) is a clinical disorder that usually appears when the parathyroid hormone (PTH) secretion by the parathyroid gland is decreased or insufficient to maintain extracellular fluid calcium in the normal range (Gotzman and Cole 2006).

PTH is an important regulator of the calcium- and phosphorus concentration in extracellular fluid. It is secreted from the parathyroid gland and the target cells are in bone, kidney and the small intestine (Benninghoff 1993). The three main effects of PTH are: 1. The mobilization of calcium from bone by stimulating the osteoclasts to reabsorb bone mineral and liberating calcium into blood. 2. The PTH stimulation of the process of calcium absorption from the small intestine, resulting in elevated blood levels of calcium. 3. The production of the active form of vitamin D in the kidney is stimulated through this process. The synthesis of a calcium-binding protein in intestinal epithelial cells, caused by vitamin D, for effective absorption of calcium into blood. The parathyroid hormone reduces the excretion of calcium in urine thereby conserving calcium in blood.

There are four reasons of hypoparathyroidism:

1) failure of parathyroid gland development
2) destruction of the parathyroid glands (removal by surgery)
3) reduced PTH production by altered parathyroid gland function
4) impaired PTH action.

Ad 1) Congenital agenesis of the parathyroid glands can produce hypoparathyroidism in the newborn child. Many cases with the DiGeorge phenotype are the result of de novo deletions, autosomal dominant inheritance is not uncommon and such families require detailed genetic examination Ad 2) In adults is surgical excision of the parathyroid glands the most common cause of hypoparathyroidism as a result of total thyroidectomy for thyroid cancer or repeated operations for primary hyperparathyroidism. Ad 3) The altered regulation of parathyroid gland function may be primary or secondary. Primary alterations of parathyroid gland secretion are most commonly caused by

activating mutations of the CaSR gene. These mutation decrease the set point for calcium, increase the sensitivity to extracellular fluid calcium concentration cause a functional hypoparathyroid state with hypocalcemia and hypercalciuria. The consequence of the activated parathyroid gland CaSR is chronic suppression of PTH secretion and the activated CaSR in kidney induces hypercalciuria that exacerbates the hypocalcemia (Gotzman and Cole 2006).

Young patients with CaSR (n=3) (age 13 to 22 yrs) (Theman et al. 2009), DiGeorge (n=2) (age 14 yrs) and idiopathic hypoPT (n=1) as well as adult patients with DiGeorge (n=1) and hypoPT by surgical removal PT gland (n=1) were investigated.

***Osteoporosis* - fragility and susceptibility to fractures:**

Osteoporosis has been defined by WHO in 1993 as “a systemic skeletal disease characterized by low bone mass and microarchitectural deterioration of bone tissue with a consequent increase in bone fragility and susceptibility to fracture” (*The American Journal of Medicine 1991;90:107-110).*

WHO working group (1994) defined BMD threshold for diagnosis of post menopausal osteoporosis (PMO) by DXA: Numbers of standard deviations below the young-adult mean value of BMD (ultimately called a “T-Score“) are used for classification: T-Score <= -2.5 osteoporosis

T-Score -1 to -2.5 osteopenia

However, a better definition of osteoporosis might be: Osteoporosis is the consequence of a stochastic process, that is, multiple genetic, physical, hormonal and nutritional factors acting alone or in concert to diminish skeletal integrity *R. Marcus (1996).*

The primary osteoporosis, which is heterogeneous in types, includes postmenopausal, senile osteoporosis and idiopathic osteoporosis. The term idiopathic osteoporosis is used for younger men and premenopausal woman with osteoporotic fragility fractures without identifiable secondary causes (Raisz 2008).

Transiliac bone biopsies from patients with postmenopausal osteoporotic women receiving Ca and Vit D (n=9) used already in previous studies were investigated (Meunier et al. 2004; Reginster et al. 2005).

Osteopetrosis:

Decreased bone turnover can also lead to skeletal abnormalities. There are several syndromes of osteopetrosis, in which bone resorption is defective because of impaired formation of osteoclasts or loss of osteoclast function (Pycnodysostosis) (Fratzl-Zelman et al. 2004). In this disorder, bone modeling as well as remodeling are impaired, and the architecture of the skeleton can be quite abnormal (increased bone volume and cortical thickness).

A transiliac bone biopsies from one patient with osteopetrosis was studied.

Osteonecrosis:

The disease osteonecrosis, also known as avascular necrosis, aseptic necrosis or ischemic necrosis of bone, is the necrosis of a bone segment, and is a result of temporary or permanent interruption of blood supply to the bone tissue.

Osteonecrotic femoral head bone tissue from patients (n=4) was investigated.

3.2. Sample Preparation

All bone samples were fixed in 70% ethanol, dehydrated in a series of ethanol, and embedded in polymethylmethacrylate. Sample blocks were trimmed using a low speed diamond saw (Isomet-R, Buehler Ltd. Lake Buff, IL, USA). Sectioned bone surfaces were sequentially grinded with sand paper with increasing grid number followed by polishing with diamond grains (size down to 0.25 microns) on hard polishing clothes by a PM5 Logitech instrument (Glasgow, Scotland). Finally the sample surface was carbon coated by vacuum evaporation with Agar SEM Carbon Coater, Agar Scientific Limited (Standsted, Essex, UK).

3.3. Quantitative Backscattered Electron Imaging (qBEI)

The validated technique of quantitative backscattered electron imaging (qBEI) allows the assessment of the degree of mineralization of polymethylmetacrylate (PMMA) embedded bone biopsies (Roschger et al. 1995; Roschger et al. 1998; Roschger 2003; Roschger et al. 2008a; Roschger et al. 2008b). The technique facilitates the description of the distribution and mean of weight percent calcium for cancellous and trabecular bone. Quantitative backscattered electron imaging is based on the visualization and quantification of bone matrix with its different degrees of mineralization, caused by bone packages of varying mineral content.

The sectioned plan-polished bone surface is scanned by an electron beam in a scanning electron microscope (SEM). Only the electrons backscattered with high energy from the sample surface are detected and used for the image generation. The intensity of the backscattered electrons (BE) is directly proportional to the atomic number of the sample material (Z-number contrast). Thus, in a mineralized tissue with calcium of an atomic number Z=20 and an organic matrix of Z~6, the calcium content is dominating the BE-signal and the grey levels in the BE-image have the meaning of Ca-content, bright reflects high and dark low Ca-content. In order to calibrate the BE-grey levels carbon (C, Z=6) and aluminum (Al, Z=13) were used as standards to calibrate the

microscope (Roschger et al. 1998). The grey levels of C and Al are adjusted always to 25 and 225, respectively, thus in all qBEI measurements the BE-grey levels are guaranteed to have the same physical meaning (a specific Z number).

For the qBEI imaging a scanning electron microscope (DSM 962, Zeiss, Oberkochen, Germany) equipped with a four quadrant semiconductor backscattered electron detector is used. The SEM is operated at 20 keV electron beam with a probe current of 110 pA. The working distance is maintained at 15 mm. The magnification is adjusted to a 50x nominal resulting with a resolution of 4 microns/pixel, so fare the BMDD of the bone sample is measured. However, for the BM-profiles, the ROI is imaged with a nominal magnification of 400x corresponding to 0.5 microns/pixel. The areas are scanned with a speed of 100 sec/frame, generated by a single frame.

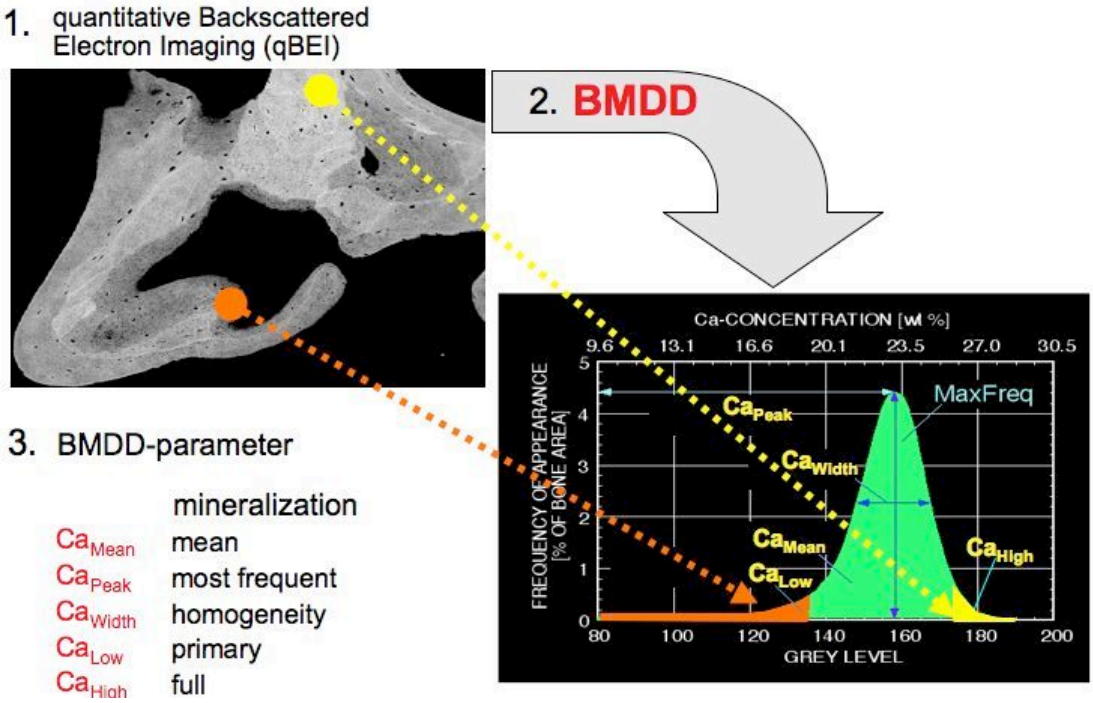

Figure 19: Quantitative backscattered electron imaging method to assess the bone mineralization density distribution (BMDD): 1. Acquirement of calibrated backscattered electron images in SEM. 2. Derivation of grey-level histograms (BMDD) describing the frequency of appearance of a certain mineral concentration throughout the bone area, which is the product of remodeling and kinetics of matrix mineralization. 3. Calculation of five BMDD parameters for characterization of the BMDD curve: Ca_{MEAN}, Ca_{PEAK}, Ca_{WIDTH}, Ca_{LOW} and Ca_{HIGH}.(Source: LBIO).

Using methods of digital image processing and analysis (NIH Image 1.63, National Institute of Health, USA) grey-level histograms (frequency distributions) are derived from the BE-images and transferred to bone mineralization density distribution (BMDD). To be able to quantify differences in the BMDD histograms and to make statistical analyses, five parameters have been established: Ca_{MEAN}, Ca_{PEAK}, Ca_{WIDTH}, Ca_{LOW}, Ca_{HIGH} (Roschger et al. 1998; Roschger et al. 2008b).

1. Ca_{MEAN}, is the weighted average Ca concentration of the mineralized bone area, obtained from the integrated area under the BMDD curve.

2. Ca_{PEAK}, is the most frequently measured wt% Ca of bone area, indicated by the peak position of the BMDD histogram.

3. Ca_{WIDTH}, measures the heterogeneity of mineralization, caused by the co-existence of bone packets with different degrees of mineralization. It is obtained by evaluating the width at half-maximum of the BMDD histogram.

4. Ca_{LOW}, is the amount (%) of bone area with a lower degree of mineralization than the value at the 5^{th} percentile of the reference BMDD, which was found to be lower than 17,68wt% Ca. Ca_{LOW} represents the amount of bone in the range of calcium concentration, which is achieved during primary mineralization (Misof et al. 2003).

5. Ca_{HIGH} indicates the % bone area exhibiting a Ca concentration above the 95^{th} percentile value of the reference BMDD, which was found to be higher than 25.30wt% Ca. It indicates fully mineralized mainly interstitial bone. A remarkable small biological variation in BMDD was found in healthy adult human trabecular bone (Roschger et al. 2008b). BMDD was independent of the skeletal sites studied, ie.: iliac crest, vertebrae, patella, femoral head and femoral neck, as well as independent of age (25 to 90 years) and ethnic origin (caucasian and afro-american) (Roschger et al. 2003). Thus a single reference BMDD for adults could be introduced (Fig. 20)

The measurements of BM-profiles are performed along lines with 4 pixels in widths perpendicular to the mineralizing front across the BSU with a step size of 0.5 µm. The pixel grey-level or the corresponding Ca-content values (Fig. 23) are plotted vs the depth into the forming BSU.

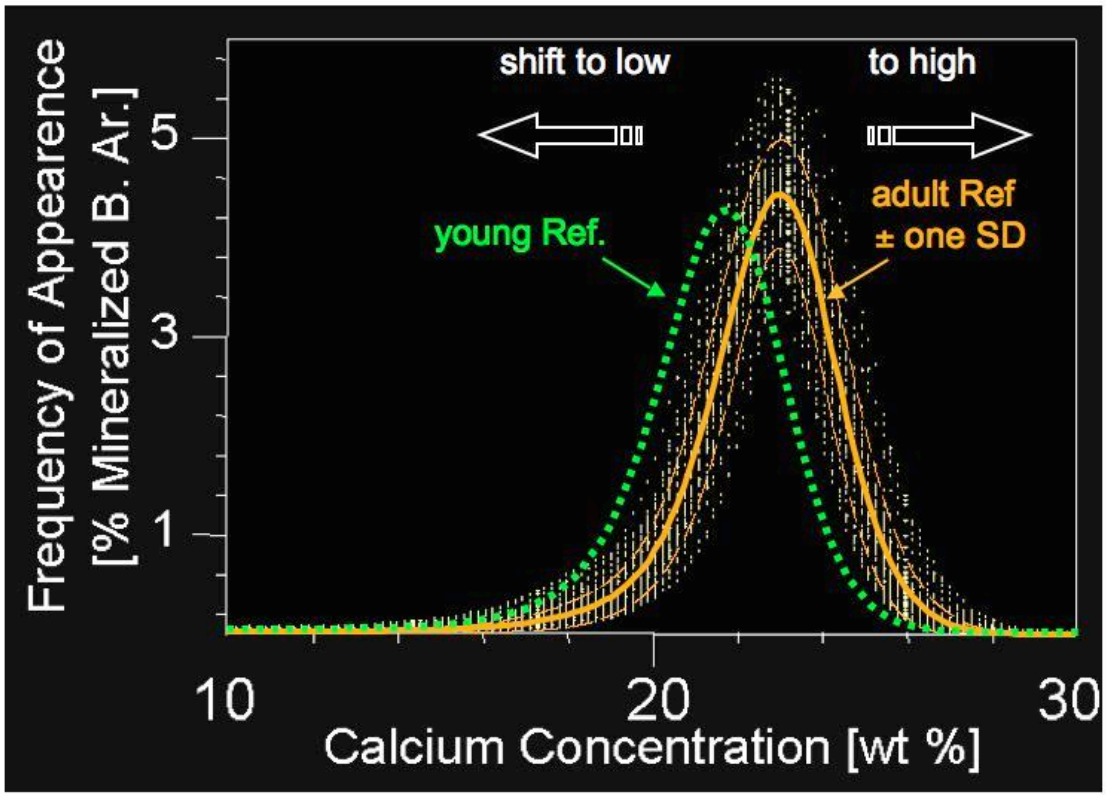

Figure 20: Reference data for bone mineralization density distributions (BMDD) of a trabecular bone for a young and an adult reference collective (see appendix). (After: Roschger et al. 2003; Roschger et al. 2008b; Fratzl-Zelman et al. 2009)

3.4. Region of Interest (ROI) - Forming BSU

During the remodeling cycle (phase 5, Fig. 16) new bone matrix (osteoid) is continuously formed by osteoblasts After a lag time the osteoid becomes mineralized following a certain time course. In a forming BSU at least three fronts are moving with a synchronized speed in the direction to the bone marrow space: 1) The coordinated action seam of osteoblasts 2) the surface of new synthesized collagen, 3) the mineralization front (Fig. 21). For this reason a histological section of such a BSU includes all phases of bone formation in a spatial sequence (Fig. 22). In consequence, the increasing Ca-content of the collagen matrix in such forming BSU reveals information about the phases and kinetics of the mineralization process.

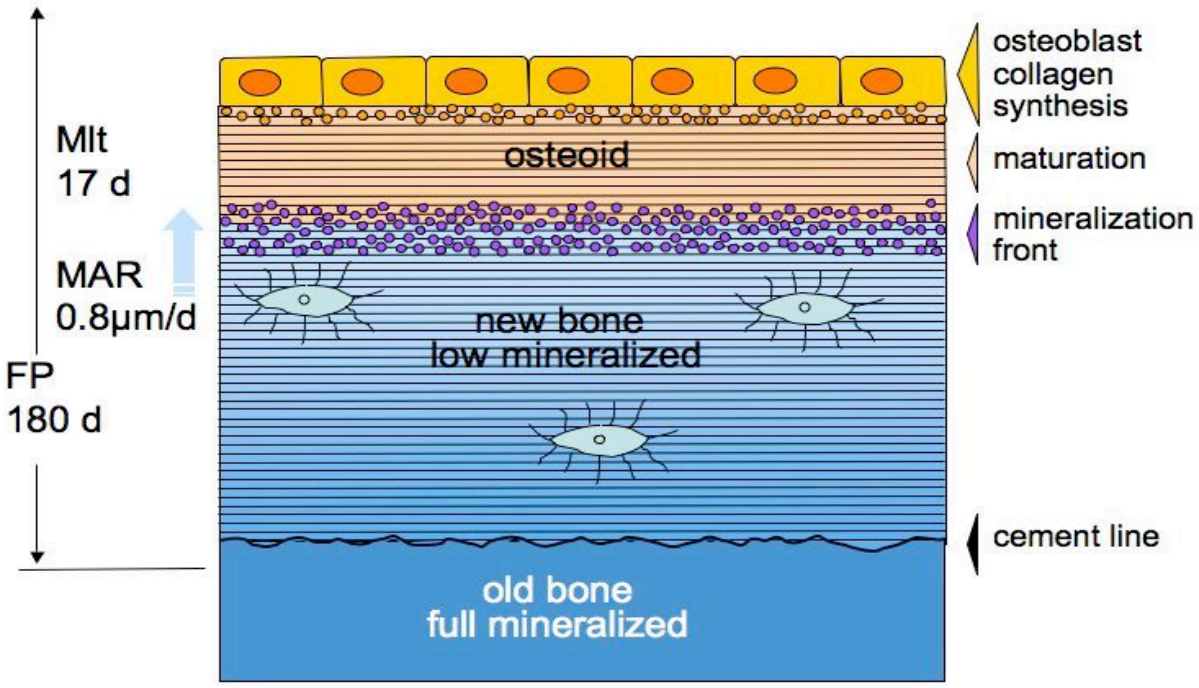

Figure 21: Sketch of a forming basic structural unit: The osteoblasts secrete collagenous matrix material (osteoid), which mineralizes after a certain mineralization lag time (Mlt). Throughout the mineralization front the mineralization starts with formation of nucleation centers. The mineralization front is moving in the direction of the osteoid with a certain speed, the mineral apposition rate (MAR). The new bone matrix is mineralized rapidly up to 70% of final mineralization. The whole forming period (FP) of a BSU is about 180 days.

Osteoid: In this zone new bone matrix not yet mineralized is found. The seam of osteoblasts on the surface of the forming BSU synthesis mainly procollagen, which is then secreted in the extra celluar space. After some extra cellular modification and self-assembling processes of the collagen molecules type I collagen fibrils are arranged in a lamellar way. Additionally, other non-collagenous proteins are incorporated in the extracellular matrix like, such as osteonectin, osteopontin, osteocalcin, bone sialoprotein, proteoglycans, phosphoproteins and proteolipids. The osteoblasts express a characteristic enzyme, the alkaline phosphatase (ALP), which plays an important role in the subsequent mineralization of the matrix. The front of osteoid is moving this way about 0.6 to 1 µm per day. Characteristically, the new osteoid matrix is not mineralized immediately but after a certain lag time of about 13 days. This means, that an osteoid seam of about 7 µm in thickness is generated between the osteoblasts and the mineralization front. It can be speculated, that this

spatial distance to the osteoblast seam is needed, because of the toxic extracellular concentration of calcium present in the mineralization zone. Moreover, a certain time for the maturation in the collagenous matrix, like cross linking and fibril modification, seems to be a prerequisite of matrix mineralization.

Mineralization Front: In this zone the mineral content is rapidly increasing from zero to a first plateau level. The underlying mechanism of initiation and progress in mineralization of osteoid is not yet fully understood. The mineralization of the collagen matrix is a highly controlled process, affected by the cross-link profile and regulated by non-collagenous proteins (NCP), which are found in the organic bone matrix. It is widely accepted, that the mineralization starts in the gap zones (Landis et al. 1996) by seeding/formation of nucleation centers followed by an rapid growth of the mineral crystals. Most likely the rapid initial growth of the crystals occur first predominantly in two dimensions (thin plates) and the bone matrix reaches the first plateau of mineralization (30% below final value) within few days (primary mineralization). Thereby the crystals are extending in the overlap zones of the collagen and form a staggered/overlapping parallel arrangement of the mineral plates (Fig. 4) of 2-4 nm thick plate like aggregates within the fibril (Gao et al. 2003). Thereby the mineralization front is moving towards the osteoid or osteoblast seam with about 0.6 to 1.0 µm per day. The so called mineral apposition rate (MAR) is measured by fluorescence double labeling of the mineralization front. For this purpose the patient receives twice tetracycline (with about 12 days between first and second dose) shortly before biopsy. Two fluorescence bands in the biopsy section mark then the progress of the mineralization front within 12 days.

Bone Matrix of Young BSU: In the zone behind the mineralization front the bone matrix increases its mineral content by a second phase of mineralization. In this phase mainly the thickness of the mineral plates is increasing (secondary mineralization) (Roschger et al. 2001; Fratzl et al. 2004a), which lasts in a time scale of months and years. In this phase of mineralization the mineralization of the bone matrix may extend also to the extra fibrilar space. Moreover, the

organic phase (cross-links) and the mineral crystals (calcium ion substitution - carbonation) are undergoing a chemical maturation process.

Cement Line/Surface: During the bone remodeling cycle, after bone resorption of osteoclasts has stopped, a thin highly mineralized layer of proteoglycans and non-collagenous proteins (NCP) is laid down on the bone surface where resorption took place (reversal phase, see. Fig. 6 and 16). It is assumed that this layer provides a contact surface for the new bone matrix and may act as a glue. In general, the lamellar orientation is changing at the cement line between the old and the new bone packet.

3.5. Analysis of BM-Profiles

Identification of a forming BSU: The forming BSUs had to be identified on the block section of trabecular or cortical bone only by criteria which the qBEI method is providing. Though the qBEI method is in principle only showing a material contrast (Ca-content) and not any histological details like osteoblast, osteoid or fluorescence double labeling bands (Fig. 26), clear criteria had to be found for the routinely identification of a forming BSU in the BE-image (demonstrated in Fig. 23). The criteria, which were sufficient for the selection for BM-profiles were:

1) The BSU had to be on the bone surface and was carrying a well defined wide dark surface seam.
2) Additionally the BSU showed evidence of an osteoid seam, which could be distinguished from embedding medium just yet by its material contrast in the BE-image (Fig. 20).

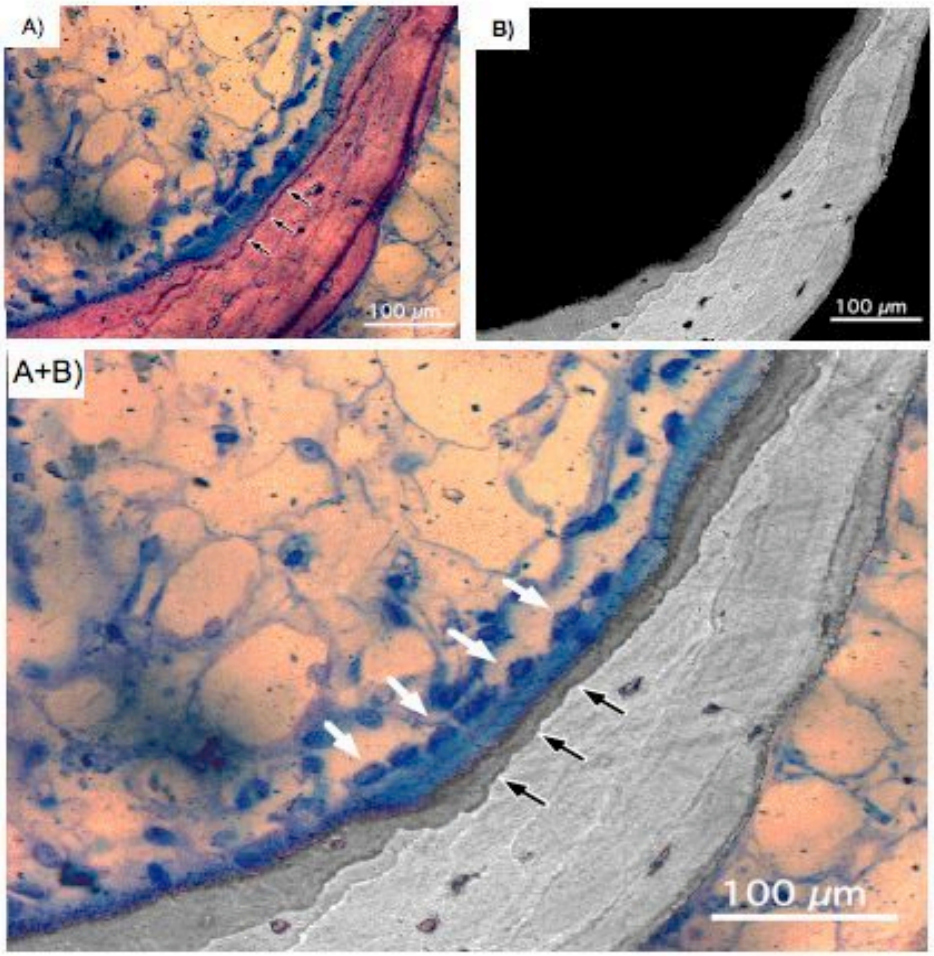

Figure 22: Identification of forming BSU: (A) Light microscopic (LM) image of a histological section shows a forming BSU stained by Giemsa staining: Pink= old mineralized bone packet; light blue= Osteoid; dark blue cellular motifs= osteoblasts. Black arrows indicate the cement line of the bone packet. (B) qBEI image of identical area of (A) showing only the mineralized part of the bone tissue. (A+B) Combination of the LM and the qBEI image: the forming BSU is characterized by a seam of osteoblasts (white arrows) followed by osteoid and an adjacent region of low mineralized bone (dark grey), the mineralization front. Black arrows indicate the cement line between forming and preexisting bone packet, source LBIO.

Selecting Lines for BM-Profile analysis: The BSUs classified as forming tissue regions (ROI) were imaged by qBEI method using a pixel resolution of 0.5 µm per pixel. Then using digital imaging processing and analysis methods a tool for generating profiles were applied (NIH Image 1.63, National Institute of Health, USA): a) Straight line areas 4 pixel wide were drawn in the digital image by "straight line" tool starting in the osteoid or embedding medium, perpendicular to the mineralizing front and ending in the adjacent old BSU (Fig.23).

b) Then the analyze mode "plot profile" was activated, which was providing the pairs of plot data. The x-axis was indicating the distances/positions along the line in steps of 0.5 µm (Fig.24). The y-axis was showing the corresponding Ca-content values to each single line position.

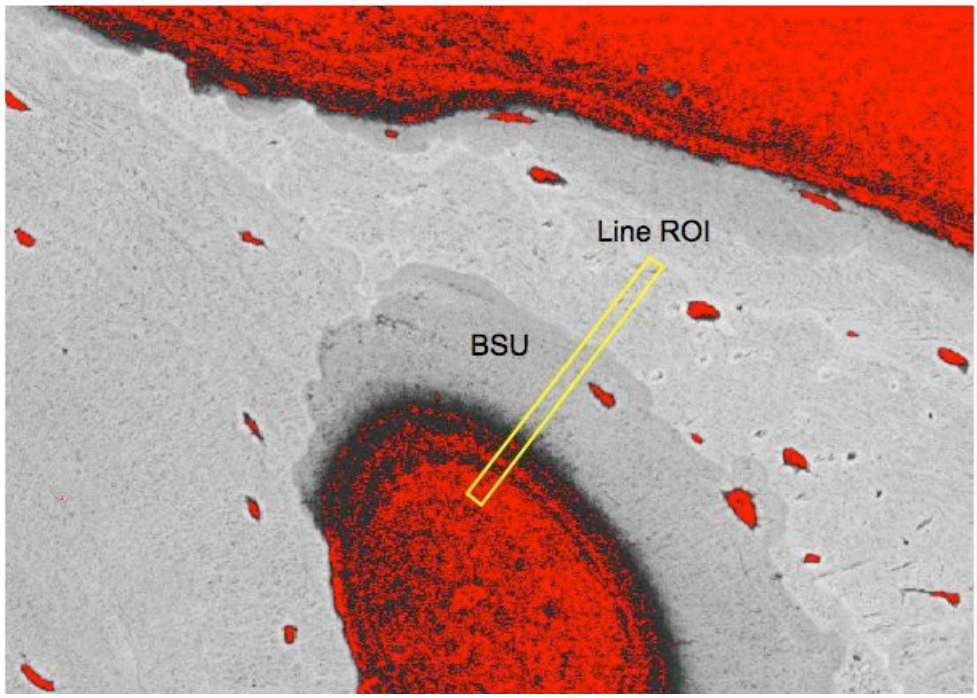

Figure 23: Measurements of bone mineralization profiles (BM-profiles): 1. qBEI images with a pixel resolution of 0.5µm x 0.5 µm were performed from forming BSU: Forming BSU is identified by its dark rim of low mineralized bone matrix. By use of density slice (red colour) the presence of osteoid is visualized. 2. Lines (4 pixels wide) were drawn perpendicular to the mineralization front for the determination of BM-profiles (source: LBIO).

The Ca content was calculated from the average grey level resulting from the four "line pixels" at each position. The reason to use a line width of four pixels instead of only one was to reduce the effect of the signal noise due to counting statistics by signal averaging. Thus, the line profile became less noisy.

Determination of the Transition Point Ca_{TURN}: The obtained plots of calcium (Ca) content and line position were analyzed by linear curve fitting in two regions of the data (Fig. 24):

1) The first line started at the beginning of the mineralization front (steep rising Ca content) and ended before the Ca values reached a plateau.

2) The second line started at the beginning of the plateau (flat rising Ca values) and ended before the profile line reached the adjacent old BSU. In cases of short plateau regions e. g. in very young forming BSU or disturbances in the bone matrix (osteocyte lacunae, non uniform fibril arrangement), the second line fit was replaced by a horizontal line through the mean of the corresponding data points.

3) The intersection of the two linear fits defined the Ca value (value at the y-axis) where the fast mineralization process was changing to the slow mineralization process designated by us as "Ca_{TURN}" (Roschger et al. 2008a; Roschger et al. 2008b). Fig. 24 is demonstrating an example for the variation in Ca_{TURN} data as obtained within an individual (male, 8.8 yrs) by multiple BM-profile measurements (n=47).

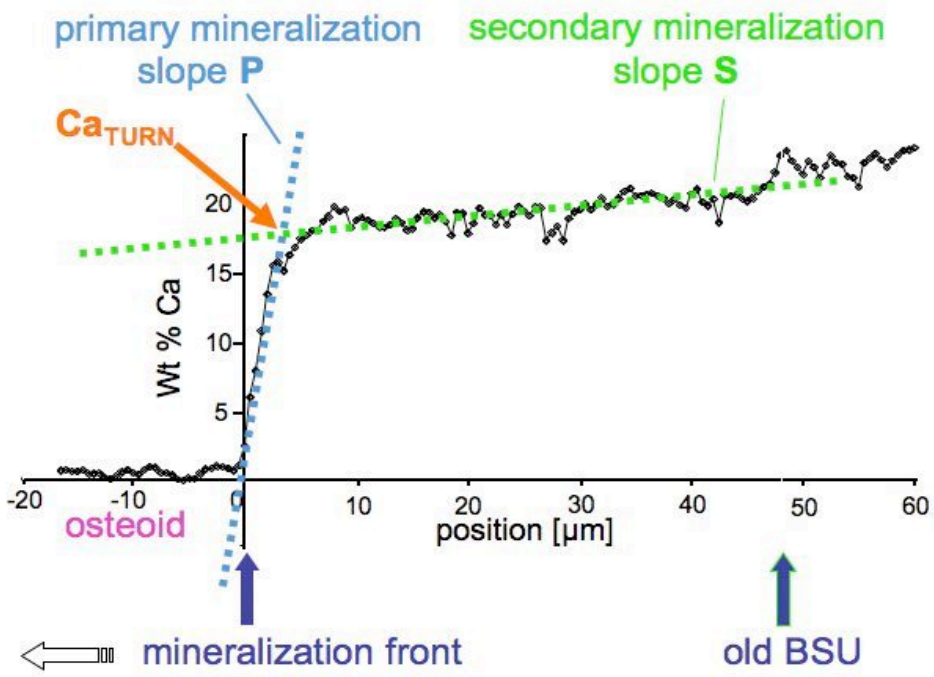

Figure 24: BM-profile as measured by qBEI - evaluation of Ca_{TURN}:
X-axis = position of measurement (distance to the mineralization front) with a step size 0.5 µm. Y-axis = corresponding calcium content in weight %. 1. Characterization of BM-profile by two linear fits: initial steep slope (P) (primary mineralization) followed by flat slope (S) (secondary mineralization). 2. Determination of the transition point Ca_{TURN} by the intersection of both linear line fits characterizing the transition from a fast to a slow mineralization process.

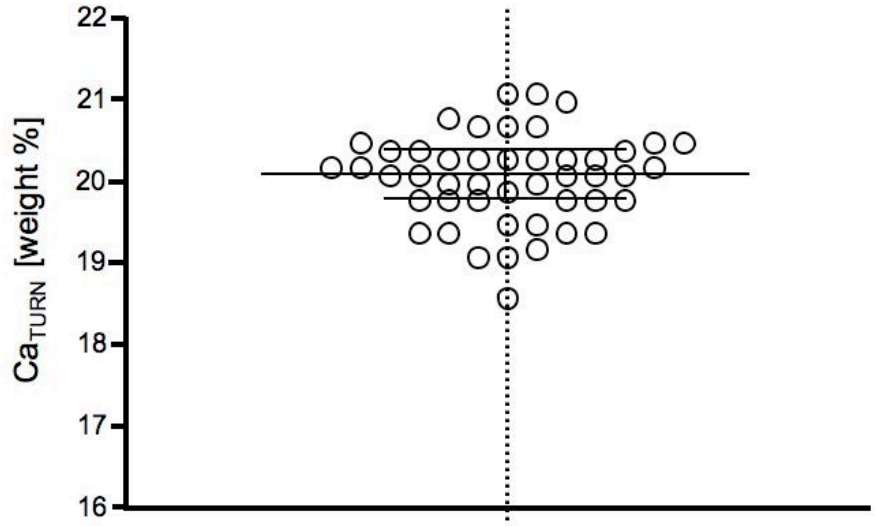

Figure 25: Example of CaTURN measurement: Scatter plot of CaTURN data from a 8.8 years old healthy boy (control) generated by evaluation of 47 line profiles of five different BSUs in a transiliac biopsy. Median [25% ; 75%] = 20,1 [19,8 ; 20,4].

Introduction of a Time Scale to the BM-Profile:

In principle the BM-profile analysis in the forming BSU gives only spatial information of mineral content of matrix volume elements along a line perpendicular the mineralization front, but does not directly provide any information about the temporal development of the mineral content of a single volume element of bone matrix. However, the forming BSU with its progressing mineralization front displays the time course of mineralization by different bone matrix volume elements as sequence of increasing distance to the mineralization front (Fig. 24).

Fluorescence labeling technique:

Bone biopsy samples are usually fluorescence labeled in a specific manner: intake of tetracycline e.g. first label - tetracycline (green) thrice-daily dosage/three days, wait of 12 days; second label - declomycin (yellow) twice-daily/three days, wait for 5 days, then performance of biopsy. Since the tetracycline binds selectively to the newly formed bone matrix (matrix at the mineralization front) two fluorescent bands are generated which can be identified by fluorescence microscopy. The distance between the fluorescent

bands is a measure how much the mineralizing front was moved forward within 12 days. This progress of the mineralization front per day averaged over the entire biopsy sample is called the mineral apposition rate (MAR) one of the primary parameters of dynamic bone formation in histomorphometry. In consequence, for a first estimate, the distances to the mineralization front can be transferred into a sequence of time points of mineralization, assuming that the mineralization front moves with a constant speed within the BSU.

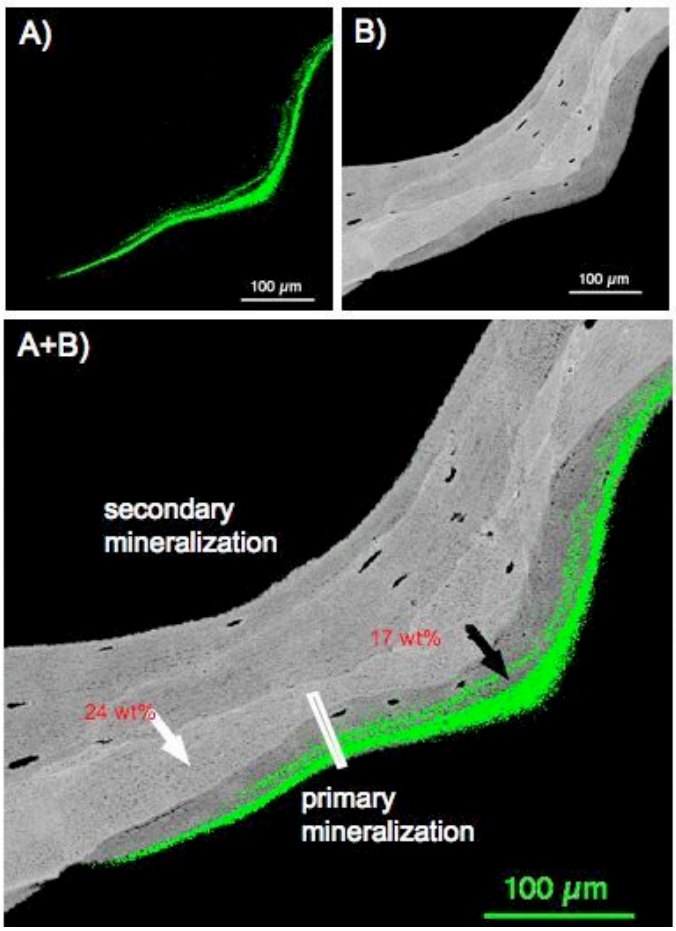

Figure 26: Time scale of a BM-profile: (A) Fluorescence double labeling of bone - Imaging by confocal laser scanning microscope (CLSM) visualizes two fluorescent bands marking the position of the moving mineralizing front at day 20 and day 6 before biopsy (see also Figure 27) (B) qBEI image of the identical bone area of (A) bone showing local calcium content of bone matrix. (A+B) Overlay of qBEI image with corresponding fluorescence image allows to relate the calcium content with time period of mineralization (tissue age) (Figure 27), (after: Misof et al. 2003)

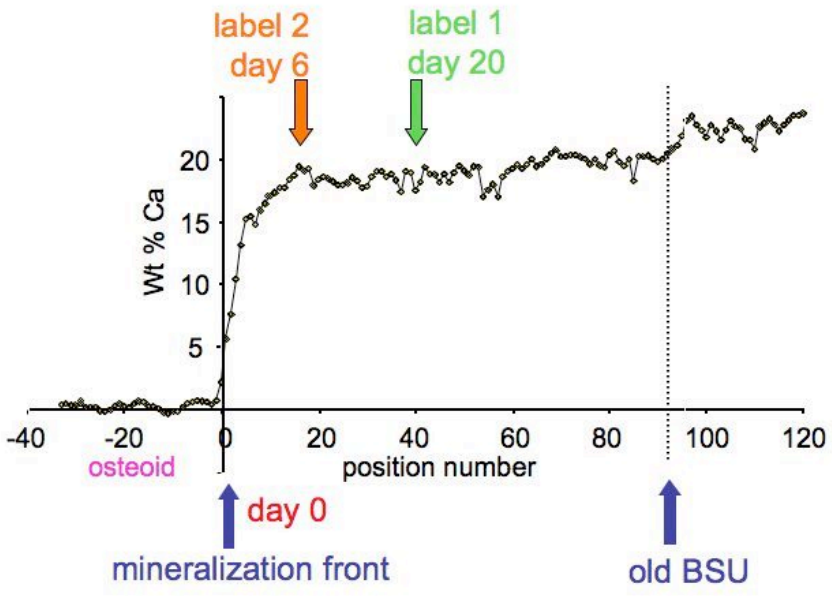

Figure 27: Profile of mineralization density at a forming BSU. The mineralization profile is combined with fluorescence double labelling. The first tetracycline labelling was done at day 20 before biopsy, the second labelling at day 6. Day zero is the day when the biopsy is taken. It can be seen that the mineralization density reaches here its plateau within six days.

A more accurate possibility for assigning the Ca-content to specific time points is a combination of CLSM and qBEI on identical BSUs. The CLSM fluorescence image is overlaid with the qBEI image of the identical BSU region and the positions of the fluorescence labels are transferred to BM-profiles directly as time markers (Fig. 27).

Consequently, in biopsy samples with fluorescence labeling the BM-profile measurements allow not only the determination of the level of mineral content when primary mineralization turns to secondary mineralization, but also how fast this point is reached defining the speed of primary mineralization.

Statistical analysis: Statistical analysis was performed using Prism 4, GraphPad Prism Version 4.0, GraphPad Software Inc., San Diego CA 2003. The median of the BM-profiles data obtained per patient was used to represent the Ca_{TURN} of the patient. The significance of differences between control and groups of patients were analyzed by Mann-Whitney tests (non-parametric analysis) (Table 1). Correlations of Ca_{TURN} of young individuals and adults with corresponding parameters of BMDD were performed using Spearman correlations (non-parametric analysis) (Table 2). All differences and correlations were considered significant at $p < 0.05$.

4. RESULTS

In this study bone biopsy samples of 75 individuals were measured for the transition point Ca_{TURN} between primary and secondary mineralization. The median of Ca_{TURN} was determined from 5 to 86 BM-profiles per individual depending on the number and size of forming BSUs found within the bone section. Further, the Ca_{TURN} values were correlated with the corresponding BMDD-parameters obtained from in the same bone sections.

4.1. Ca_{TURN} of Young Individuals (age range 2.1 to 20.8 years)

Controls: A subgroup of the young reference group, which were used to establish normative data for BMDD of young individuals were analyzed (see appendix (Fratzl-Zelman et al. 2009)). A median of 19.75 weight% Ca for Ca_{TURN} was found for the young controls. The Ca_{TURN} value and the corresponding BMDD parameters are listed in Table 1. Correlation analysis of age and Ca_{TURN} did not show any correlation ($r=0.26$, $p=0.39$) (Fig. 32). Estimate of time point when Ca_{TURN} is reached (T_{TURN}) is 16 days based on an average MAR of young individuals (0.9µm/day).

Children with OI type I & OI type VII: In these groups five patients with OI type I and four patients with OI type VII were measured for Ca_{TURN}. Statistical comparison revealed a significant increased of Ca_{TURN}, for OI-I +9.0%, $p<0.001$ and for OI-VII +5.2%, $p<0.01$, respectively, compared to controls (Table 1, Fig. 28).

Young Individuals with CaSR: In these group two patients with age of 13, 14 years and one with 19 yrs were measured for Ca_{TURN}. Statistical comparison revealed a significant decrease in Ca_{TURN}, (-16%, $p<0.001$), compared to controls (Table 1, Fig. 28).

Correlation Ca_{TURN} vs BMDD Parameters for all Young Individuals: Fig. 28 displays examples of single BM-profiles from three individuals (one control, two with bone diseases) together with the corresponding bone mineralization density

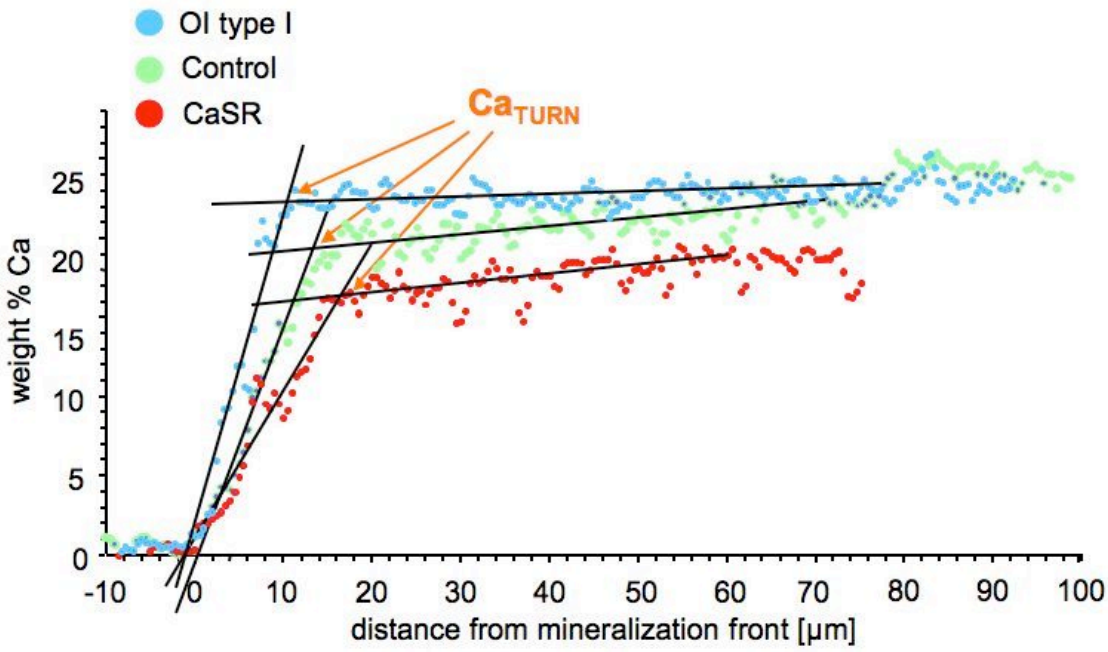

Figure 28: Example of individual BM-profiles from children with genetic disorders: Control = healthy individual, OI type I= patients with osteogenesis imperfecta type I, CaSR = patient with an activating mutation of the calcium sensing receptor. The deviations from control Ca_{TURN} indicate disturbances of the primary mineralization process in these patients.

distribution (BMDD) curves to demonstrate the relationship between Ca_{TURN} and BMDD-parameters. When Ca_{TURN} values were correlated with the corresponding BMDD parameters describing the average (Ca_{MEAN}) and the most frequent (Ca_{PEAK}) Ca-content of the entire cancellous bone compartment, a strong positive linear correlation was obtained. For BMDD parameters Ca_{WIDTH} the correlation was negative, while for Ca_{LOW} no significant correlation was found (Table 2).

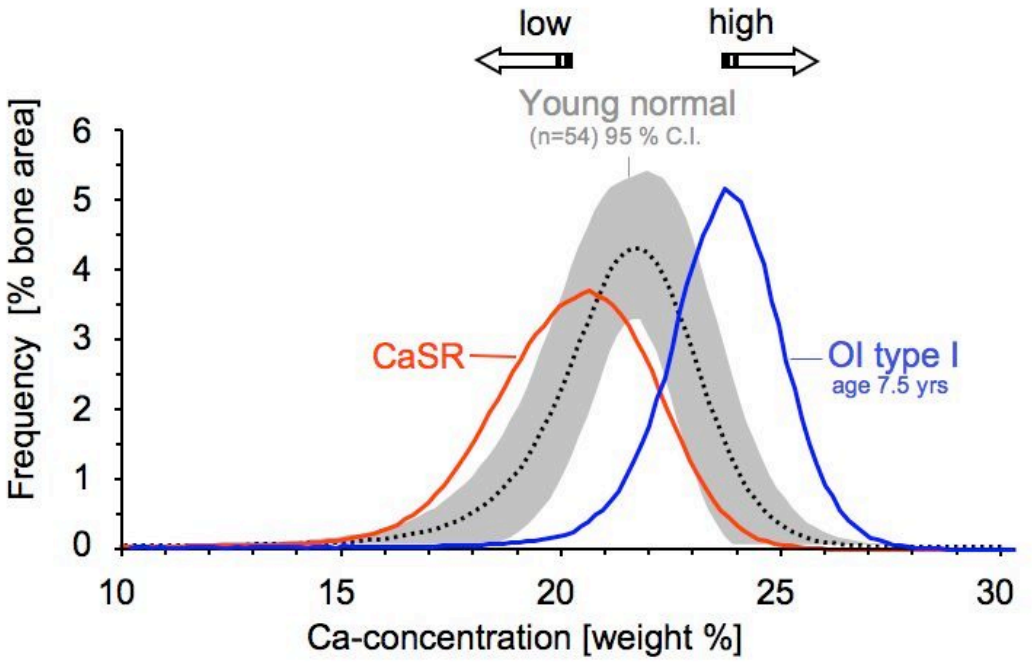

Figure 29: Example of bone mineralization density distributions (BMDD) of a patient with an activating mutation of the calcium-sensing receptor (CaSR) (age, 13 to 22 yrs and with osteogenesis imperfecta (OI type I) (age, 3 to 14 yrs) compared that of a young control reference group (Fratzl-Zelman et al. 2009). The CaSR patient has the BMDD shifted towards lower mineralization density and the heterogeneity is increased. The OI type I patient has the BMDD shifted towards higher mineralization density and the heterogeneity is reduced

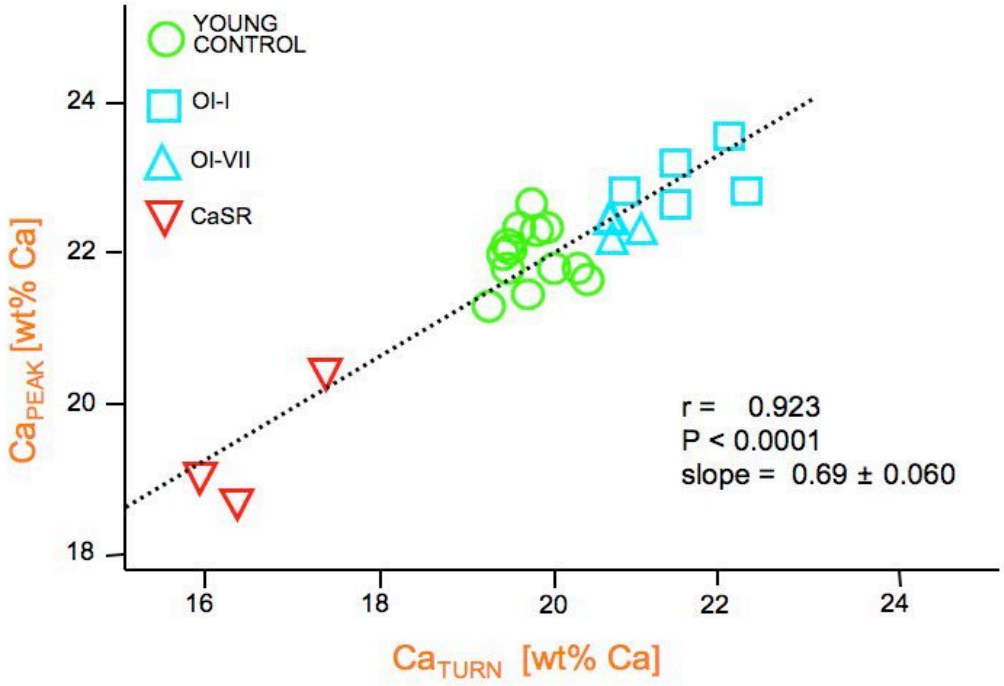

Figure 30: Correlation between Ca_{TURN} and Ca_{PEAK} values of CaSR, OI patients and young controls.

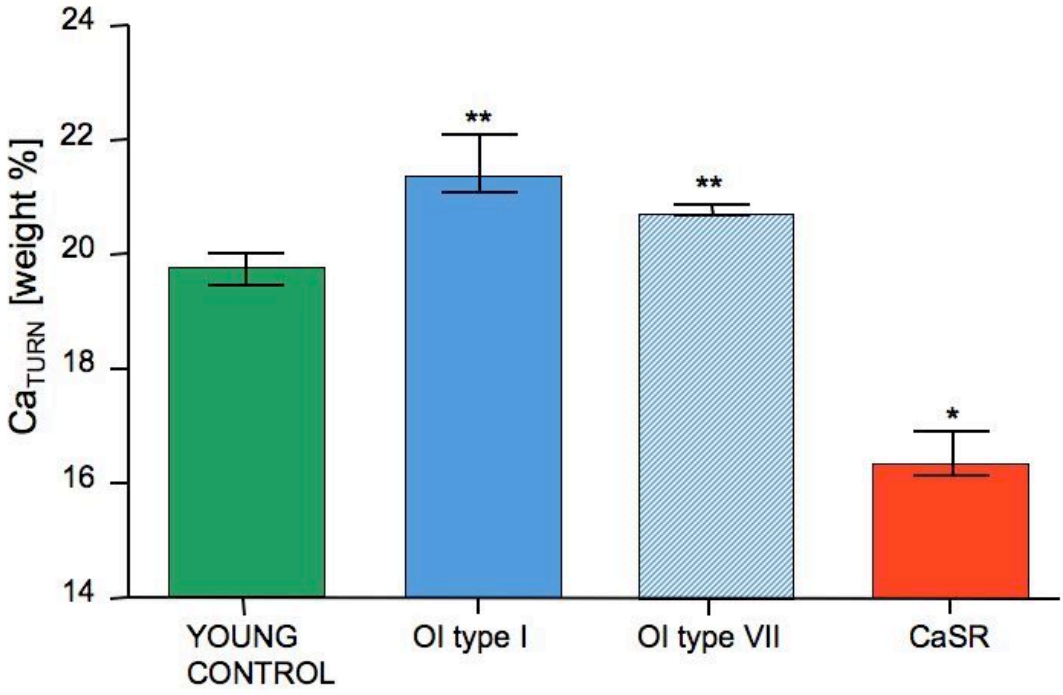

*Figure 31: Comparison of median Ca_{TURN} values of healthy young controls (YOUNG CONTROL) and osteogenesis imperfecta type I (OI-I), osteogenesis imperfecta type VII (OI-VII) and activating mutation of calcium sensing receptor (CaSR). *p<0.5, **p<0.01 sigificance level of differences with respect to young control.*

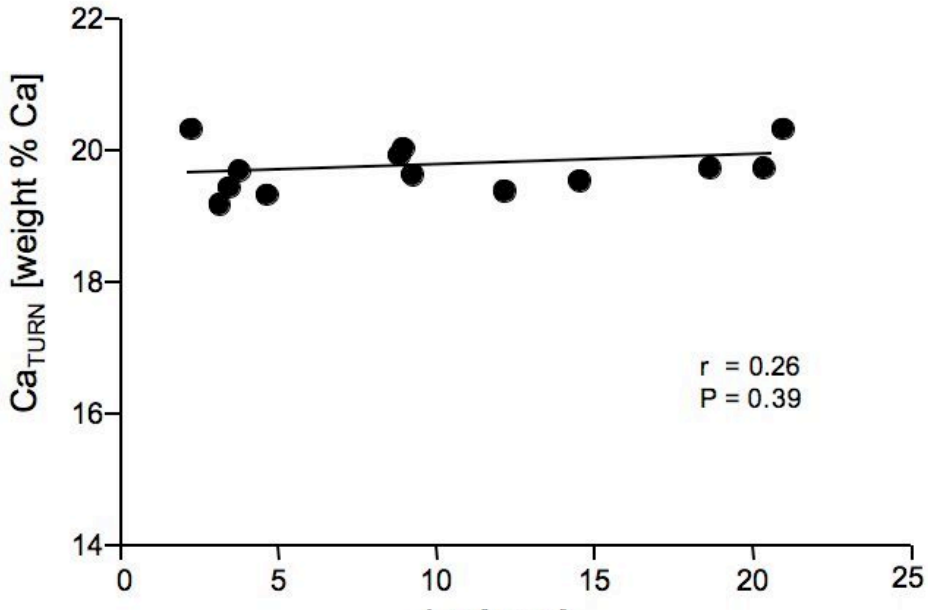

Figure 32: Correlation analysis between age and Ca_{TURN} of young healthy individuals revealed no age dependency of Ca_{TURN}.

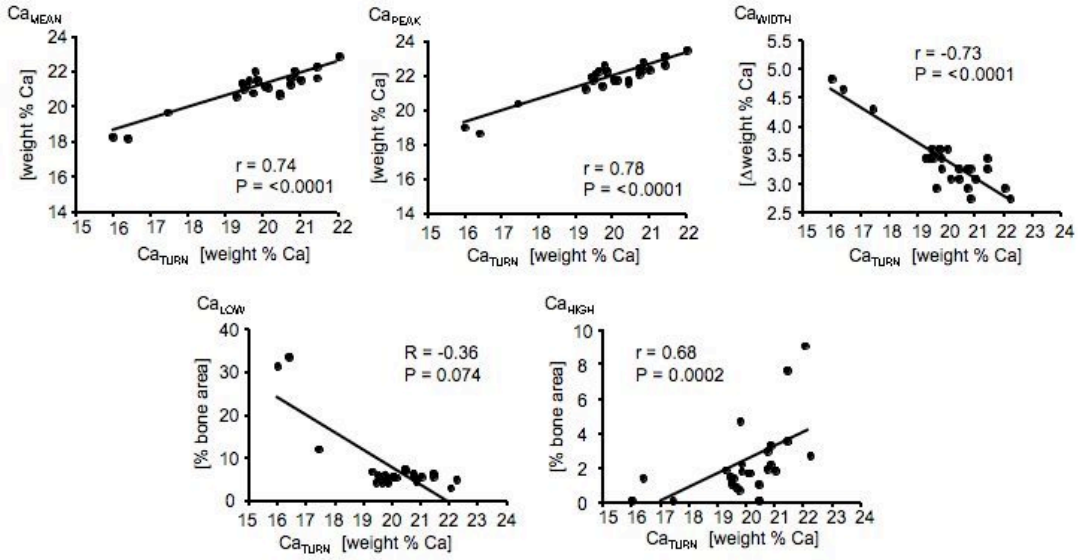

Figure 33: Correlation analysis between Ca_{TURN} and the five bone mineral density distribution (BMDD) parameters: Ca_{MEAN}, Ca_{PEAK}, Ca_{HIGH} are positively, while Ca_{WIDTH} and Ca_{LOW} are negatively correlated with Ca_{TURN}.

4.2. Ca_{TURN} of Adult Individuals (age range 21 to 58 years)

Controls: As controls served biopsies from 8 individuals (premenopausal women) without any sign of metabolic bone diseases. A median of 19.75 wt % Ca for Ca_{TURN} was found for the adult controls, which was equal to that of the young controls. The Ca_{TURN} value and the corresponding BMDD parameters are listed in Table 1. Estimate of time point when Ca_{TURN} is reached (T_{TURN}) is 25 days based on an average MAR of adults (0.6µm/day).

Patients with Osteoporosis (treated with Ca and Vit D): Postmenopausal osteoporotic women treated with Ca and Vit-D exhibited a Ca_{TURN} of 18.40 wt% Ca, which was numerically lower than that of the controls, but this difference did not reach level of significance. The only significant difference with respect to controls was Ca_{WIDTH} (+18%, p=0.008) (Table 1).

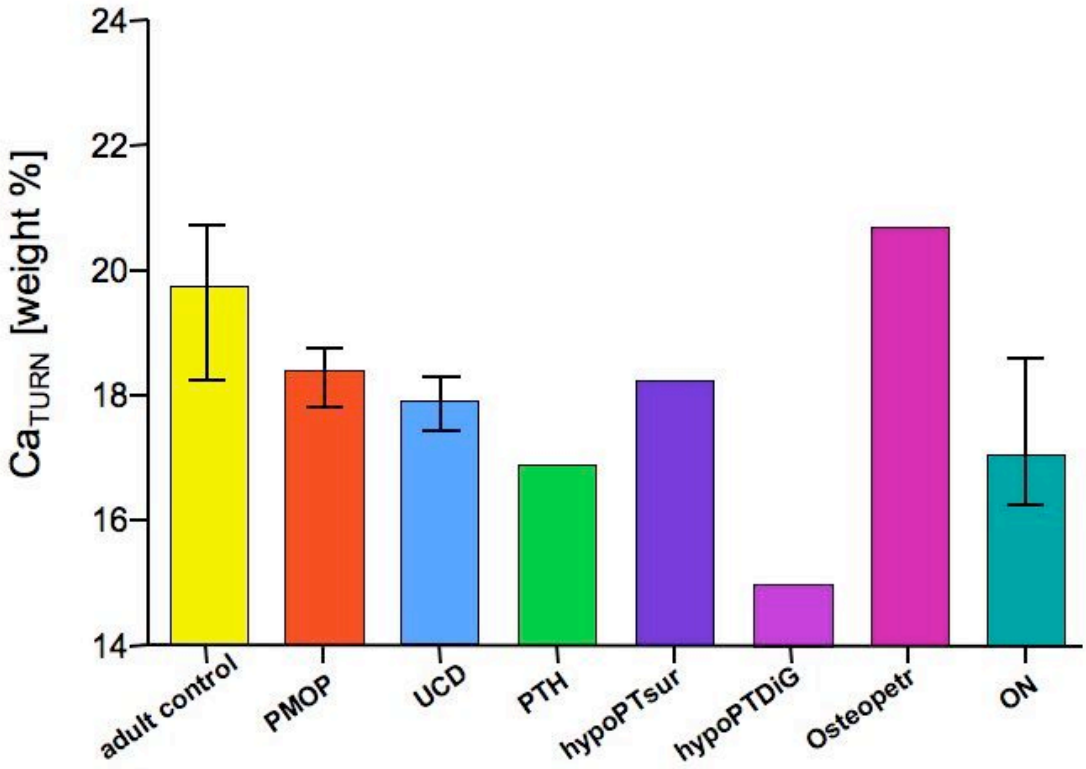

Figure 34: Comparison of median Ca_{TURN} values of healthy adult controls and disease cases: PMOP = postmenopausal osteoporosis (calcium & VitD treated) (n=9), UCD = not clarified bone disease (n=10); PTH = PTH treatment of OP (n=1); hypoPTsur = hypoparathyroidism after surgery (n=1); hypoPTDiG = hypoparathyroidism due to developmental disoder - DiGeorge syndrom (n=1); Osteopetrosis (n=1); Osteonecrosis of femoral head (n=4).

Patients with Unclear Differential Diagnosis: This patient group presented a Ca_{TURN} of 17.90 weight % Ca, which was significant lower (-9.4%, p=0.021) compared to control. Additionally, CaWidth (+12.7, p=0.043) was increased

Two Patients with HypoPT (Surgery and Di George): The hypoPT patient who had a surgical remove of the PT gland exhibited no statistical differences compared to adult control, while the hypoPT patient with DiGeorge showed a significant lower Ca_{TURN} (-24%, p=0.008), when analysed by Wilcoxon signed-rank test.

Patient with PTH treatment: Ca_{TURN} of this osteoporotic patient treated for 18 months with intermittent PTH was found to be lower (-14.4%, p=0.008) compared to controls.

Patient with Osteopetrosis: The Ca_{TURN} (+4.8%, ns) was numerically higher than that of controls but the difference did not reach level of significance.

Patients with Osteonecrosis: The group of patients (n=4) with osteonecrosis in the femoral head displayed a slightly lower Ca_{TURN} (-13.7%, p=0.048) as controls at this skeletal site.

Correlation Ca_{TURN} vs BMDD Parameters for all Adult Individuals: Correlation analysis between Ca_{TURN} and corresponding BMDD parameters of all adult individuals did not reveal any correlations (Table 2).

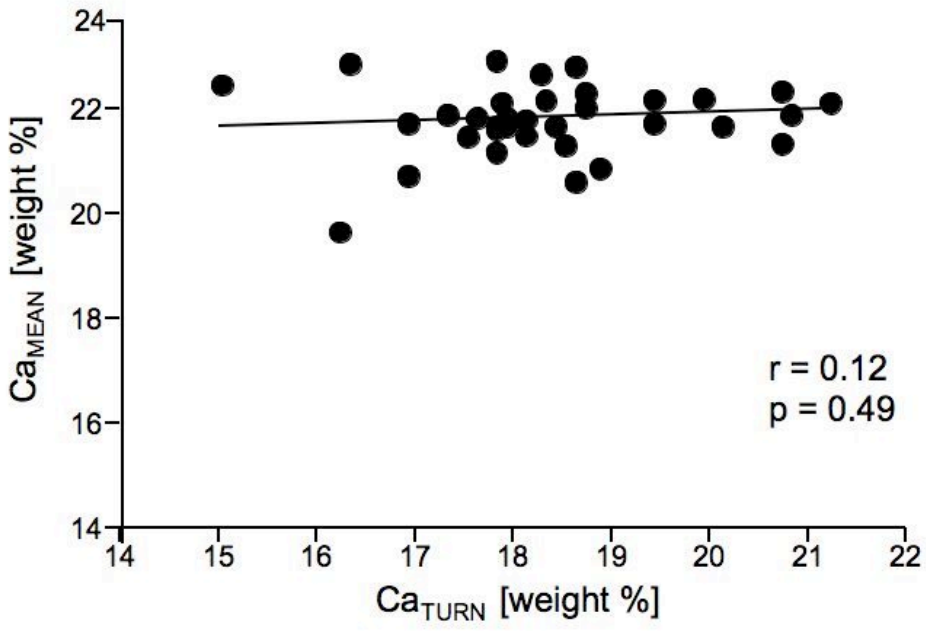

Figure 35: Correlation analysis between Ca_{TURN} and Ca_{MEAN} of adult individuals (healthy and diseased) revealed no dependency on Ca_{TURN}.

.

diseases/ controls	n	age range	Ca_{TURN} [Ca wt%]	Ca_{MEAN} [Ca wt%]	Ca_{PEAK} [Ca wt%]	Ca_{WIDTH} [DCa wt%]	Ca_{LOW} [% B.Ar]	Ca_{HIGH} [% B.Ar]
Control young	13	2-20	19.75 [19.50;20.00]	21.26 [20.80;21.58]	21.84 [21.84;22.36]	3.47 [3.29;3.64]	6.06 [4.84;6.62]	1.53 [1.10;1.86]
OI type I	5	3-14	21.40** [21.40;22.00]	22.13 [22.08;22.37]	22.88 [22.88;23.22]	2.95 [2.77;3.29]	5.47 [4.86;6.08]	3.62 [2.78;7.72]
OI type VII	4	2-12	20.75** [20.70;20.85]	21.65 [21.54;21.73]	22.43 [22.36;22.46]	3.21 [3.08;3.29]	6.04 [5.87;6.26]	2.52 [1.97;3.12]
CaSR	3	13-22	16.35* [16.15;16.88]	18.36 [18.32;19.05]	19.06 [18.89;19.76]	4.68 [4.51;1.77]	31.66 [22.09;32.75]	0.17 [0.15;0.82]
hypoPT DiGorge	2	14	16.45* [16.08;16.83]	19.35 [18.87;19.84]	19.93 [19.32;20.54]	5.03 [4.68;5.37]	24.30 [18.18;30.42]	2.99 [2.55;3.43]
HypoPT idiopathic	1	22	15.9* [15.45;16.3]	22.49	23.22	3.12	4.49	7.52
Control adult	8	pre-meno-pausal	19.75 [18.43;20.73]	21.83 [21.68;22.00]	22.53 [22.49;22.57]	3.38 [3.12;3.47]	5.54 [3.93;6.50]	3.18 [2.64;5.56]
Osteoporosis	9	post-meno-pausal	18.40 [17.85;18.70]	22.08 [21.23;22.21]	22.88 [22.01;22.88]	3.99 [3.64;4.16]	5.17 [4.96;6.33]	
Unclear diseases	10	21-58	17.90* [17.65;18.10]	21.81 [21.68;21.87]	22.53 [22.40;22.66]	3.81 [3.64;3.94]	5.29 [4.51;6.00]	5.36 [3.31;7.18]
PTH-treament	1	49	16.9** [16.4;17.5]	20.79	21.66	4.33		
Osteo-petrosis	1	24	20.7 [20.6;21.0]	22.40	23.33	4.33	5.77	
HypoPT surgery	1	49	18.25 [17.8;18.85]	22.71	23.40	3.64	3.86	10.40
HypoPT DiGeorge	1	40	15.0** [14.7;15.9]	22.51	23.05	3.12	3.88	6.49
Osteo-nekrosis	4	Jochen?	17.05* [16.28;18.20]	21.97 [21.21;22.40]	23.22 [22.83;23.57]	3.21 [3.12;4.03]	7.17 [3.10;14.67]	5.14 [1.89;8.52]

*Table 1: Medians of Ca_{TURN} and corresponding BMDD-parameters obtained from the group of patients and/or single patients; *p<0.05, **p<0.01 indicates significantly difference to corresponding controls.*

	Young		Adult
CaMean	r=0.7395	p<0.0001	ns
CaPeak	r=0.7945	p<0.0001	ns
CaWidth	r=-0.7276	p<0.0001	ns
CaLow	r=-0.3636	p=0.0740	ns

Table 2: correlation analysis (nonparametric, after Spearman) between Ca_{TURN} and the BMDD-parameters.

5. DISCUSSION

In the present work bone mineralization density profiles (BM-profiles) were measured in sites of forming bone mirroring the time course of matrix mineralization starting from level zero (osteoid). This information together with the bone turnover is of important clinical interest, because Ca_{TURN} and bone turnover determine the mineralization status (BMDD) of the bone material of the patient. It is a crucial factor of bone strength and thus an important determinant of fracture risk.

Biphasic mineralization law

Since the micrographic imaging of osteonal or trabecular bone by (Jowsey 1964) it is evident that the bone matrix mineralizes with a special time course, so that the young bone osteons or bone packets have lower mineral content then the older ones. This was confirmed by the method of fluorescence labeling by which the mineralizing front at a bone forming site is marked at two different time points usually about 12 days apart. By this method the labeled tissue age as well the dynamic parameters of bone formation like mineral apposition rate and mineralizing surface can be histological determined. First the combination of the fluoresence labeling with the qBEI method allowed to allocate the local Ca-content with the duration of mineralization. The results showed that there must be a fast initial mineralization process in which already 70 % of final mineralization density is performed followed by a slower process (Misof et al. 2003). Interestingly, as the generation of BMDDs was simulated by mathematical computing model, the out come was that a peak shaped BMDD can only be produced by an underlying mineralization process, which is biphasic, an initial fast and followed by a slow phase (Ruffoni et al. 2007; Ruffoni et al. 2008). The presented experimental results based on the analysis of bone mineralization density profiles across the mineralization front is completely in agreement with this theoretical approach.

Mineralization law of children

Healthy growing children have an 2.5 fold increased bone turnover compared to that of adults (Glorieux et al. 2000; Rauch and Glorieux 2004). The bone (re)modeling balance is also positive and the bone mass is rapidly increasing by this way. Further, the BMDD of children showed a shift towards lower mineralization (Ca_{MEAN} -5%) compared to adults (Fratzl-Zelman et al. 2009). This would be consistent with the increased bone turnover situation in children. Indeed, the BM-profile measurements revealed no significant differences between children and adults confirming that these differences in BMDD is rather not due to changes in the mineralization law than rather due to the increased bone turnover. Surprisingly, the BMDD of the young individuals was found to be independent of age in the range from 2 to 20 years. This can be understood by the fact that in a growing bone the average tissue age remain at a similar low level due to the high bone turnover situation. In contrast the BMDD of adults was also constant at a higher level in the age range from 25 to 90 yrs, because of rather constant lower level of bone turnover (Roschger et al. 2003).

A further interesting novel outcome was, that the investigated children with genetic disorder presenting an atypic bone phenotype with characteristic changes in the BMDD, which were clearly the results of changes in the mineralization law. In the cases of Osteogenesis imperfecta it was a shift towards higher mineralization density resulting into a more brittle bone, while in the cases with CaSR the shift was towards lower mineralization density, which leads to a less stiff bone material.

Osteogenesis Imperfecta: Until now it was well known that the OI generates bone with increased mineral content, but the underlying mechanism was still not elucidated (Roschger et al. 2008a). It was common sense that the increased mineralization density is due to the altered collagen structure as the consequence of gene mutation in the collagen gene. However, recent qBEI measurements could prove that the different OI types show about the same increase in mineralization independent of severity of OI and type of collagen mutation or modification. Thus, for example there were no differences in degree

of matrix mineralization in OI type I with quantitative (intact collagen but half amount) and qualitative mutation (altered collagen structure) (Roschger et al. 2008a). Further it was found that the bone turnover rate in these children are increased compared to healthy control children, which would expect rather a shift of the BMDD towards lower mineralization density than to higher mineralization (Ruffoni et al. 2007). All together, this leads to the hypothesis, that the mineralization process is somehow accelerated most probably due to altered osteoblast function. The accelerated mineralization would result then to higher mineral contents in all the bone packets formed compared to that of controls. Indeed, our finding strongly confirms this hypothesis. In the OI cases the Ca_{TURN} value, which describes the mineral level where the mineralization changes from the rapid primary to the slow secondary mineralization, is remarkably increased. This would explain, that, though in OI the bone turnover is higher, the BMDD is not shifted towards lower mineralization, because already the very new bone packets have increased mineral content. Further, it seems that initial lead in mineralization density with respect to controls remain during the secondary mineralization phase when the bone packets became older.

CaSR patients: This etiology of hypoparathryoidism is associated with an activating mutation of the calcium sensing recpector at the parathyroid gland. The genetic mutation mimics high calcium levels in the serum, though the level is low. In consequence the PTH level is also reduced, because there is no need to provide more calcium through activity of osteoclasts. In consequence also the bone turnover is markedly suppressed. This scenario would expect, that the BMDD is shifted towards higher mineralization and the distribution became more narrow, however, the reverse is the case. The BMDD of these patient are shifted towards lower mineralization and the BMDD peak was wider. Considering the Ca_{TURN} of these patients, one can see that this value is markedly decreased compared to control children indicating a change in the mineralization law towards lower level of primary mineralization, which does not seem to be compensated later in the phase of secondary mineralization. Thus, the BMDD of CaSR patient decribes a low mineralization status, though the

bone turnover is suppressed. About the mechanism of this change in mineralization kinetics can only be speculated. Maybe the osteoblast has also a CaSR receptor, which is somehow involved in the control of the mineralization process.

Mineralization law of adults

Adults have a lower bone turnover rate compared to children, but a Ca_{TURN} in the Ca-concentration range as in children was found. Consistently, the BMDD was shifted towards higher mineralization density compared to children.

Postmenaupausal osteoporosis: In general these patients have a somewhat increased bone turnover acompanied mostly with deficient Calcium and Vit D. This lead to a BMDD shifted towards lower mineralization negatively influencing the bone strength. Further the remodeling balance between bone formation and resorption is negative in this age, that leads to loss of bone mass and structural quality. Again this contributes to a reduction of the mechanical competence of bone. All together it results in an increase of the fracture incidence in these patients. Cacium and Vit D supplementation was found to have a beneficial effect on the BMDD (shifts back to normal). Considering the Ca_{TURN} in such treated patient we could not found differences compared to adult controls. It can be concluded therefore that this type of bone fracture disease is rather a problem of controlling remodeling activity, while the mineralization process seems to be not affected.

Idiopathic Osteoporosis: Most of the investigated biopsies from patients with unclear differential diagnosis exhibited a BMDD shifted towards lower mineralization, which was not necessarily coupled to an increased bone turnover. Interestingly, the Ca_{TURN} values of all these patients were decreased compared to controls. Hence in this disease it is likely that the mineralization process is affected. This novel outcome is of important clinical interest, because new therapeutic strategies different from osteoporosis (remodeling disease) have to be applied or developed for such patients.

Conclusion

In conclusion the measurements of bone mineralization density profiles in bone biopsies allows to distinguish between changes of the bone mineralization density distribution due to bone turnover and due to disturbances in the mineralization process. This differential analysis of the bone matrix mineralization status provides a new clinical tool for better diagnosis, and treatment decisions in bone diseases. Further it will help to develop new therapeutic strategies targeting more accurately the underlying mechanism of the disease.

6. REFERENCES

Ashby M.F. (1983) The mechanical-properties of cellular solids. Phys Metall Mater Sci 14:1755-1769.

Aubin J.E. & Liu F. (1996) The osteoblasts lineage. In: Principles of Bone Biology (Bilezikian JP, Raisz LG, Rodan GA, eds), pp 51-67. New York, San Diego, London, Boston, Sydney, Tokyo, Toronto: Academic Press.

Baron R.E. (1999) Anatomy and Ultrastructure of Bone. In: Primer on the Metabolic Bone Diseases and Disorders of Mineral Metabolism (Favus MJ, ed), pp 3-10. Philadelphia, New York: Lippincott Williams & Wilkins.

Benninghoff A. (1993) Anatomie - Makroskopische Anatomie, Embryologie und Histologie des Menschen, ed 15th. München, Wien, Baltimore: Urban & Schwarzenberg.

Bilezikian J.P., Raisz L.G. & Rodan G.A. (1996) Principles of Bone Biology. San Diego: Academic Press.

Blair J.M., Zheng Y. & Dunstan C.R. (2007) RANK ligand. Int J Biochem Cell Biol 39:1077-1081.

Blouin S., Thaler H.W., Korninger C., Schmid R., Hofstaetter J.G., Zoehrer R., Phipps R., Klaushofer K., Roschger P. & Paschalis E.P. (2009) Bone matrix quality and plasma homocysteine levels. Bone 44:959-964.

Boivin G. & Meunier P.J. (2002) Changes in bone remodeling rate influence the degree of mineralization of bone. Connect Tissue Res 43:535-537.

Bonewald L.F. (2008) Osteocytes. In: Primer on the Metabolic Bone Diseases and Disorders of Mineral Metabolism (Rosen cJ, ed), pp 22-27. Washington, DC: American society for bone and mineral research.

Bonewald L.F. & Johnson M.L. (2008) Osteocytes, mechanosensing and Wnt signaling. Bone 42:606-615.

Boskey A.L. (2006) Mineralization, Structure and Function of Bone. In: Dynamics of Bone and Cartilage Metabolism, pp 201- 212. New York, San Diego, London, Boston, Sydney, Tokyo, Toronto: Academic Press.

Bouxsein M.L. (2003) Bone quality: where do we go from here? Osteoporos Int 14 Suppl 5:S118-127.

Boyle W.J., Simonet W.S. & Lacey D.L. (2003) Osteoclast differentiation and activation. Nature 423:337-342.

Burger C., Zhou H.W., Wang H., Sics I., Hsiao B.S., Chu B., Graham L. & Glimcher M.J. (2008) Lateral packing of mineral crystals in bone collagen fibrils. Biophys J 95:1985-1992.

Burr D.B. (2002) The contribution of the organic matrix to bone's material properties. Bone 31:8-11.

Cashman K.D. (2002) Calcium intake, calcium bioavailability and bone health. Br J Nutr 87 Suppl 2:S169-177.

Dempster D.W. (2006) Anatomy and Functions of the adult skeleton. In: Primer on the metabolic bone diseases and disorders of mineral metabilism (Murray JF, ed), pp 7-11. Washington, DC: American society for bone and mineral research.

Eriksen E.F., Axelrod D.W. & Melsen F. (1994) Bone Histomorphometry. New York: Raven Press.

Fernandez-Tresguerres-Hernandez-Gil I., Alobera-Gracia M.A., del-Canto-Pingarron M. & Blanco-Jerez L. (2006a) Physiological bases of bone regeneration I.

Histology and physiology of bone tissue. Med Oral Patol Oral Cir Bucal 11:E47-51.
Fernandez-Tresguerres-Hernandez-Gil I., Alobera-Gracia M.A., del-Canto-Pingarron M. & Blanco-Jerez L. (2006b) Physiological bases of bone regeneration II. The remodeling process. Med Oral Patol Oral Cir Bucal 11:E151-157.
Fratzl P. (2006) Material Properties: Mineral Crystals. In: The bone quality book: a guide to factors influencing bone strength (Dempster DW, Felsenberg D, Geest Vd, eds), pp 56-63. Amsterdam, Netherland: Excerpta Medica.
Fratzl P., Gupta H.S., Paschalis E. & Roschger P. (2004a) Structure and mechanical quality of the collagen-mineral nano-composite in bone. Journal of Materials Chemistry 14:2115-2123.
Fratzl P., Gupta H.S., Paschalis E.P. & Roschger P. (2004b) Structure and mechanical quality of the collagen-mineral nano-composite in bone. Journal of Materials Chemistry:2115-2123.
Fratzl P., Roschger P., Eschberger J., Abendroth B. & Klaushofer K. (1994) Abnormal bone mineralization after fluoride treatment in osteoporosis: a small-angle x-ray-scattering study. J Bone Miner Res 9:1541-1549.
Fratzl P. & Weinkamer R. (2007) Nature's hierarchical materials. Progress in Materials Science 52:1263-1334.
Fratzl-Zelman N., Roschger P., Misof B.M., Pfeffer S., Glorieux F.H., Klaushofer K. & Rauch F. (2009) Normative data on mineralization density distribution in iliac bone biopsies of children, adolescents and young adults. Bone
Fratzl-Zelman N., Valenta A., Roschger P., Nader A., Gelb B.D., Fratzl P. & Klaushofer K. (2004) Decreased bone turnover and deterioration of bone structure in two cases of pycnodysostosis. J Clin Endocrinol Metab 89:1538-1547.
Frost H.M. (1963) Bone Remodeling Dynamics. Springfield, IL: Charles C. Thomas.
Gao H., Ji B., Jager I.L., Arzt E. & Fratzl P. (2003) Materials become insensitive to flaws at nanoscale: lessons from nature. Proc Natl Acad Sci U S A 100:5597-5600.
Glorieux F.H., Travers R., Taylor A., Bowen J.R., Rauch F., Norman M. & Parfitt A.M. (2000) Normative data for iliac bone histomorphometry in growing children. Bone 26:103-109.
Gotzman D. & Cole D.E.C. (2006) Hypoparathyroidism. In: Primer on the Metabolic Bone Diseases and Disorders of Mineral Metabolism (Favus MJ, ed), pp 216 - 219. Washington, DC: American Society for Bone and Mineral Research.
Gupta H.S., Schratter S., Tesch W., Roschger P., Berzlanovich A., Schoeberl T., Klaushofer K. & Fratzl P. (2005) Two different correlations between nanoindentation modulus and mineral content in the bone-cartilage interface. J Struct Biol 149:138-148.
Gupta H.S., Seto J., Wagermaier W., Zaslansky P., Boesecke P. & Fratzl P. (2006) Cooperative deformation of mineral and collagen in bone at the nanoscale. Proc Natl Acad Sci U S A 103:17741-17746.
Hadjidakis D.J. & Androulakis, II (2006) Bone remodeling. Ann N Y Acad Sci 1092:385-396.
Han Z.H., Palnitkar S., Rao D.S., Nelson D. & Parfitt A.M. (1996) Effect of ethnicity and age or menopause on the structure and geometry of iliac bone. J Bone Miner Res 11:1967-1975.

Jager I. & Fratzl P. (2000) Mineralized collagen fibrils: a mechanical model with a staggered arrangement of mineral particles. Biophys J 79:1737-1746.
Jowsey J. (1964) Variations in bone mineralization with age and disease. In: Bone biodynamics (Frost HM, ed), pp 461 - 479. Boston MA: Little, Brown & Company.
Kazanci M., Wagner H.D., Manjubala N.I., Gupta H.S., Paschalis E., Roschger P. & Fratzl P. (2007) Raman imaging of two orthogonal planes within cortical bone. Bone 41:456-461.
Krause C., de Gorter D.J.J., Karperien M. & ten Dijke P. (2008) Signal Transduction Cascades Controlling Osteoblast Differention. In: Primer on the Metabolic Bone Diseases and Disorders of Mineral Metabolism (Rosen CJ, ed), vol 7th, pp 10-16. Washington D.C.: The American Society for Bone and Mineral Research.
Kuivaniemi H., Tromp G. & Prockop D.J. (1991) Mutations in collagen genes: causes of rare and some common diseases in humans. Faseb J 5:2052-2060.
Landis W.J., Hodgens K.J., Arena J., Song M.J. & McEwen B.F. (1996) Structural relations between collagen and mineral in bone as determined by high voltage electron microscopic tomography. Microsc Res Tech 33:192-202.
Legros R., Balmain N. & Bonel G. (1987) Age-related changes in mineral of rat and bovine cortical bone. Calcif Tissue Int 41:137-144.
Lips P., van Schoor N.M. & Bravenboer N. (2009) Vitamin D-Related Disorders. In: Primer on the Metabolic Bone Diseases and Disorders of Mineral Metabolism (Rosen CJ, ed), pp 329-335. Washington D.C.: American Society for Bone and Mineral Research.
Lowik C.W. & van Bezooijen R.L. (2006) Wnt signaling is involved in the inhibitory action of sclerostin on BMP-stimulated bone formation. J Musculoskelet Neuronal Interact 6:357.
Mackie E.J., Ahmed Y.A., Tatarczuch L., Chen K.S. & Mirams M. (2008) Endochondral ossification: how cartilage is converted into bone in the developing skeleton. Int J Biochem Cell Biol 40:46-62.
Maes C., Kobayashi T. & Kronenberg H.M. (2007) A Novel Transgenic Mouse Model to study the Osteoblast Lineage in Vivo. In: Annals of the New York Academy of Science 1116, pp 149-164. New York: New York Academy of Sciences.
Manolagas S.C. (2000) Birth and death of bone cells: basic regulatory mechanisms and implications for the pathogenesis and treatment of osteoporosis. Endocr Rev 21:115-137.
Manolagas S.C., Jilka R.L., Bellido T., O'Brian C.A. & Parfitt A.M. (1996) Interleukin-6-type cytokines and their receptors. In: Principles of Bone Biology (Bileikian JP, Raisz, L. G., Rodan, G. A., ed), pp pp 701-713. San Diego, CA: Academic Press.
Marini J.C. (2006) Osteogenesis Imperfecta. In: Primer on the Metabolic Bone Diseases and Disorders of Mineral Metabolism (Favus MJ, ed), pp 418 - 421. Washington, DC: American Society for Bone and Mineral Research.
Marks S.C., Jr. & Hermey D.C. (1996) The Structure and Development of Bone. In: Principles of Bone Biology (Bilezikian JP, Raisz LG, Rodan GA, eds). New York, San Diego, London, Boston, Sydney, Tokyo, Toronto: Academic Press.
Marshall D., Johnell O. & Wedel H. (1996) Meta-analysis of how well measures of bone mineral density predict occurrence of osteoporotic fractures. Bmj 312:1254-1259.

McLean R.R., Jacques P.F., Selhub J., Tucker K.L., Samelson E.J., Broe K.E., Hannan M.T., Cupples L.A. & Kiel D.P. (2004) Homocysteine as a predictive factor for hip fracture in older persons. N Engl J Med 350:2042-2049.
Meunier P.J., Roux C., Seeman E., Ortolani S., Badurski J.E., Spector T.D., Cannata J., Balogh A., Lemmel E.M., Pors-Nielsen S., Rizzoli R., Genant H.K. & Reginster J.Y. (2004) The effects of strontium ranelate on the risk of vertebral fracture in women with postmenopausal osteoporosis. N Engl J Med 350:459-468.
Misof B.M., Roschger P., Cosman F., Kurland E.S., Tesch W., Messmer P., Dempster D.W., Nieves J., Shane E., Fratzl P., Klaushofer K., Bilezikian J. & Lindsay R. (2003) Effects of intermittent parathyroid hormone administration on bone mineralization density in iliac crest biopsies from patients with osteoporosis: a paired study before and after treatment. J Clin Endocrinol Metab 88:1150-1156.
Morello R., Bertin T.K., Chen Y., Hicks J., Tonachini L., Monticone M., Castagnola P., Rauch F., Glorieux F.H., Vranka J., Bachinger H.P., Pace J.M., Schwarze U., Byers P.H., Weis M., Fernandes R.J., Eyre D.R., Yao Z., Boyce B.F. & Lee B. (2006) CRTAP is required for prolyl 3- hydroxylation and mutations cause recessive osteogenesis imperfecta. Cell 127:291-304.
Nawrot-Wawrzyniak K., Varga F., Nader A., Roschger P., Sieghart S., Zwettler E., Roetzer K.M., Lang S., Weinkamer R., Klaushofer K. & Fratzl-Zelman N. (2009) Effects of Tumor-Induced Osteomalacia on the Bone Mineralization Process. Calcif Tissue Int
Ortner D.J. & Turner-Walker G. (2003) The Biology of Skeletal Tissues. In: Identification of Pathological Conditions in Human Skeletal Remains, pp 11-25.
Parfitt A.M. (1994) Osteonal and hemi-osteonal remodeling: the spatial and temporal framework for signal traffic in adult human bone. J Cell Biochem 55:273-286.
Parfitt A.M. (1998) Osteoclast precursors as leukocytes: importance of the area code. Bone 23:491-494.
Paris O., Zizak I., Lichtenegger H., Roschger P., Klaushofer K. & Fratzl P. (2000) Analysis of the hierarchical structure of biological tissues by scanning X-ray scattering using a micro-beam. Cell Mol Biol (Noisy-le-grand) 46:993-1004.
Parisien M.V., McMahon D., Pushparaj N. & Dempster D.W. (1988) Trabecular architecture in iliac crest bone biopsies: infra-individual variability in structural parameters and changes with age. Bone 9:289-295.
Paschalis E. (2006) Material Properties: Collagen. In: The Bone Quality Book: A guide to factors influencing bone strength (Dempster DW, Felsenberg D, Van der Geest S, eds), pp 42-48. Amsterdam, Netherland: Excerpta Medica.
Paschalis E.P., Verdelis K., Doty S.B., Boskey A.L., Mendelsohn R. & Yamauchi M. (2001) Spectroscopic characterization of collagen cross-links in bone. J Bone Miner Res 16:1821-1828.
Peterlik H., Roschger P., Klaushofer K. & Fratzl P. (2006) From brittle to ductile fracture of bone. Nat Mater 5:52-55.
Prockop D.J., Constantinou C.D., Dombrowski K.E., Hojima Y., Kadler K.E., Kuivaniemi H., Tromp G. & Vogel B.E. (1989) Type I procollagen: the gene-protein system that harbors most of the mutations causing osteogenesis imperfecta and probably more common heritable disorders of connective tissue. Am J Med Genet 34:60-67.
Raisz L.G. (2008) Overview of Pathogenesis. In: Primer on the Metabolic Bone Diseases and Disorders of Mineral Metabolism (Rosen CJ, ed), vol 7th, pp 203-206. Washington D.C.: ASBMR.

Rauch F. & Glorieux F.H. (2004) Osteogenesis imperfecta. Lancet 363:1377-1385.
Reginster J.Y., Seeman E., De Vernejoul M.C., Adami S., Compston J., Phenekos C., Devogelaer J.P., Curiel M.D., Sawicki A., Goemaere S., Sorensen O.H., Felsenberg D. & Meunier P.J. (2005) Strontium ranelate reduces the risk of nonvertebral fractures in postmenopausal women with osteoporosis: Treatment of Peripheral Osteoporosis (TROPOS) study. J Clin Endocrinol Metab 90:2816-2822.
Rinnerthaler S., Roschger P., Jakob H.F., Nader A., Klaushofer K. & Fratzl P. (1999) Scanning small angle X-ray scattering analysis of human bone sections. Calcif Tissue Int 64:422-429.
Roschger P. (2003) Characterization of mineralized tissue in vertebrates by scanning microscopic methods for material science and medicine. In: Institut für Materialphysik, Leoben: Montanuniversität Leoben.
Roschger P., Fratzl P., Eschberger J. & Klaushofer K. (1998) Validation of quantitative backscattered electron imaging for the measurement of mineral density distribution in human bone biopsies. Bone 23:319-326.
Roschger P., Fratzl P., Klaushofer K. & Rodan G. (1997) Mineralization of cancellous bone after alendronate and sodium fluoride treatment: a quantitative backscattered electron imaging study on minipig ribs. Bone 20:393-397.
Roschger P., Fratzl-Zelman N., Misof B.M., Glorieux F.H., Klaushofer K. & Rauch F. (2008a) Evidence that Abnormal High Bone Mineralization in Growing Children with Osteogenesis Imperfecta is not Associated with Specific Collagen Mutations. Calcif Tissue Int 82:263-270.
Roschger P., Grabner B.M., Rinnerthaler S., Tesch W., Kneissel M., Berzlanovich A., Klaushofer K. & Fratzl P. (2001) Structural development of the mineralized tissue in the human L4 vertebral body. J Struct Biol 136:126-136.
Roschger P., Gupta H.S., Berzlanovich A., Ittner G., Dempster D.W., Fratzl P., Cosman F., Parisien M., Lindsay R., Nieves J.W. & Klaushofer K. (2003) Constant mineralization density distribution in cancellous human bone. Bone 32:316-323.
Roschger P., Paschalis E.P., Fratzl P. & Klaushofer K. (2008b) Bone mineralization density distribution in health and disease. Bone 42:456-466.
Roschger P., Plenk H., Jr., Klaushofer K. & Eschberger J. (1995) A new scanning electron microscopy approach to the quantification of bone mineral distribution: backscattered electron image grey-levels correlated to calcium K alpha-line intensities. Scanning Microsc 9:75-86; discussion 86-78.
Ross F.P. (2008) Osteoclast Biology and Bone Resorption. In: Primer on the Metabolic Bone Diseases and Disorders of Mineral Metabolism (Rosen CJ, ed), vol 7th, pp 16-22. Washington D.C.: The American Society for Bone and Mineral Research.
Ruffoni D., Fratzl P., Roschger P., Klaushofer K. & Weinkamer R. (2007) The bone mineralization density distribution as a fingerprint of the mineralization process. Bone 40:1308-1319.
Ruffoni D., Fratzl P., Roschger P., Phipps R., Klaushofer K. & Weinkamer R. (2008) Effect of temporal changes in bone turnover on the bone mineralization density distribution: a computer simulation study. J Bone Miner Res 23:1905-1914.
Seeman E. (2008) Bone quality: the material and structural basis of bone strength. J Bone Miner Metab 26:1-8.
Stein M.S., Feik S.A., Thomas C.D., Clement J.G. & Wark J.D. (1999) An automated analysis of intracortical porosity in human femoral bone across age. J Bone Miner Res 14:624-632.

Teitelbaum S.L. & Ross F.P. (2003) Genetic regulation of osteoclast development and function. Nat Rev Genet 4:638-649.
Teitelbaum S.L., Tondravi M.M. & Ross F.P. (1997) Osteoclasts, macrophages, and the molecular mechanisms of bone resorption. J Leukoc Biol 61:381-388.
ten Dijke P., Krause C., de Gorter D.J., Lowik C.W. & van Bezooijen R.L. (2008) Osteocyte-derived sclerostin inhibits bone formation: its role in bone morphogenetic protein and Wnt signaling. J Bone Joint Surg Am 90 Suppl 1:31-35.
Theman T.A., Collins M.T., Dempster D.W., Zhou H., Reynolds J.C., Brahim J.S., Roschger P., Klaushofer K. & Winer K.K. (2009) PTH(1-34) replacement therapy in a child with hypoparathyroidism caused by a sporadic calcium receptor mutation. J Bone Miner Res 24:964-973.
Urist M.U. (1980) Fundamental and clinical bone physiology. Philadelphia, Toronto: J. B. Lippincot Company.
Vashishth D., Gibson G.J., Khoury J.I., Schaffler M.B., Kimura J. & Fyhrie D.P. (2001) Influence of nonenzymatic glycation on biomechanical properties of cortical bone. Bone 28:195-201.
Veis A. (2003) Mineralization in organic matrix frameworks. Biomineralization 54:249-289.
Ward L.M., Rauch F., Travers R., Chabot G., Azouz E.M., Lalic L., Roughley P.J. & Glorieux F.H. (2002) Osteogenesis imperfecta type VII: an autosomal recessive form of brittle bone disease. Bone 31:12-18.
Wojtowicz A., Dziedzic-Goclawska A., Kaminski A., Stachowicz W., Wojtowicz K., Marks S.C., Jr. & Yamauchi M. (1997) Alteration of mineral crystallinity and collagen cross-linking of bones in osteopetrotic toothless (tl/tl) rats and their improvement after treatment with colony stimulating factor-1. Bone 20:127-132.

7. APPENDIX

Bone 44 (2009) pp.1043–1048)

Normative data on mineralization density distribution in iliac bone biopsies of children, adolescents and young adults

N. Fratzl-Zelman[a], P. Roschger[a], B.M. Misof[a], S. Pfeffer[a], F.H. Glorieux[b], K. Klaushofer[a], F. Rauch[b]

a Ludwig Boltzmann Institute of Osteology at the Hanusch Hospital of WGKK and AUVA Trauma Centre Meidling, 4th Med. Dept., Hanusch Hospital, Heinrich Collin Str. 30, 1140 Vienna, Austria
b Genetics Unit, Shriners Hospital for Children and McGill University, Montreal, Quebec, Canada H3G 1A6

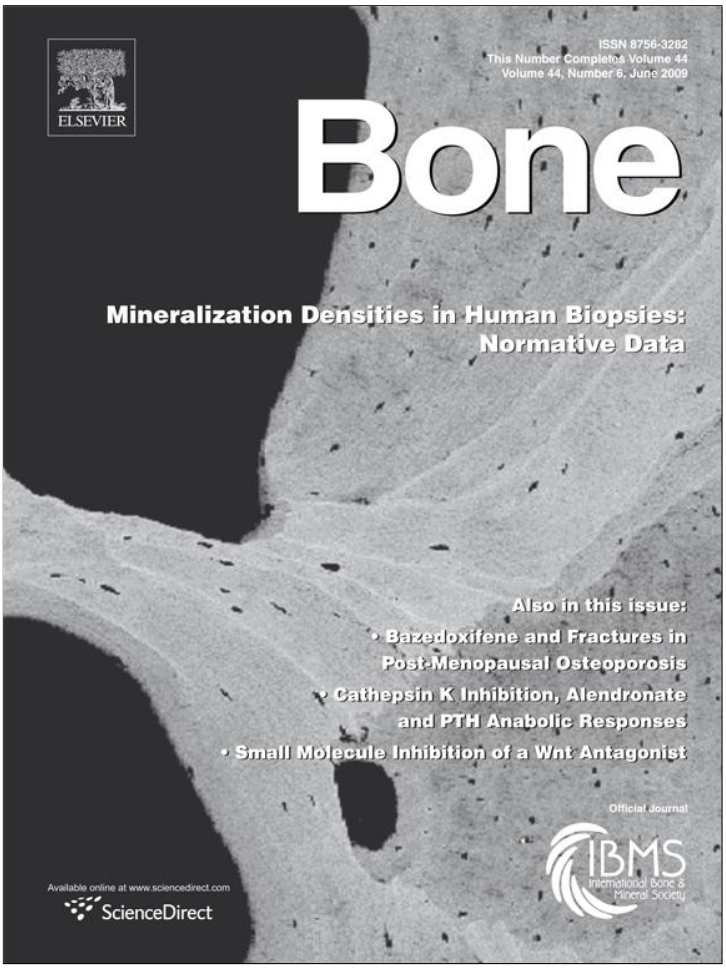

Bone 44 (2009) 1043–1048

Contents lists available at ScienceDirect

Bone

journal homepage: www.elsevier.com/locate/bone

Normative data on mineralization density distribution in iliac bone biopsies of children, adolescents and young adults

N. Fratzl-Zelman [a,*], P. Roschger [a], B.M. Misof [a], S. Pfeffer [a], F.H. Glorieux [b], K. Klaushofer [a], F. Rauch [b]

[a] Ludwig Boltzmann Institute of Osteology at the Hanusch Hospital of WGKK and AUVA Trauma Centre Meidling, 4th Med. Dept., Hanusch Hospital, Heinrich Collin Str. 30, 1140 Vienna, Austria
[b] Genetics Unit, Shriners Hospital for Children and McGill University, Montreal, Quebec, Canada H3G 1A6

ARTICLE INFO

Article history:
Received 22 September 2008
Revised 15 February 2009
Accepted 19 February 2009
Available online 4 March 2009

Edited by: R. Baron

Keywords:
Bone mineralization density distribution (BMDD)
Quantitative backscattered electron imaging (qBEI)
Iliac bone
Normative data
Children

ABSTRACT

Bone mineralization density distribution (BMDD) as assessed by quantitative backscattered electron imaging (qBEI) in iliac crest bone biopsies has become in the last years a powerful diagnostic tool to evaluate the effect of metabolic bone diseases and/or therapeutic interventions on the mineralization status of the bone material. However until now, normative reference data are only available for adults. The aim of the present study is to close this gap and establish normative data from children and compare them with reference BMDD data of adults.

qBEI analyses were performed on bone samples from 54 individuals between 1.5 and 23 years without metabolic bone diseases, which were previously used as study population to establish normative histomorphometric standards.

In the trabecular compartment, none of the BMDD parameters showed a significant correlation with age. The BMDD was shifted towards lower mineralization density (CaMean −5.6%, $p<0.0001$; CaPeak −5.6%, $p<0.0001$; CaLow +39.0% $p<0.001$; CaHigh −80.7%, $p<0.001$) and the inter-individual variation was higher compared to the adult population.

The cortices appeared to be markedly less mineralized (CaMean −3.1%, $p<0.0001$) than cancellous bone due to higher amounts of low mineralized secondary bone. However, the cortical BMDD parameters showed a strong correlation ($r=0.38$ to 0.85, with $p<0.001$ to <0.0001) with cancellous BMDD parameters.

In conclusion, this study provides evidence that BMDD parameters in growing healthy subjects are relatively constant and that these data can be used as normative references in pediatrics osteology. The larger inter-individual variability compared to adults is most likely related to alterations of the bone turnover rate during growth.

Introduction

There is rising interest to include aspects of bone material quality [1–4] into the diagnosis of bone diseases, the estimation of fracture risk and treatment decisions. At present, assessment of bone material quality requires the examination of bone biopsy samples. One of the key parameters of material quality is mineral density content of the bone matrix, which determines the stiffness and toughness of bone material [3]. The local mineralization density of bone tissue can be measured by various techniques, such as microradiography [5,6], synchrotron radiation microcomputed tomography [7,8] and quantitative backscattered electron imaging (qBEI) [9].

The bone mineralization density distribution (BMDD) provides important information about the effect of metabolic bone diseases and therapeutic interventions on the mineralization of the bone material [9–12]. Reference data for trabecular BMDD in adults are available for the age range from 25 to 90 years [13]. These show a remarkably small inter-individual variation (coefficient of variation of less than 1.7%) in BMDD, suggesting that even small deviations have biological relevance. Indeed, low matrix mineralization was found in osteoporosis [14,15] and mild primary hyperparathyroidism [16] while a shift towards higher mineralization was found in osteogenesis imperfecta [17,18].

At present, the use of BMDD in pediatric populations is hampered by the lack of reference data for the age range below 25 years. In previous studies we therefore compared BMDD values of children and adolescents either with adults [19] or with individually age-matched controls [9,18,20]. However, comparison with adult data is certainly not ideal, as preliminary data suggest that trabecular bone matrix is less mineralized in children than in adults [7,21]. Comparison with age-matched controls is cumbersome and requires access to the raw data of control subjects. Establishing pediatric reference data for BMDD is therefore important for assessing pediatric bone diseases by qBEI and would also yield new insights into normal bone

* Corresponding author. Ludwig Boltzmann Institute of Osteology, UKH Meidling, Kundratstrasse 37, A-1120 Vienna, Austria. Fax: +43 1 60150 2651.
E-mail address: nadja.fratzl-zelman@osteologie.at (N. Fratzl-Zelman).

8756-3282/$ – see front matter © 2009 Elsevier Inc. All rights reserved.
doi:10.1016/j.bone.2009.02.021

development. We therefore performed qBEI analyses of complete transiliac bone biopsy specimen from children, adolescents and young adults without metabolic bone diseases.

Materials and methods

Subjects

The study population comprised 54 Caucasian subjects aged from 1.5 to 23 years (32 female, 22 male). Bone biopsies were performed during surgery for various orthopedic conditions, such as lower limb deformities, scoliosis, clubfeet and other problems that require corrective surgery (exostoses, cubitus valgus and equinovarus of the foot). All subjects were ambulatory, had normal renal function as assessed by measurement of serum creatinine and had no evidence of any metabolic bone disease. None was immobilized prior to surgery or received medications known to affect bone metabolism. This cohort is part of a larger population that has been presented before to establish reference data for histomorphometric parameters in cancellous and cortical bone [22–24].

Quantitative backscattered electron imaging (qBEI)

Quantitative backscattered electron imaging was employed to visualize and quantify the local mineralization density in transiliac bone biopsy samples. The physical principle of the technique is based on a quantification of the intensity of electrons backscattered from the surface of a sectioned bone area. The obtained signal is proportional to the weight fraction of calcium (Ca wt.%) present locally in the embedded bone tissue. Full details of the technique have been described elsewhere [10,13]. Blocks containing polymethylmethacrylate-embedded undecalcified iliac bone samples were prepared for

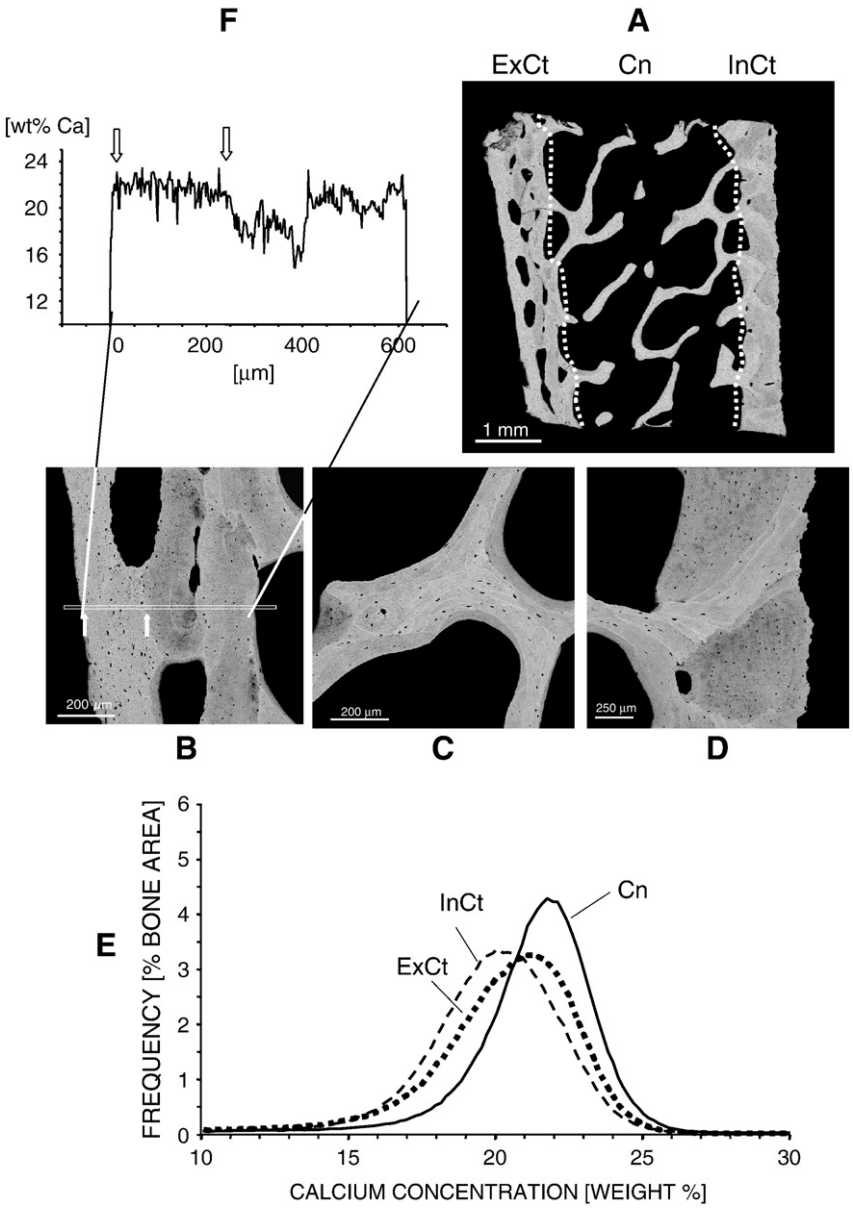

Fig. 1. Backscattered electron images and corresponding BMDD of a transiliac bone biopsy of a 12-year-old study participant. Overview of the entire biopsy sample showing the asymmetric aspect of the two cortices: (A) The external cortex (Ex.Ct) is characterized by periosteal primary bone and endocortical cancellation while the internal cortex (In.Ct) is characterized by periosteal eroded surfaces and endocortical encroaching of trabecular features. (B) Detail of external cortex. (C) Detail of cancellous bone. (D) Detail of internal cortex. (E) BMDD curves corresponding to the Ex.Ct and internal In.Ct as well as cancellous bone (Cn). (F) Calcium content profile through the external cortex from the periosteal to the endocortical surface as indicated by the white line. Arrows indicate the region of primary periosteal bone.

qBEI by grinding and polishing in order to obtain plane and parallel surfaces. The sample surface was then carbon coated. Quantitative BEI was performed in a digital scanning electron microscope (DSM 962, Zeiss, Oberkochen, Germany) equipped with a four-quadrant semiconductor backscattered electron detector. The microscope was operated at 20 keV electron energy and a probe current of 110 pA.

A series of backscattered electron images using a pixel resolution of 2 µm (as shown in Figs. 1B to D) were performed covering the entire biopsy area including both cortices and the cancellous bone compartment. Mineralized bone tissue were segmented from soft tissue including osteoid and marrow space filled with embedding medium by grey level thresh holding [10,11]. Cancellous bone was separated from the cortical bone as indicated by the dashed line in Fig. 1A. Thereby the line was following the bone tissue where the compact bone character is changing into a cancellous one (subjectively). In the age range of 1.5 to 14 years morphological features as visualized by qBEI allowed us to assign the two cortices to external (Ex.Ct) and to internal (In.Ct) cortices (see Fig. 1) [24]. However, for ages above 14 years the above mentioned morphological features disappeared and hampered the discrimination between external and internal cortices. Hence, for the entire age range 1.5 to 23 years only one set of the BMDD data for cortical bone, the average of the two cortices was determined.

From the grey level images obtained by the area scans, grey level frequency histograms were derived and converted by calibration [10] to BMDD. BMDD curves indicate the frequency of pixels corresponding to specific calcium contents occurring throughout the sample area. BMDD curves were evaluated separately for the trabecular compartment and the two cortical compartments (Fig. 1 E).

For statistical analysis, five parameters characterizing the BMDD curve were determined, as described in detail elsewhere [9,13] (see Fig. 2):

- CaMean, the weighted mean calcium concentration of the bone area obtained by the integrated area under the BMDD curve;
- CaPeak, the peak position of the histogram, which indicates the most frequently occurring calcium concentration (calcium value with the highest number of pixels) in the bone area;
- CaWidth, the full width at half maximum of the distribution, describing the variation in mineralization density;
- CaLow, the percentage of bone area that is mineralized below the 5th percentile of the reference BMDD of normal adults [13], that is below 17.68 wt.% calcium. This parameter corresponds to the amount of bone area undergoing primary mineralization.
- CaHigh, the percentage of bone area that is mineralized above the 95th percentile of the reference BMDD of normal adults that is above 25.30 wt.% calcium. This parameter corresponds to the amount of bone having achieved plateau level of normal mineralization and includes also the contribution of highly mineralized cement lines [9].

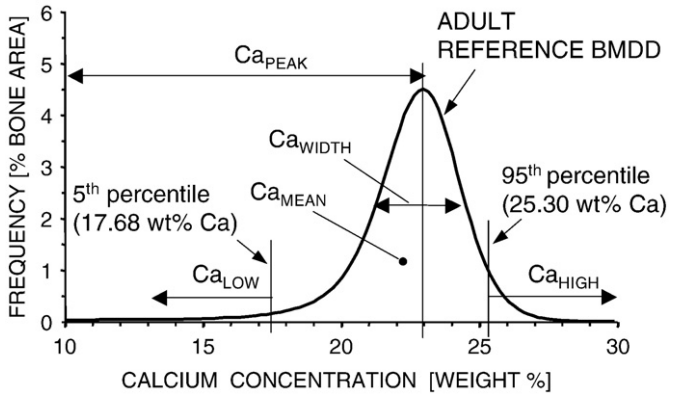

Fig. 2. The BMDD curve of normal human adult trabecular bone. All BMDD parameters used in this article (CaMean, CaPeak, CaWidth, CaLow, CaHigh) are indicated in this curve. Note that CaLow and CaHigh are defined in relation to this reference BMDD of adults [9].

Table 1
Cancellous BMDD parameters in the present study population compared to reference data for cancellous BMDD in adults [13] and to cortical BMDD parameters of the present study population.

	Adults	Present study population	
	Cancellous bone ($n=52$)	Cancellous bone ($n=54$)	Cortex ($n=53$)
CaMean [wt.% Ca]	22.20 (0.45)	20.95[a] (0.57)	20.31[b] (0.93)
CaPeak [wt.% Ca]	22.94 (0.39)	21.66[a] (0.52)	21.14[b] [20.62; 21.75]
CaWidth [Δwt.% Ca]	3.29 [3.12; 3.47]	3.47 [3.12; 3.64]	3.81[b] [3.38; 4.38]
CaLow [%]	4.52 [3.87; 5.79]	6.14[a] [4.90; 7.99]	9.06[b] [6.22; 15.00]
CaHigh [%]	4.62 [3.52; 6.48]	0.89[a] [0.43; 1.47]	0.46[b1] [0.28; 1.22]

Data shown are mean (SD) or median [25%; 75%].
[a] significant difference ($p<0.0001$) in cancellous bone results between adults and the present study population.
[b, b1] significant difference ($p<0.0001$, $p<0.01$) to cancellous bone result in the present study population.

Statistical analyses

Statistical analysis was performed using SigmaStat for Windows Version 2.03 (SPSS Inc.). The relationship between BMDD parameters and age was tested by Spearman rank order correlation tests. Comparisons of BMDD parameters between the present study group and those of an adult reference population were done by *t*-test or nonparametric by Mann–Whitney test when appropriate. Differences of BMDD parameters between spongiosa, and cortical bone were tested by Friedman repeated measures ANOVA on ranks followed by Tukey pairwise comparison. Not normally distributed data are given by median and interquartile range in Table 1. Correlations between results in trabecular and cortical bone were calculated by Pearson or Spearman correlation coefficients when appropriate (Table 2).

Results

Trabecular bone

In trabecular bone, none of the BMDD parameters varied significantly with age (Fig. 3A). Statistical *t*-test between the male and female group did not reveal differences in BMDD parameters either. The corresponding *p*-values ranged from 0.31 to 0.95. Consequently, a single reference BMDD of trabecular bone could be constructed for the entire age range from 1.5 to 23 years (Fig. 3B). Table 1 presents these results in numerical format.

Compared to the adult reference population [13], the present study population had lower average mineralization density, as expressed by 5.6% lower results for CaMean and CaPeak (Table 1, Fig. 3B). Correspondingly, samples from the younger population contained 39% more areas with low mineralization, and 81% less areas with fully mineralized bone ($p<0.001$ in both cases; Table 1). The average intraindividual heterogeneity of mineralization (i.e., CaWidth) was not significantly different between groups ($p=0.52$). However, the

Table 2
Correlations of cortical with cancellous BMDD parameters of the present study population.

	Cortical vs. cancellous bone
Ca_{Mean}	$r=0.85$, $p<0.0001$
Ca_{Peak}	$r=0.83$, $p<0.0001$
Ca_{Width}	$r=0.38$, $p<0.01$
Ca_{Low}	$r=0.75$, $p<0.0001$
Ca_{High}	$r=0.72$, $p<0.0001$

Data shown are the correlation coefficient *r* and the corresponding *p*-value.

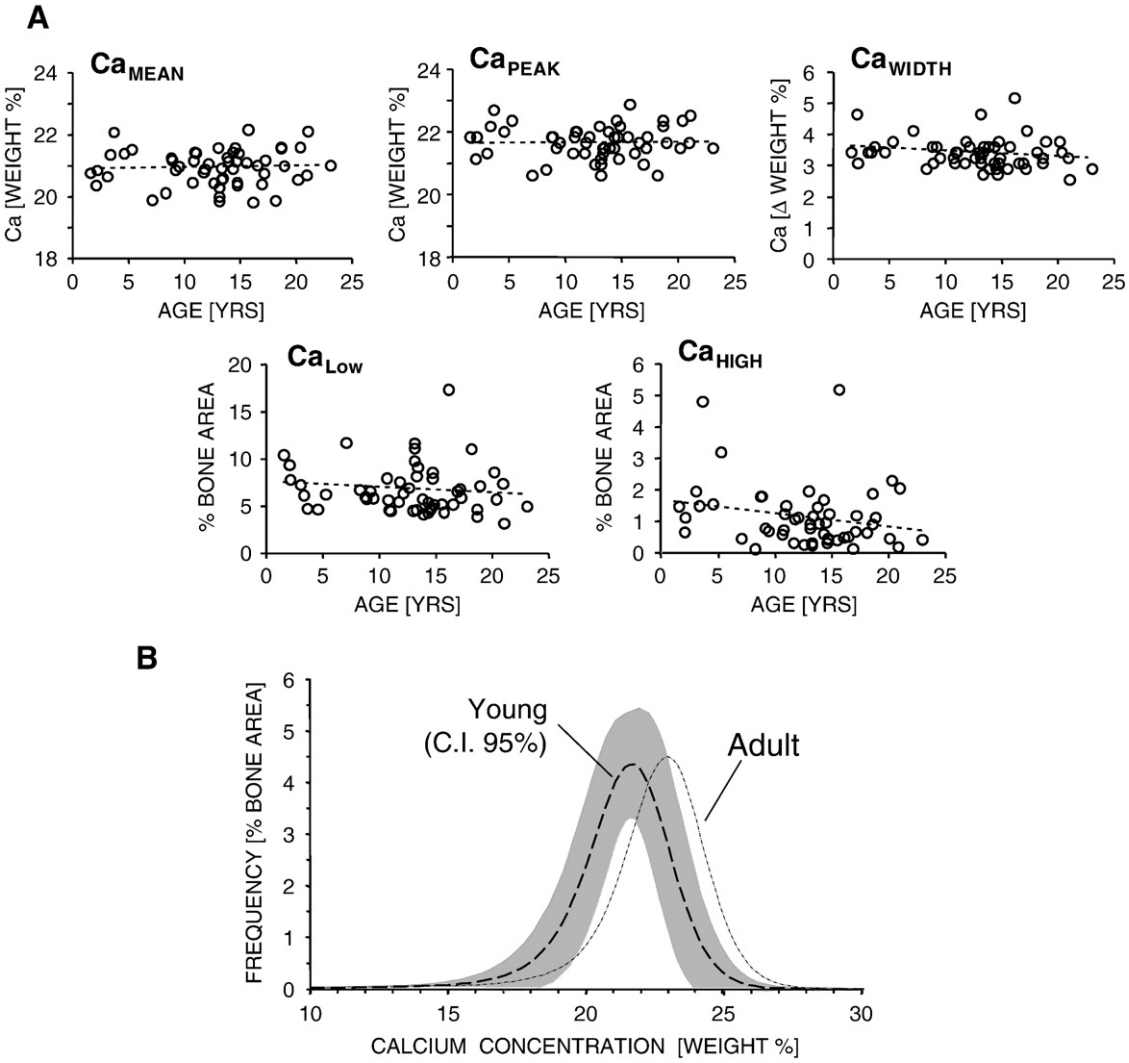

Fig. 3. Relationship of BMDD parameters with age. (A) The dotted lines indicate the linear fits. However none of the parameters showed a significant correlation with age. (B) Reference BMDD curve for trabecular bone for the age range from 1.5 to 23 years. The grey band indicates the 95% confidence interval (C.I.) for the individual histogram values. For comparison the reference BMDD curve of adults (25 to 90 years of age) is shown too.

interindividual variability of mineralization density was slightly higher in the present study population than in adults. E.g., the interindividual coefficient of variation in CaPeak was 1.7% in the adult group and 2.4% in our present cohort (Table 1).

Cortical bone

BMDD parameters of cortical bone (mean of both cortices) were significantly correlated to those of trabecular bone (Table 2). Nevertheless, the mineralization density of cortical bone was markedly lower and more heterogeneous than that of trabecular bone (Table 1, Fig. 1). This was explained by the observation that cortical bone contained more areas undergoing primary mineralization and fewer areas of fully mineralized bone (Fig. 1, Table 1).

Though in the age range 1.5 to 14 years the two cortices, the external and internal cortices, exhibited an asymmetric aspect, the mineralization density (CaMean −0.98%) was only slightly lower for internal compared to external cortex (data not shown). In the external cortex, bone tissue close to the periosteal surface was more highly mineralized than bone adjacent to the endocortical surface (Figs. 1B and F). The internal cortex contained remnants of highly mineralized trabeculae. The areas between these trabecular remnants were 'filled' with large amounts of newly formed and lower mineralized bone (Fig. 1D). The periosteal surface of the internal cortex often presented an eroded aspect (Fig. 1D).

Discussion

The main findings of this study are that BMDD parameters of iliac trabecular bone are constant from 1.5 to 23 years of age and that matrix mineralization density is lower in cortical than in trabecular bone. In addition there was a strong correlation of the BDDD parameters between cortical and trabecular bone. These observations need to be interpreted in light of the mineralization process and of normal iliac bone development.

The lack of age dependency of BMDD parameters in these biopsies during growth of individuals, which is consistent with a previous study [17], is somewhat surprising and requires closer analysis: First, in children and adolescents, the site of biopsy is located at approximately 1 cm below the apophyseal iliac growth plate. During human skeletal development, this growth plate is one of the last to fuse [25]. It can therefore be assumed that in most of our study participants this growth plate was active when the biopsy was performed. This means that even though our study population varied widely in chronological age, the age of the bone tissue at the site of biopsy was presumably similar between study participants. Second, it

has been shown that trabecular bone in the growing skeleton is subjected to a high rate of bone turnover with a small positive balance towards new bone acquisition [26]. Hence, in a situation of high bone turnover – and independently of age – the BMDD is shifted towards lower mineralization [9,12,14,16,27]. This is due to the fact that newly formed bone matrix is rapidly mineralized (within a few days) up to only 70% (primary mineralization) of fully mineralized bone matrix and the full mineralization lasts years (secondary mineralization). Consistently, a recent mathematical model showed that the most frequently occurring calcium concentration (CaPeak) decreases in situations of high bone turnover [28]. Therefore, the average degree of mineralization depends on the age of the bone tissue. High bone turnover decreases the average age of bone tissue and therefore is associated with increased CaLow and decreased CaPeak and CaMean [28,29]. Presumably, the continuing endochondral bone formation process and the subsequent high remodeling activity thus contribute to maintain bone tissue age fairly constant, which explains why the mineralization density of the bone matrix did not change with the chronological age of study participants. Once the growth process is completed, the bone tissue 'ages' rapidly. This means that mineralization density increases rapidly until a new steady state is achieved, the level of which depends on the prevailing remodeling rate [28]. Therefore, the mineralization density of iliac trabecular bone is higher in adults than during development.

Further, the BMDD data reflected the distinctive development of the cortices. According to previous studies, the developing ilium increases in width due to a lateral modeling drift of both cortices [23,26]. The outer cortex is expanding through periosteal bone apposition and is partially resorbed and transformed into trabecular bone on the endocortical side. In contrast, the inner cortex expands by endocortical apposition, and thus encroaches on the trabecular compartment. During this process, trabeculae are incorporated into the inner cortex and the space between trabeculae is filled up with new bone tissue.

The qBEI method shows that the primary bone produced by the periosteal osteoblasts of the external cortex is more highly mineralized than the adjacent bone tissue that has undergone intracortical remodeling and thus constitutes secondary bone. As the amount of this high-density primary bone is generally much less than that of the low-density secondary bone, the overall mineralization density of the external cortex is lower and more heterogeneous than that of the cancellous bone. Interestingly, this primary periosteal bone matrix with increased mineralization density, which has already described using microradiography [30], is known to have a different lamellar structure than secondary bone [23]. It seems that the mineralization process of this bone matrix is accelerated. Otherwise, the mineralization density would be distinctly lower, because of its relatively young age in this cortical bone region. Such rapid formation of highly mineralized periosteal bone tissue in the developing skeleton might represent an efficient mechanism to establish rapidly some mechanical competence by forming first a rigid scaffold, which is remodeled and optimized later on. This strategy seems to be analogous to the formation of highly mineralized callus tissue in fracture healing [31,32].

In contrast, the internal cortex of the ilium does not contain primary bone in growing individuals, as the formation drift occurs on the endocortical surface [23,26]. Consequently, the internal cortex is composed of a mixture between relatively old and highly mineralized trabecular remnants and new bone matrix with low mineralization. The average mineralization density therefore is below that of trabecular bone. Thus, consistent with previous observations that were made with a different experimental approach, the average mineralization density during development is lower in cortical than in trabecular bone [17]. As discussed, this is presumably the result of modeling drifts. When the modeling drifts come to a halt at the end of bone development, the mineralization density of cortical bone should increase. In adults, CaPeak of cortical bone is indeed similar or higher than that of trabecular bone [33].

Moreover, it is remarkable, that the cortical BMDD parameters were strongly correlated to those of trabecular bone. This suggests a certain "coupling" of bone turnover rate between cortical and trabecular bone compartments in these young individuals.

In conclusion, the present study shows that trabecular BMDD of transiliac biopsy samples remains constant from 1.5 to 23 years of age and that the cortical BMDD is different, but strongly correlated to the trabecular BMDD in each individual. Therefore, the reference values for trabecular and cortical bone as well its correlation to each other derived in this study can be used for the entire age range. It should be emphasized, that due to the higher variability in BMDD, the usage of the normative data deduced from 54 individuals might be more reliable than the usage of age-matched controls. These data should increase the use of qBEI in the assessment of pediatric bone biopsy samples.

Acknowledgments

We thank G. Dinst, Ph. Messmer, D. Gabriel and S. Thon for careful sample preparations and qBEI measurements at the bone material laboratory of the Ludwig Boltzmann-Institute of Osteology, Vienna, Austria, and Rose Travers for histomorphometric analyses at the Genetics Unit of the Shriners Hospital in Montreal, Canada. This study was supported by the AUVA (Research funds of the Austrian workers compensation board), by the WGKK (Viennese sickness insurance funds) and the Shriners of North America. F.R. is a Chercheur-Boursier Clinicien of the Fonds de la Recherche en Santé du Québec.

References

[1] Currey JD. Bones-Structure and Mechanics. Princeton: Princeton University Press; 2002.
[2] Currey JD. Bone architecture and fracture. Curr Osteoporos Rep 2005;3:52–6.
[3] Fratzl P, Gupta H, Paschalis E, Roschger P. Structure and mechanical quality of the collagen-mineral nano-composite in bone. Journal of Material Chemistry 2004;14:2115–23.
[4] Seeman E. Bone quality: the material and structural basis of bone strength. J Bone Miner Metab 2008;26:1–8.
[5] Eschberger J, Eschberger D. Microradiography. In: FA VR, editor. Handbook of biomaterials evaluation. New York: Macmillan Publishing Company; 1986. pp. 461–500.
[6] Boivin G, Meunier PJ. The degree of mineralization of bone tissue measured by computerized quantitative contact microradiography. Calcif Tissue Int 2002;70:503–11.
[7] Nuzzo S, Peyrin F, Cloetens P, Baruchel J, Boivin G. Quantification of the degree of mineralization of bone in three dimensions using synchrotron radiation microtomography. Med Phys 2002;29:2672–81.
[8] Borah B, Ritman EL, Dufresne TE, et al. The effect of risedronate on bone mineralization as measured by micro-computed tomography with synchrotron radiation: correlation to histomorphometric indices of turnover. Bone 2005;37:1–9.
[9] Roschger P, Paschalis EP, Fratzl P, Klaushofer K. Bone mineralization density distribution in health and disease. Bone 2008;42:456–66.
[10] Roschger P, Fratzl P, Eschberger J, Klaushofer K. Validation of quantitative backscattered electron imaging for the measurement of mineral density distribution in human bone biopsies. Bone 1998;23:319–26.
[11] Roschger P, Fratzl P, Klaushofer K, Rodan G. Mineralization of cancellous bone after alendronate and sodium fluoride treatment: a quantitative backscattered electron imaging study on minipig ribs. Bone 1997;20:393–7.
[12] Zoehrer R, Roschger P, Paschalis EP, et al. Effects of 3- and 5-year treatment with risedronate on bone mineralization density distribution in triple biopsies of the iliac crest in postmenopausal women. J Bone Miner Res 2006;21:1106–12.
[13] Roschger P, Gupta HS, Berzlanovich A, et al. Constant mineralization density distribution in cancellous human bone. Bone 2003;32:316–23.
[14] Roschger P, Rinnerthaler S, Yates J, Rodan GA, Fratzl P, Klaushofer K. Alendronate increases degree and uniformity of mineralization in cancellous bone and decreases the porosity in cortical bone of osteoporotic women. Bone 2001;29:185–91.
[15] Boivin G, Meunier PJ. Effects of bisphosphonates on matrix mineralization. J Musculoskelet Neuronal Interact 2002;2:538–43.
[16] Roschger P, Dempster DW, Zhou H, et al. New observations on bone quality in mild primary hyperparathyroidism as determined by quantitative backscattered electron imaging. J Bone Miner Res 2007;22:717–23.
[17] Boyde A, Travers R, Glorieux FH, Jones SJ. The mineralization density of iliac crest bone from children with osteogenesis imperfecta. Calcif Tissue Int 1999;64:185–90.

[18] Weber M, Roschger P, Fratzl-Zelman N, et al. Pamidronate does not adversely affect bone intrinsic material properties in children with osteogenesis imperfecta. Bone 2006;39:616–22.
[19] Fratzl-Zelman N, Valenta A, Roschger P, et al. Decreased bone turnover and deterioration of bone structure in two cases of pycnodysostosis. J Clin Endocrinol Metab 2004;89:1538–47.
[20] Roschger P, Fratzl-Zelman N, Misof BM, Glorieux FH, Klaushofer K, Rauch F. Evidence that abnormal high bone mineralization in growing children with osteogenesis imperfecta is not associated with specific collagen mutations. Calcif Tissue Int 2008;82:263–70.
[21] Roschger P, Grabner BM, Rinnerthaler S, et al. Structural development of the mineralized tissue in the human L4 vertebral body. J Struct Biol 2001;136:126–36.
[22] Glorieux FH, Travers R, Taylor A, et al. Normative data for iliac bone histomorphometry in growing children. Bone 2000;26:103–9.
[23] Rauch F, Travers R, Glorieux FH. Cellular activity on the seven surfaces of iliac bone: a histomorphometric study in children and adolescents. J Bone Miner Res 2006;21:513–9.
[24] Rauch F, Travers R, Glorieux FH. Intracortical remodeling during human bone development-a histomorphometric study. Bone 2007;40:274–80.
[25] Dimeglio A. Growth in pediatric orthopedics. In: Lovell W, Weinstein S, Morrissy R, editors. Lovell and Winter's pediatric orthopaedics. Philadelphia: Lippincott Williams and Wilkins; 2006. pp. 33–62.
[26] Parfitt AM, Travers R, Rauch F, Glorieux FH. Structural and cellular changes during bone growth in healthy children. Bone 2000;27:487–94.
[27] Fratzl P, Roschger P, Fratzl-Zelman N, Paschalis EP, Phipps R, Klaushofer K. Evidence that treatment with risedronate in women with postmenopausal osteoporosis affects bone mineralization and bone volume. Calcif Tissue Int 2007;81:73–80.
[28] Ruffoni D, Fratzl P, Roschger P, Klaushofer K, Weinkamer R. The bone mineralization density distribution as a fingerprint of the mineralization process. Bone 2007;40:1308–19.
[29] Ruffoni D, Fratzl P, Roschger P, Phipps R, Klaushofer K, Weinkamer R. The effect of temporal changes in bone turnover on the bone mineralization density distribution: a computer simulation study. J Bone Miner Res 2008;12:1905–14.
[30] Leblond CP, Wilkinson GW, Belanger LF, Robichon J. Radio-autographic visualization of bone formation in the rat. Am J Anat 1950;86:289–341.
[31] Gerstenfeld LC, Alkhiary YM, Krall EA, et al. Three-dimensional reconstruction of fracture callus morphogenesis. J Histochem Cytochem 2006;54:1215–28.
[32] Uthgenannt BA, Kramer MH, Hwu JA, Wopenka B, Silva MJ. Skeletal self-repair: stress fracture healing by rapid formation and densification of woven bone. J Bone Miner Res 2007;22:1548–56.
[33] Misof BM, Roschger P, Dempster D, Fratzl P, Klaushofer K. Relationship between trabecular and cortical bone mineralization density distribution (BMDD) in iliac crest biopsies from healthy individuals and cases of primary hyperparathyroidism. Bone 2006;39:S17.

LEBENSLAUF

Persönliches:

Name:	Mag. Sonja Andrea PFEFFER
Geburtsdatum:	12. Juni 1971
Geburtsort:	Salzburg
Familienstand:	ledig
Staatsbürgerschaft:	österreichisch

Schulbildung und Studium:

1977 – 1986	Pflichtschule
1986 – 1989	Handelsakademie I, Sbg.
1989 – 1992	Kaufmännische Berufsschule VI, Sbg. mit Lehrabschlussprüfung
1991 – 1994	Abendgymnasium für Berufstätige, Sbg.
22.10.1997	Studienberechtigungsprüfung, Universität Innsbruck
WS 1997/98 – SS 2005	Diplomstudium Biologie, Universität Salzburg Thema der Diplomarbeit: *Immunologische Signifikanz der Stickoxidsynthase (NOS) in der Epidermis bei Xenopus Laevis*
WS 2005/06 – SS 2009	Doktoratstudium der Naturwissenschaften, Universität Wien Thema der Dissertation: *Measurements of mineralization density profiles in bone forming sites: a novel tool for diagnosis of disturbances in primary mineralization of bone*

Berufspraxis:

01.09.1989 – 31.08.1992	Lehre als Bürokauffrau Ludwig Pfeffer GmbH, 5020 Salzburg
01.09.1992 – 31.05.1993	Sekretariat Ludwig Pfeffer GmbH, 5020 Salzburg
01.06.1993 – 30.09.1997	Sekretariat Österr. Institut für Menschenrechte

	5020 Salzburg
01.09.2000 – 31.03.2004	Sekretariat Ludwig Pfeffer GmbH, 5020 Salzburg
15.07.2005 – 30.06.2009	Wissenschaftl. Mitarbeiterin Ludwig Boltzmann Inst. für Osteologie 1120 Wien

Ausbildung und Training:

- European Calcified Tissue Society (ECTS) Ph D-Trainingscourse in Oxford, September 2007
- SE Finanzierung, Kommunikation und Abwicklung von Projekten, Uni Wien 2006

Scientific Meetings:

- International Conference on Progress in Bone and Mineral Research, November 2006, Vienna, Austria
- Osteologie Kongress März 2007: Wien im Zentrum der deutschsprachigen Osteologie, Wien, Austria
- ÖGKM-Jahrestagung 2008, Wien, Austria
- ECTS 36th European Symposium on calcified Tissue, May 2009, Vienna, Austria

Memberships:

- European Calcified Tissue Society (ECTS)
- Austrian Society for Bone and Mineral Research (ÖGEKM)

Wien, 16. Februar 2009 .....